

(12) LEVEL II

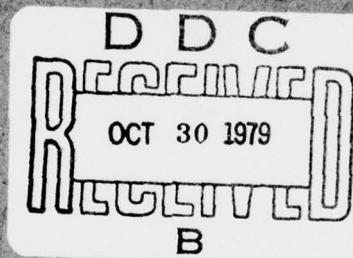
AD

**TECHNICAL REPORT
NATICK/TR-79/023**

**FINITE ELEMENT ANALYSIS OF A
STATICALLY LOADED ISO TACTICAL
SHELTER**

AD A025807

DDC FILE COPY



by
**Arthur R. Johnson
and
Vlty P. Ciras**

Approved for public release;
distribution unlimited.

JANUARY 1979

**UNITED STATES ARMY
NATICK RESEARCH and DEVELOPMENT COMMAND
NATICK, MASSACHUSETTS 01760**



Aero-Mechanical Engineering Laboratory

79 10 29 057

Approved for public release; distribution unlimited.

Citation of trade names in this report does not constitute an official indorsement or approval of the use of such items.

Destroy this report when no longer needed. Do not return it to the originator.

UNCLASSIFIED

SECURITY CLASSIFICATION OF THIS PAGE (When Data Entered)

REPORT DOCUMENTATION PAGE		READ INSTRUCTIONS BEFORE COMPLETING FORM
1. REPORT NUMBER NATICK/TR-79/023	2. GOVT ACCESSION NO.	3. RECIPIENT'S CATALOG NUMBER <i>Technical rept.</i>
4. TITLE (and Subtitle) FINITE ELEMENT ANALYSIS OF A STATICALLY LOADED ISO TACTICAL SHELTER	5. TYPE OF REPORT & PERIOD COVERED	
7. AUTHOR(s) Arthur R. Johnson Vitty P. Ciras	6. PERFORMING ORG. REPORT NUMBER	
9. PERFORMING ORGANIZATION NAME AND ADDRESS US Army Natick Research & Development Command Aero-Mechanical Engineering Laboratory Natick, MA 01760	8. CONTRACT OR GRANT NUMBER(s)	
11. CONTROLLING OFFICE NAME AND ADDRESS US Army Natick Research & Development Command Aero-Mechanical Engineering Laboratory Natick, MA 01760	10. PROGRAM ELEMENT, PROJECT, TASK AREA & WORK UNIT NUMBERS 62723A 1L162723A427 01003BG	
14. MONITORING AGENCY NAME & ADDRESS (if different from Controlling Office) <i>12-159</i>	12. REPORT DATE January 1979	
	13. NUMBER OF PAGES	
	15. SECURITY CLASS. (of this report) UNCLASSIFIED	
16. DISTRIBUTION STATEMENT (of this Report) Approved for public release; distribution unlimited.		
17. DISTRIBUTION STATEMENT (of the abstract entered in Block 20, if different from Report) DDC RECEIVED OCT 30 1979 B		
18. SUPPLEMENTARY NOTES <i>ISO (International Standard Organization)</i>		
19. KEY WORDS (Continue on reverse side if necessary and identify by block number)		
ISO SHELTERS FINITE ELEMENT ANALYSIS ARMY SHELTERS SHELTERS	SHIPPING CONTAINERS FREIGHT CONTAINERS CONTAINERS CARGO	LOAD CARRYING PANELS (STRUCTURAL) SANDWICH PANELS TACTICAL SHELTERS
20. ABSTRACT (Continue on reverse side if necessary and identify by block number) A finite element analysis of a 2.4 m x 2.4 m x 6.1 m (8 ft x 8 ft x 20 ft) 3-for-1 expandable ISO Army Shelter has been made for static loads designated in the specifications for Army ISO Tactical Shelters. The report includes a description of the load paths, an investigation of the load-carrying capability of the structure both with and without wall panels as structural members, recommendations for improving the design for static load response, a buckling analysis for the ISO stacking test, and a comparison of calculated and measured data for a series of tests performed on the prototype shelter analyzed in this report.		

DD FORM 1 JAN 73 1473 EDITION OF 1 NOV 65 IS OBSOLETE

UNCLASSIFIED

SECURITY CLASSIFICATION OF THIS PAGE (When Data Entered)

PREFACE

This work represents part of an effort to develop a standard family of rigid wall tactical shelters. Other ongoing efforts involve both the manufacture of and field testing of prototype shelters. The data provided in this effort will help guide the development of future shelters by providing a better understanding of the structural response of these shelters to static loads. Future work will include the dynamic response of tactical shelters.

ACCESSION for	
NTIS	White Section <input checked="" type="checkbox"/>
DDC	Buff Section <input type="checkbox"/>
UNANNOUNCED	<input type="checkbox"/>
JUSTIFICATION _____	
BY _____	
DISTRIBUTION/AVAILABILITY CODES	
Dist. Avail. and/or SPECIAL	
A	

TABLE OF CONTENTS

	Page
LIST OF FIGURES	4
LIST OF TABLES	9
1. INTRODUCTION	11
2. COMPUTER MODEL	11
a. Description of Shelter	11
b. Finite Elements Used	13
c. Finite Element Mesh	17
d. Computation of Structural Properties	27
3. STATIC ANALYSIS	33
a. Load No. 1 - Stacking	44
b. Load No. 2 - Top Lift	52
c. Load No. 3 - Bottom Lift	59
d. Load No. 4 - Restraint	64
e. Load No. 5 - Racking	69
f. Load No. 6 - Lashing	75
g. Load No. 7 - End Wall Uniform Load	85
h. Load No. 8 - Side Wall Uniform Load	85
i. Load No. 9 - Roof Concentrated Load	92
4. COMPARISON OF MEASURED DATA AND COMPUTED DATA	92
5. BUCKLING ANALYSIS FOR STACKING LOAD	104
6. CONCLUSIONS AND RECOMMENDATIONS	111
REFERENCES	116
APPENDIX - DATA DECKS FOR FINITE ELEMENT MODELS	117

LIST OF FIGURES

	Page
Figure 1. General view of a 2.4-m x 2.4-m x 6.1-m ISO Army shelter	12
Figure 2. Major components of a 3-for-1 Army shelter	14
Figure 3. Components of 3-for-1 shelter used for static analysis	16
Figure 4. Global coordinate system and skeleton view of model for static analysis	18
Figure 5. Transverse sectional view A-A of shelter	19
Figure 6. Longitudinal sectional view B-B of shelter	20
Figure 7. Plan sectional view C-C of shelter	21
Figure 8. Grid point identification	23
Figure 9. Plate element identification	24
Figure 10. Beam element identification	25
Figure 11. Three-dimensional plot of finite element model	26
Figure 12. A 2.4 m x 2.4 m panel fixed at one end with shear load at other end	29
Figure 13. End wall mesh convergence data, top left corner only	30
Figure 14. Beam number 1 properties	34
Figure 15. Beam number 2 properties	35
Figure 16. Beam number 3 properties	36
Figure 17. Beam number 4 properties	37
Figure 18. Beam number 5 properties	38
Figure 19. Beam number 6 properties	39
Figure 20. Beam number 7 properties	40

LIST OF FIGURES (Continued)

	Page
Figure 21. Beam number 8 properties	41
Figure 22. Beam number 9 properties	42
Figure 23. Beam number 10 properties	43
Figure 24. Test No. 1, stacking	45
Figure 25. Undeformed and deformed structure plot superimposed for beams — stacking load	46
Figure 26. Deformed structure plot — stacking load	47
Figure 27. Personnel door end. Stacking load. In plane bending moments in outer frame	48
Figure 28. Personnel door end. Stacking load. Axial load in outer frame	49
Figure 29. Side wall nearest XZ plane. Stacking load. In plane bending moments in outer frame	50
Figure 30. Floor beams. Stacking load. Bending moments in vertical plane	51
Figure 31. Stacking load. Side wall nearest XZ plane. Stress in vertical direction for outer skin	53
Figure 32. Test No. 2, lifting from top	54
Figure 33. Deformed structure plot - lifting from top	55
Figure 34. Lifting from top. Bending moments in XZ plane for corner post	57
Figure 35. Lifting from top. Bending moments in XZ plane for I beam under floor	58
Figure 36. Lifting from top. Hecky-von Mises stress in top skin of floor plate	60

LIST OF FIGURES (Continued)

	Page
Figure 37. Test No. 3, lifting from bottom	61
Figure 38. Deformed structure plot — case with no wall and roof panels. Lifting from bottom	62
Figure 39. Lifting from bottom. Bending moments in XZ plane for door frame member	63
Figure 40. Lifting from bottom. Bending moments in XZ plane for extrusion in edge of floor	65
Figure 41. Test No. 4, restraint	66
Figure 42. Restraint. Superimposed plot for undeformed and deformed floor panel	67
Figure 43. Restraint. Axial load in I-beam under floor	68
Figure 44. Restraint. Side wall farthest from XZ plane. Horizontal stress distribution	70
Figure 45. Test No. 5, racking	71
Figure 46. Racking. Load No. 1, deformed body plot	72
Figure 47. Racking. Load No. 1, deformed body plot, personnel door end	73
Figure 48. Racking. Personnel door end. In plane bending moments in outer frame	74
Figure 49. Test No. 6, lashing	76
Figure 50. Lashing. Load No. 1, deformed body plot, personnel door end	77
Figure 51. Lashing. Load No. 3, deformed body plot, personnel door end	78
Figure 52. Lashing. Load No. 5, deformed body plot, personnel door end	79

LIST OF FIGURES (Continued)

	Page
Figure 53. Lashing. Load No. 8, deformed body plot	80
Figure 54. Lashing. Load No. 8, deformed body plot, side wall farthest from XZ plane	81
Figure 55. Lashing. Axial loads in end wall frame	82
Figure 56. Lashing. Axial loads in side wall frame farthest from XZ plane	84
Figure 57. Test No. 7, end wall uniform load	86
Figure 58. Deformed structure plot — uniform load on end wall	87
Figure 59. Uniform load on end wall. Superimposed plot for undeformed and deformed end wall	88
Figure 60. Test No. 8, side wall uniform load	89
Figure 61. Deformed structure plot — uniform load on side wall	90
Figure 62. Uniform load on side wall. Superimposed plot for undeformed and deformed side wall	91
Figure 63. Test No. 9, roof concentrated load	93
Figure 64. Deformed structure plot — roof concentrated load	94
Figure 65. Roof concentrated load. Superimposed plot for undeformed and deformed roof	95
Figure 66. Stacking test. Computed and measured strains in corner post	97
Figure 67. Restraint. Computed and measured strains in floor I-beam	99
Figure 68. Restraint. Detailed view of floor frame near ISO fitting	100
Figure 69. Lashing. Computed and measured strains in roof beam	101
Figure 70. Lashing. Detailed view of roof near ISO fitting	102

LIST OF FIGURES (Continued)

		Page
Figure 71.	Lashing. Computed and measured strains in corner post	103
Figure 72.	Lashing. Computed and measured strains for lower transverse compression test	105
Figure 73.	Lashing. Computed and measured strains for lower transverse tension test	106
Figure 74.	Lashing. Detailed view of transverse channel and channel cross sectional area	107
Figure 75.	Buckling mode No. 1 for complete structure subjected to stacking load	110
Figure 76.	Buckling mode No. 1 for structure with no wall and roof panels subjected to stacking load	112
Figure 77.	Buckling mode No. 2 for structure with no wall and roof panels subjected to stacking load	113

LIST OF TABLES

	Page
Table 1. Computed scale factors for end wall in-plane behavior	31
Table 2. Physical properties for plate elements	32
Table 3. Computed Eigenvalues for buckling under stacking load	109

FINITE ELEMENT ANALYSIS OF A STATICALLY LOADED ISO TACTICAL SHELTER

1. INTRODUCTION

The Army has been using shelters which are made from honeycomb panels and beams for many years. The detailed design of the shelters has changed over the years since shelters were designed for special tasks. Due to the quantity of shelters in the system and due to a desire of the Army to have shelters capable of meeting the basic requirements for cargo containers¹ the Army has decided to standardize its shelters.

There have been few complete analyses of shelters in the past. None of the past studies appeared to have investigated the effects of the panels as load-carrying members to determine suitable panel and beam combinations or at least indicate numerically how the panels and beams share the applied loads.

This study is a straightforward structural analysis of a prototype Army shelter originally designed to the International Standard Organization's (ISO) specifications for dimensions of freight containers. The objectives of this study are to:

- (1) Develop a finite element structural model for an ISO Army shelter which is 2.4 m x 2.4 m x 6.1 m (8 ft x 8 ft x 20 ft) in its shipping configuration.
- (2) Investigate the load-carrying capability of the structure by applying the ISO loads and investigating the load paths determined by finite element analyses.
- (3) Investigate the load-carrying capability of the structure both with and without panels to determine the effects of neglecting panels in design or the effects of using weak panels to save fabrication costs.

Section 2 of this report describes the shelter and finite element model chosen for the analysis. Section 3 contains a description of the static loads and reports the results of the analysis for these loads. A comparison of measured data and computed data is made in Section 4. Buckling is considered for the stacking load in Section 5 and Section 6 contains the results and conclusions obtained from this numerical study.

2. COMPUTER MODEL

a. Description of Shelter

A general view of a 3-for-1 expandable shelter is shown in Figure 1. The major structural components of the shelter are aluminum beams and paper honeycomb core

¹ANSI MH 5.1-1971, "Basic Requirements for Cargo Containers," November 18, 1971.

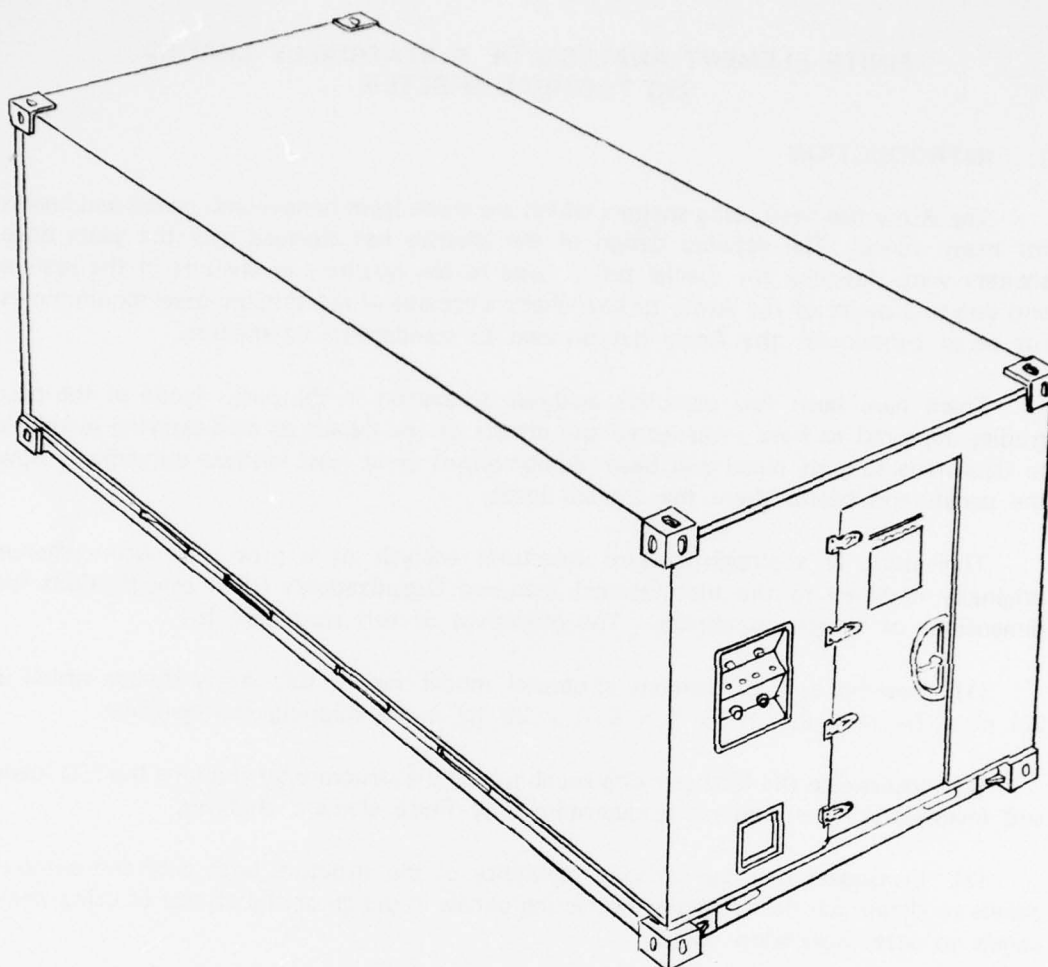


FIGURE 1. GENERAL VIEW OF A 2.4m X 2.4m X 6.1m ISO ARMY SHELTER

sandwich panels with aluminum facings. An expanded view with the major component breakdown for structural components in the shelter is given in Figure 2. It is not obvious in Figure 2 that major load-carrying aluminum beams are built into the edges of the panels shown, but this information is detailed below. Also, there is a hinge connection between the fixed roof and the foldout expandable roof which acts as a side wall in the shipping configuration and the foldout roof is not connected to the floor when the shelter is in the shipping configuration.

When the shelter is tested for static loads the major load-carrying elements are those shown in Figure 3. It is assumed that the foldout end walls, side walls, and floors contribute little to the static load-carrying ability of the shelter through their hinge-type connections to the structural components shown in Figure 3. Also, although the door frames are considered as structural members, the doors are not, so this report contains the structural response without including any structural interaction which may occur between the door frames and the doors.

b. Finite Elements Used

A Government version (level 15.5.0) of the NASTRAN finite element program was used for this analysis. Thus, the elements chosen for the analysis were taken from the family of elements available in this version of NASTRAN. Since the shelter is made from beams and sandwich plates the choice of elements was dictated by the problem. This was true because there is only one type of beam element and only one type of sandwich plate element available in this version of NASTRAN. Modeling of hinges required the use of scalar spring elements. Thus, a beam element, a sandwich plate element, and a scalar spring element was considered a sufficient variety for modeling the static behavior of the 3-for-1 shelter. A short description of the beam and plate elements follows. Detailed information is available in the "NASTRAN Theoretical Manual."²

(1) Beam Element

The standard straight beam element was used. It allows for a cubic interpolation of the transverse displacement field associated with bending, a linear interpolation of the axial displacement, and transverse shear and torsion displacements are treated with linear interpolation in the beam. The element coordinates are the three displacements and three rotations at each end of the beam. Bending is allowed in two orthogonal planes.

(2) Sandwich Plate Element

Triangular Element: The transverse displacement is interpolated with an incomplete bicubic polynomial whose coefficients are the generalized coordinates.

² Richard H. MacNeal, "The NASTRAN Theoretical Manual (Level 15)," COSMIC, University of Georgia, Georgia, April 1972.

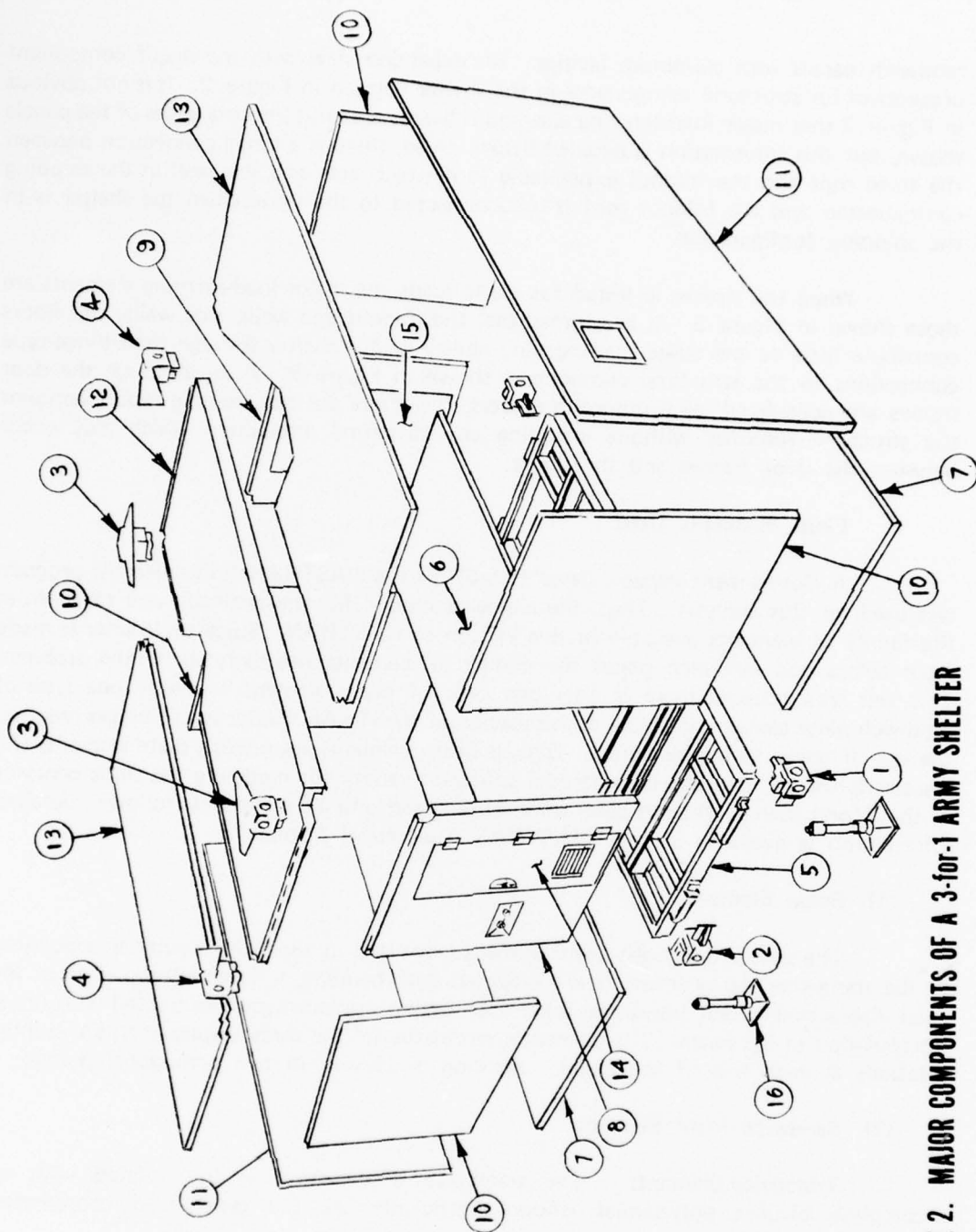


FIGURE 2. MAJOR COMPONENTS OF A 3-for-1 ARMY SHELTER

3 for 1

MAJOR SUBASSEMBLIES

<u>ITEM</u>	<u>DESCRIPTION</u>
1	ISO FITTING - LOWER R. H. (Two)
2	ISO FITTING - LOWER L. H. (Two)
3	ISO FITTING - UPPER R. H. (Two)
4	ISO FITTING - UPPER L. H. (Two)
5	FRAME
6	FLOOR PANEL
7	HINGED FLOOR PANEL
8	FIXED END PANEL - PERSONNEL DOOR
9	FIXED END PANEL - CARGO DOOR
10	HINGED END PANEL
11	HINGED SIDE PANEL
12	FIXED ROOF PANEL
13	HINGED ROOF PANEL
14	DOOR - PERSONNEL
15	DOOR - CARGO
16	JACK

**FIGURE 2. MAJOR COMPONENTS OF A 3 FOR 1 ARMY SHELTER
(CONTINUED)**

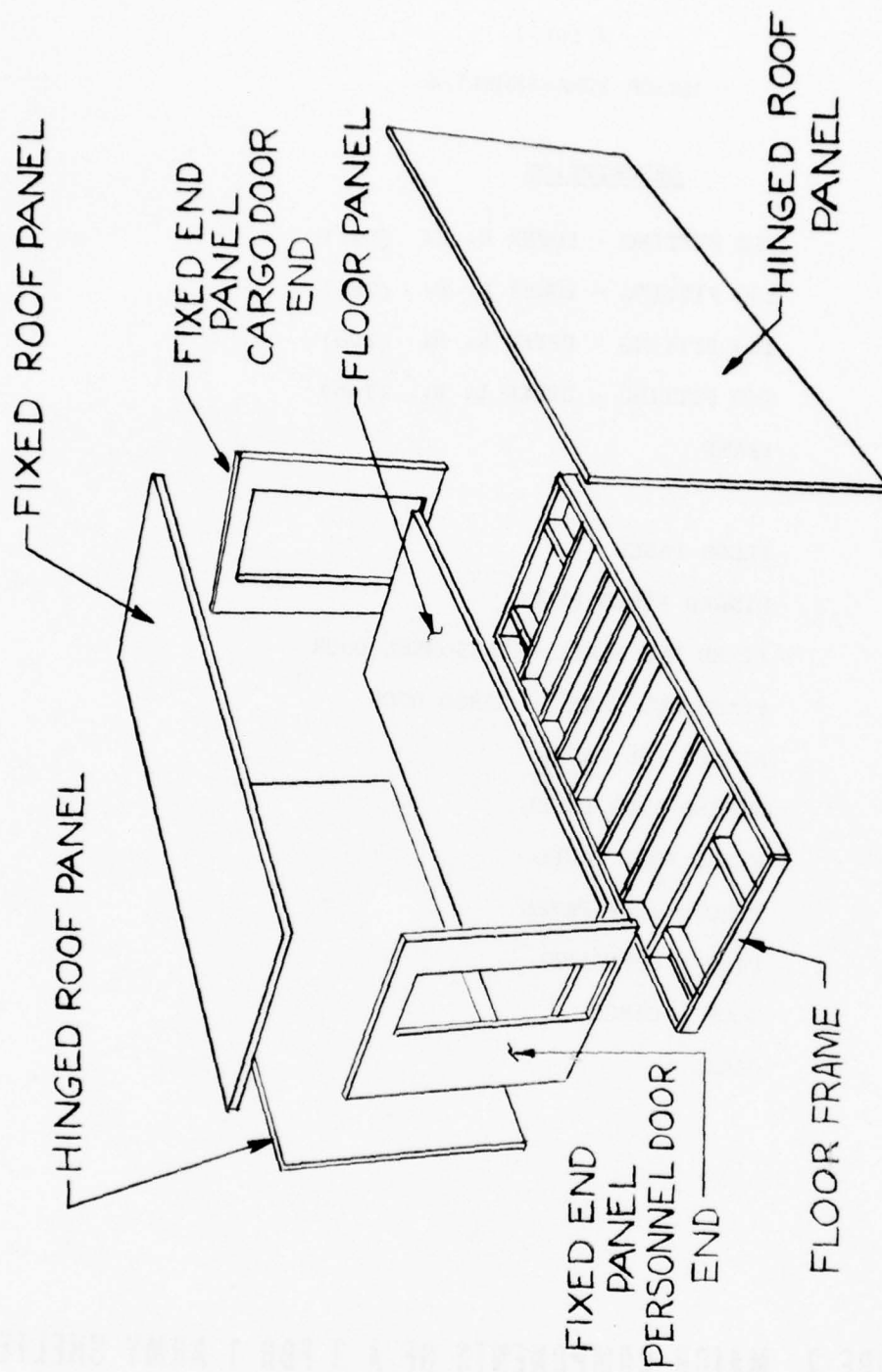


FIGURE 3. COMPONENTS OF 3-for-1 SHELTER USED FOR STATIC ANALYSIS

Computation of stiffness for bending and transverse shear is accomplished by expressing the element's potential energy as a function of bending moments, curvatures, shear forces, and shear strains. The material stress-strain laws and the equilibrium equations are used to obtain the moments and shear forces in terms of the material properties and strains. The incomplete bicubic polynomial and the relation between the shear strains, slopes, and rotations are used to compute the strains and curvatures as a function of the generalized coordinates. The stiffness is then computed relative to these generalized coordinates by integration. Finally, the transformation between the element coordinates and the generalized coordinates is used to obtain the stiffness matrix in terms of the nodal coordinates.

Quadrilateral Element: The stiffness matrix is computed by locating a median plane midway between the diagonals of the intended quadrilateral. A new quadrilateral made by projecting the four sides of the original intended quadrilateral (the original four points may not be in a plane) onto the median plane is used to compute the element stiffness matrix. One diagonal is used to divide this new quadrilateral into two triangles. The stiffness matrices of these triangles are then computed, as stated above, with respect to the degrees of freedom at the nodes of the quadrilateral. This process is repeated for the other diagonal. The triangular stiffness matrices are then weighted by $1/2$ and added to yield the quadrilateral stiffness matrix.

c. Finite Element Mesh

A skelton view of the shelter and the direction of the axes of the global coordinates is shown in Figure 4. Figures 5, 6, and 7 are detailed transverse, longitudinal, and plan sectional views of the structural components to be modeled with the finite elements. At first sight it is noticed that the shelter would require an extremely large number of elements, degrees of freedom, and special constraints if some lumping of the structural elements is not done before discretizing the structure. Thus, the following assumptions were made:

(1) Details of the floor plate and supporting beam interaction will not be sought in this analysis. The fact that the longitudinal spacing between the transverse beams under the floor is such that sandwich plate theory is not even a valid method of analysis for these plates justifies not adding degrees of freedom to more accurately approximate an invalid answer. However, it is hoped (not proved here) that choosing a mesh which should give a description of the floor's bending behavior as a large rectangular plate without the beams supporting it will be sufficiently fine for modeling the floor plate and beams as a major structural component of the 3-for-1 shelter. Thus, a fine mesh for the floor plate (to obtain floor plate data valid between the floor beams) was not made.

(2) Extrusions in the roof, end walls, and side walls that abut and bolt together in the shipping configuration are assumed to be one composite beam. This reduces the modeling effort by eliminating the requirement for special constraints which properly connect the degrees of freedom of two separate beams to represent the structural behavior of the bolted beams that may slide on each other.

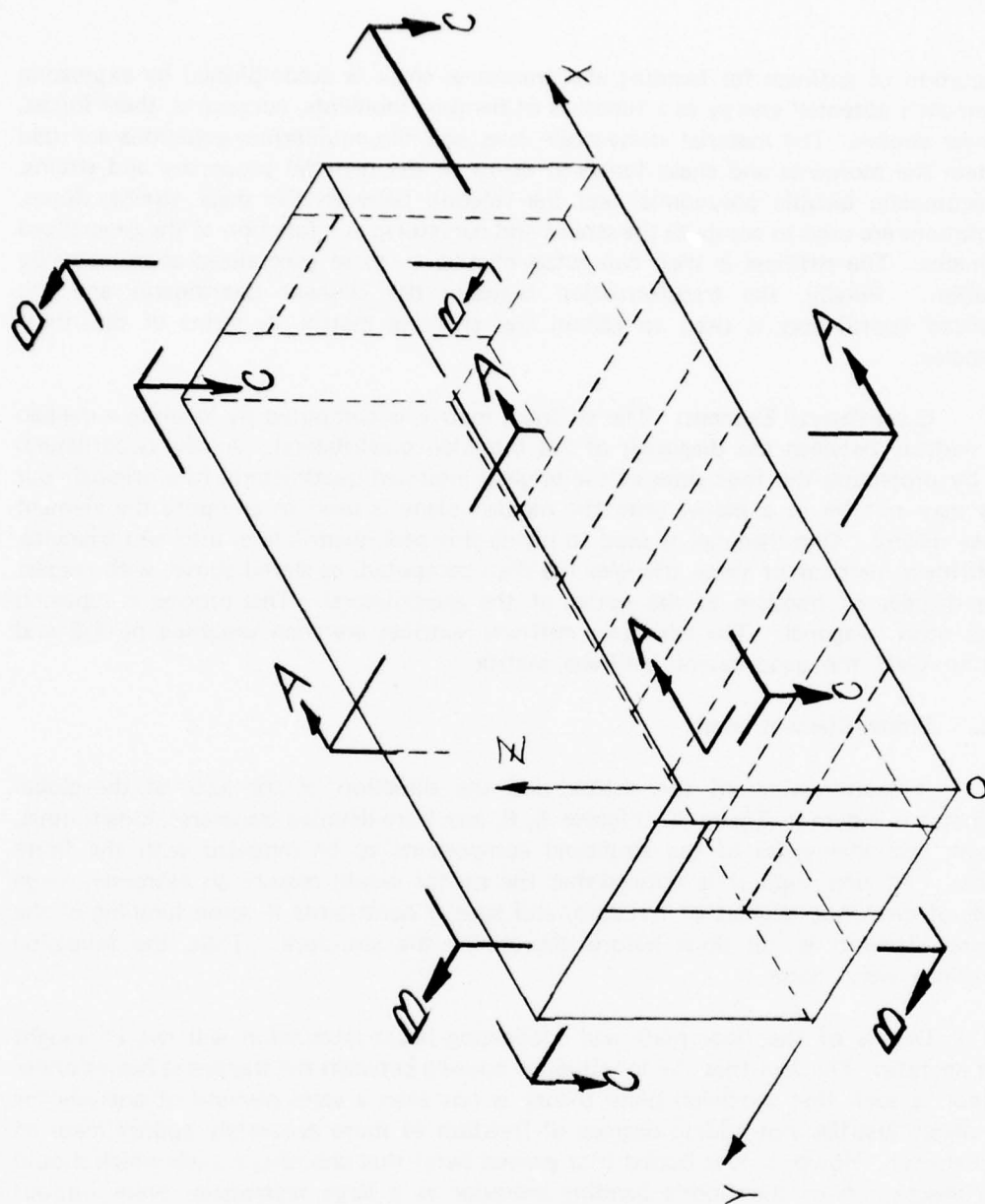


FIGURE 4. GLOBAL COORDINATE SYSTEM AND SKELETON VIEW OF MODEL FOR STATIC ANALYSIS

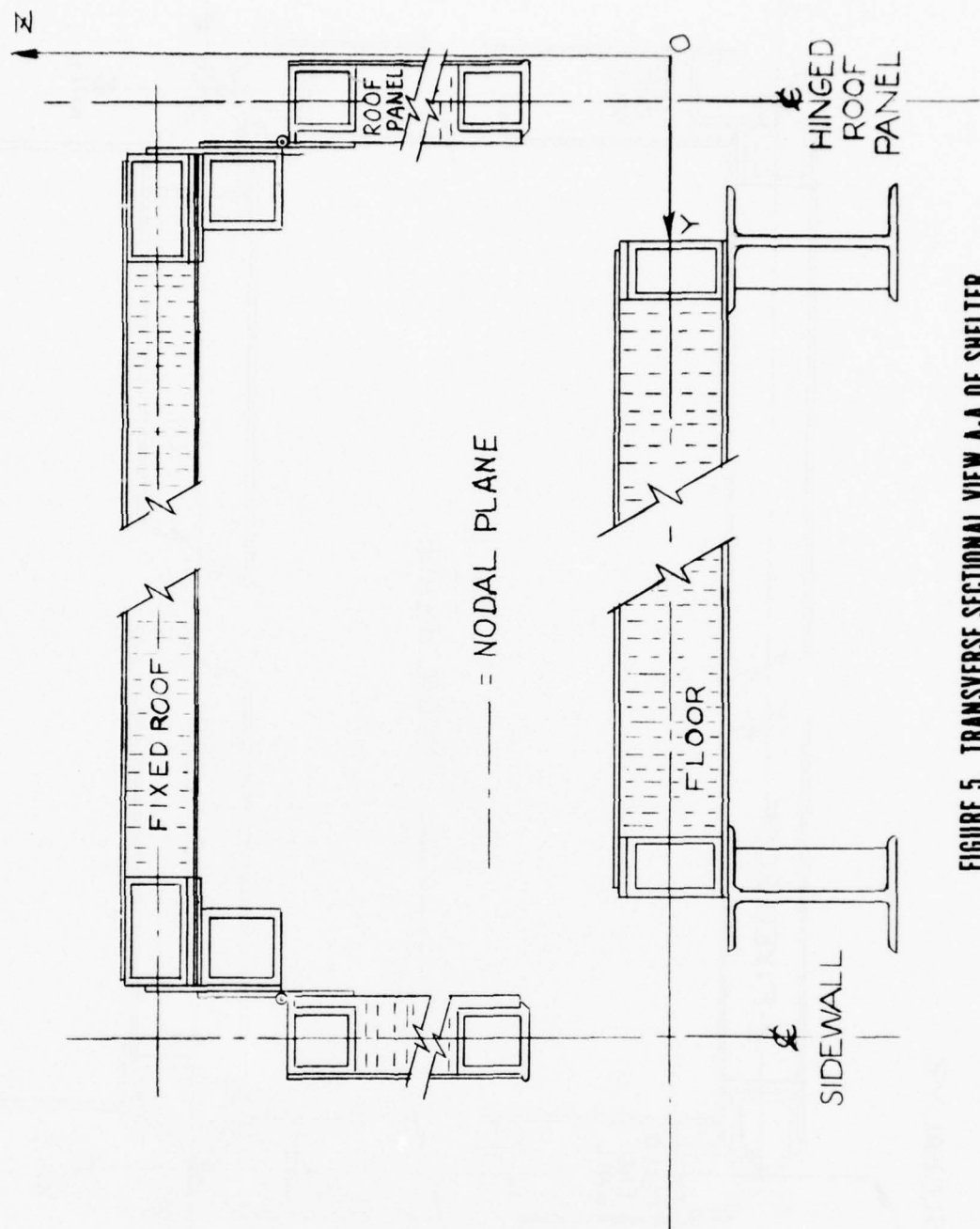


FIGURE 5. TRANSVERSE SECTIONAL VIEW A-A OF SHELTER.

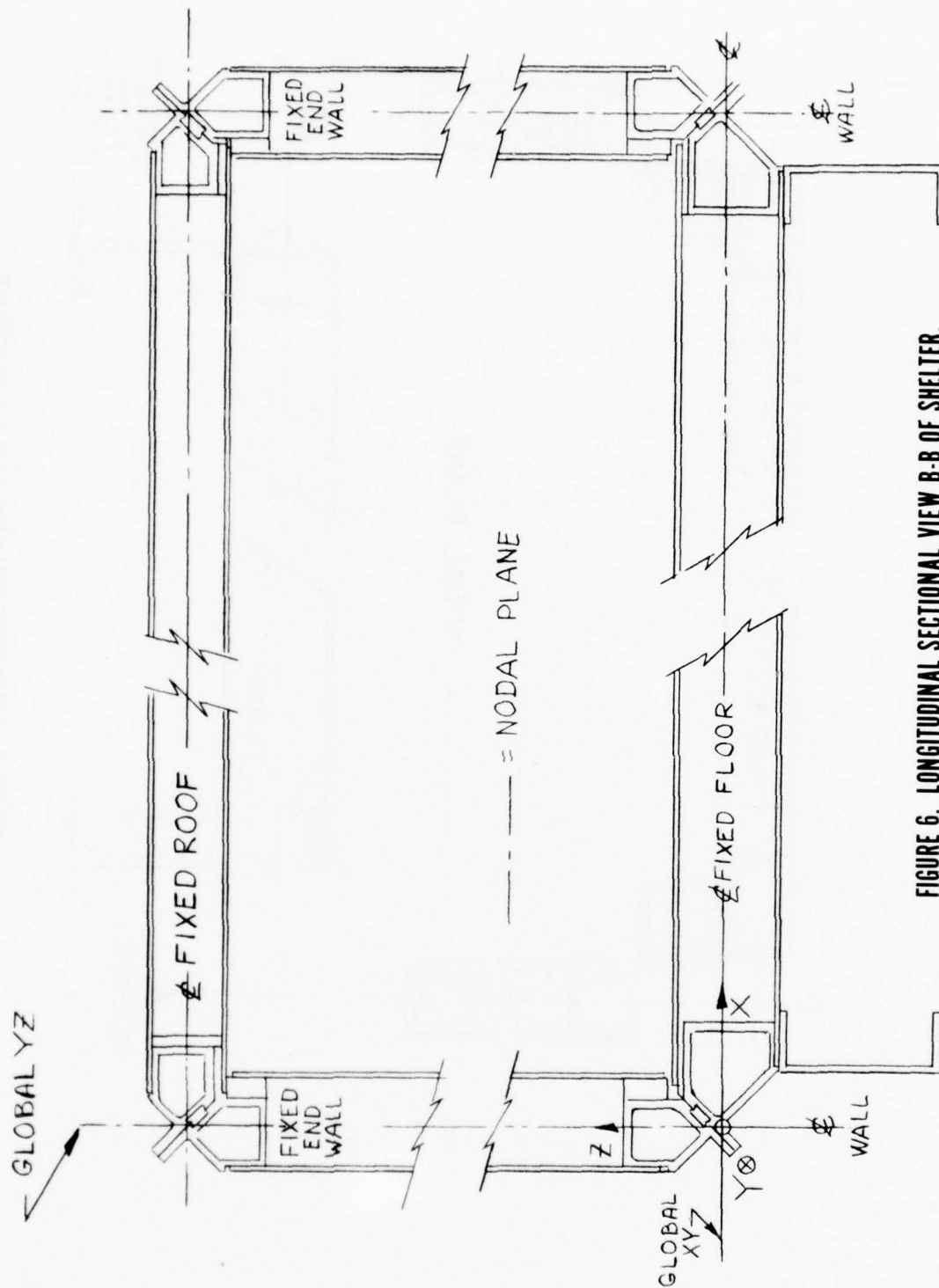


FIGURE 6. LONGITUDINAL SECTIONAL VIEW B-B OF SHELTER.

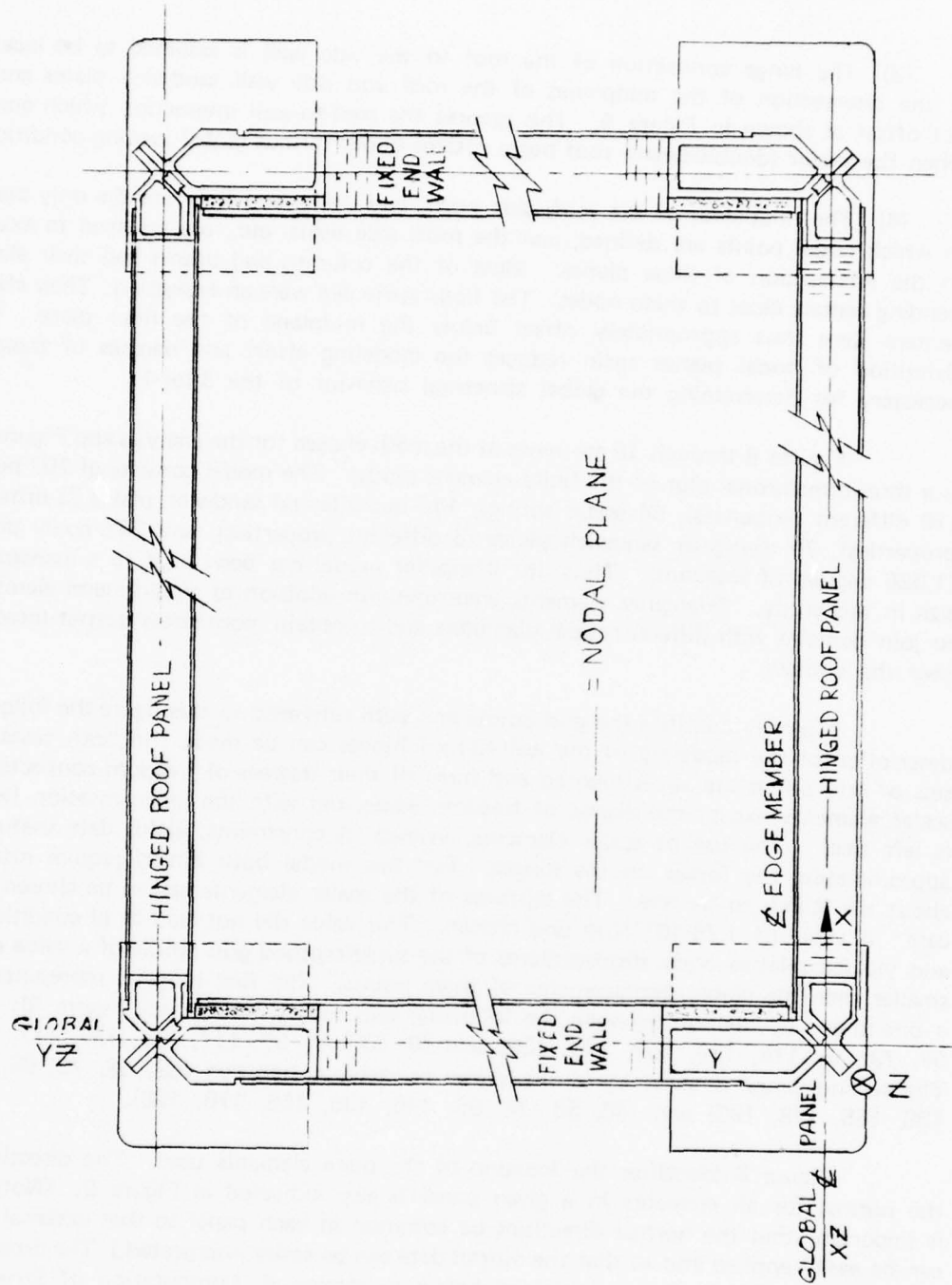


FIGURE 7. PLAN SECTIONAL VIEW C-C OF SHELTER.

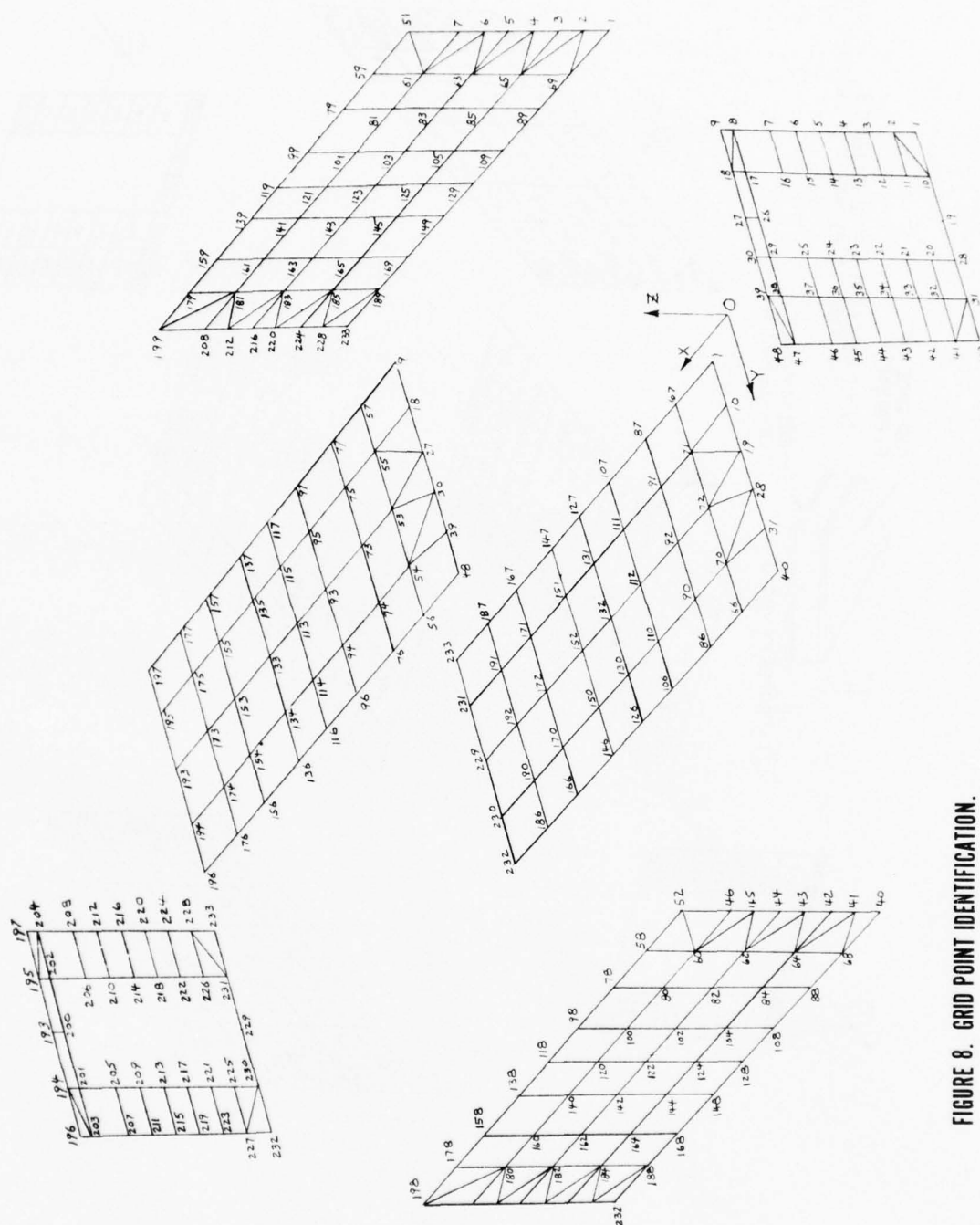
(3) The hinge connection of the roof to the side wall is assumed to be located at the intersection of the midplanes of the roof and side wall sandwich plates and is not offset as shown in Figure 5. This ignores the roof-to-wall interaction which occurs when the major (double-beam) roof beam rotates under various global loading conditions.

(4) The midplanes of the roof, side walls, end walls, and floor are the only planes in which nodal points are defined, and the roof, side walls, etc., are assumed to extend to the intersection of these planes. Most of the columns and beams had their elastic bending centers close to these nodes. The floor stiffeners were an exception. Their elastic centers were thus appropriately offset below the midplane of the floor plate. This definition of nodal planes again reduces the modeling effort and degrees of freedom necessary for determining the global structural behavior of the 3-for-1.

Figures 8 through 10 are views of the mesh chosen for the analysis and Figure 11 is a three-dimensional plot of the finite element model. The model consists of 207 beams (10 different properties), 54 scalar springs, 144 quadrilateral sandwich plates (3 different properties), 70 triangular sandwich plates (3 different properties), and 231 nodal points (1,386 degrees of freedom). Thus, the computer model has been kept to a manageable size in this study. Triangular elements were used (in addition to quadrilateral elements) to join domains with different mesh diameters and to obtain more stress output locations near the corners.

Figure 8 identifies the grid points and with reference to this figure the following description of the modeling of the wall-to-roof hinges can be made. In both cases two sets of grid points are superimposed and have all their degrees of freedom connected by scalar elements except the degree of freedom associated with the hinge rotation (which is left free). The use of scalar elements, instead of constraints, yields data useful for approximating the forces on the hinges. For this model both hinges require rotation about the X-axis to be free. The stiffness of the scalar elements had to be chosen with care. A value of $1.75 \cdot 10^{12}$ N/m was chosen. This value did not lead to ill conditioning and yielded relative nodal displacements of the superimposed grid points of a value much smaller than the global displacements of these points. The first hinge is represented by a one-to-one connection between the following two sets of points (see Figure 8): (51, 59, 79, 99, 119, 139, 159, 179, 199) and (9, 57, 77, 97, 117, 137, 157, 177, 197). The second hinge is given by a one-to-one connection between (52, 58, 78, 98, 118, 138, 158, 178, 198) and (48, 56, 76, 96, 116, 136, 156, 176, 196).

Figure 9 identifies the location of the plate elements used. The direction of the normal for all elements in a given panel is also indicated in Figure 9. (Note: It is important that the normal directions be common in each panel so that external loads can be easily applied and so that the output data can be easily interpreted.) The properties referred to in Figure 9 are explained below in section d, Computation of Structural Properties.



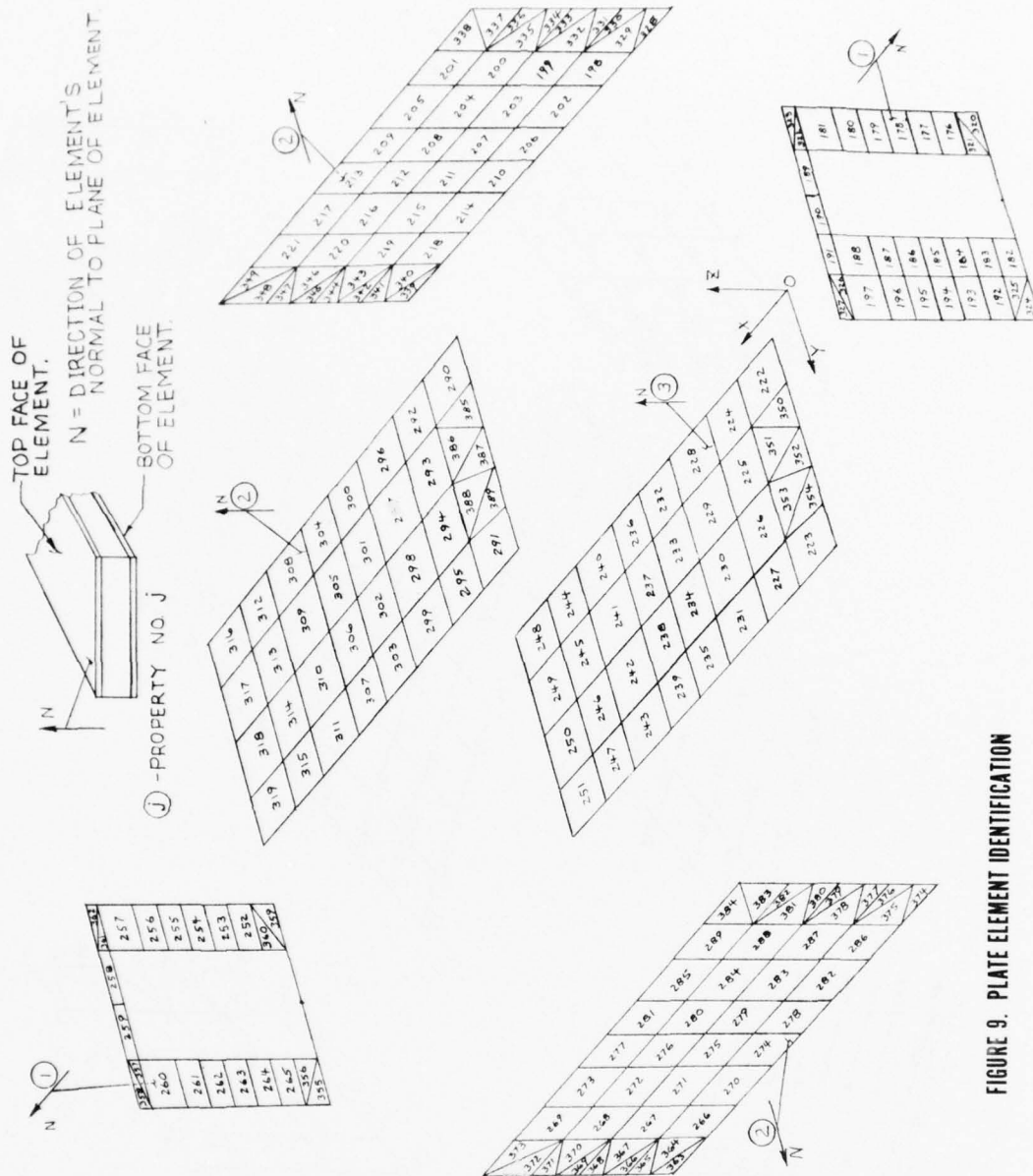


FIGURE 9. PLATE ELEMENT IDENTIFICATION

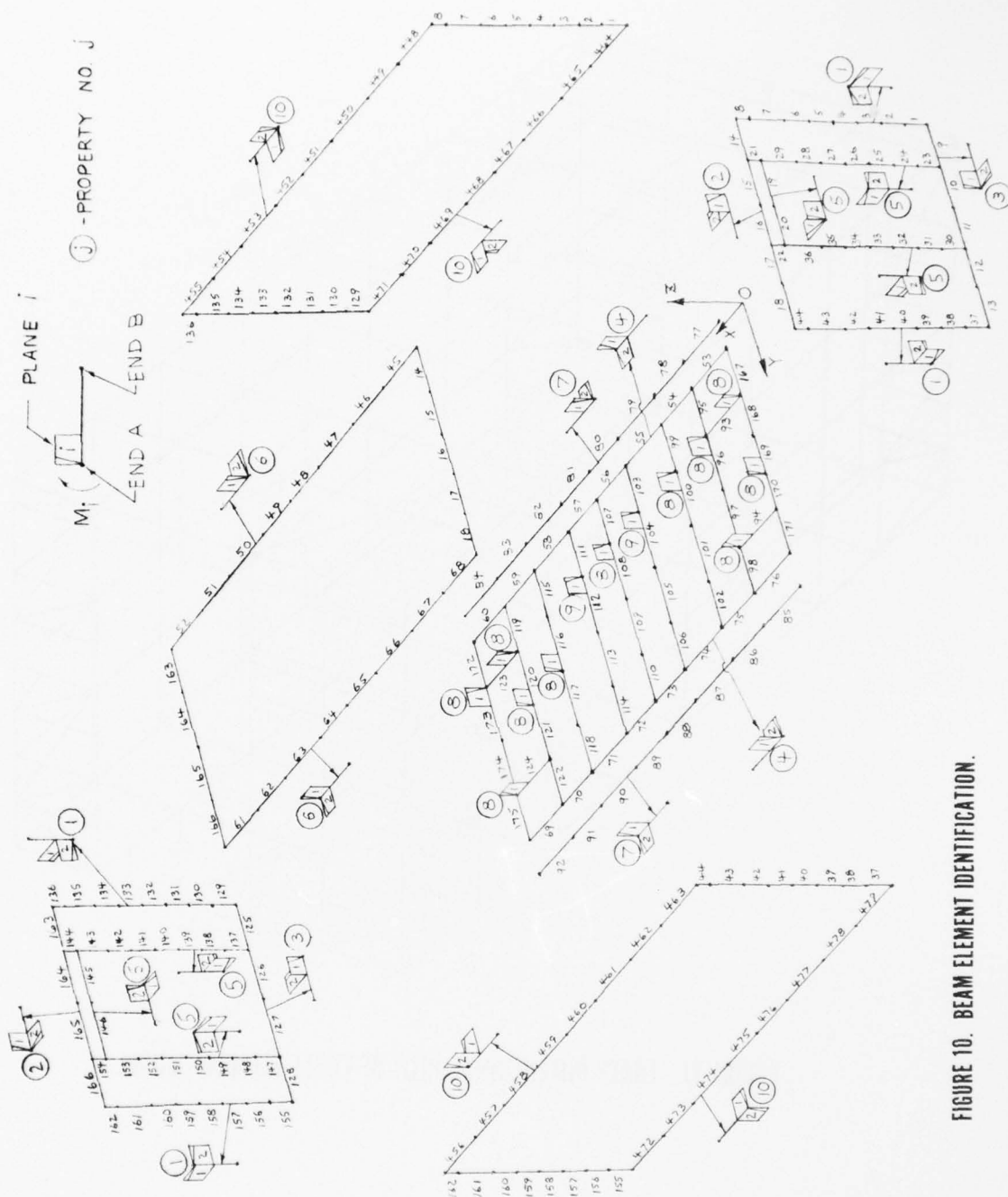


FIGURE 10. BEAM ELEMENT IDENTIFICATION.

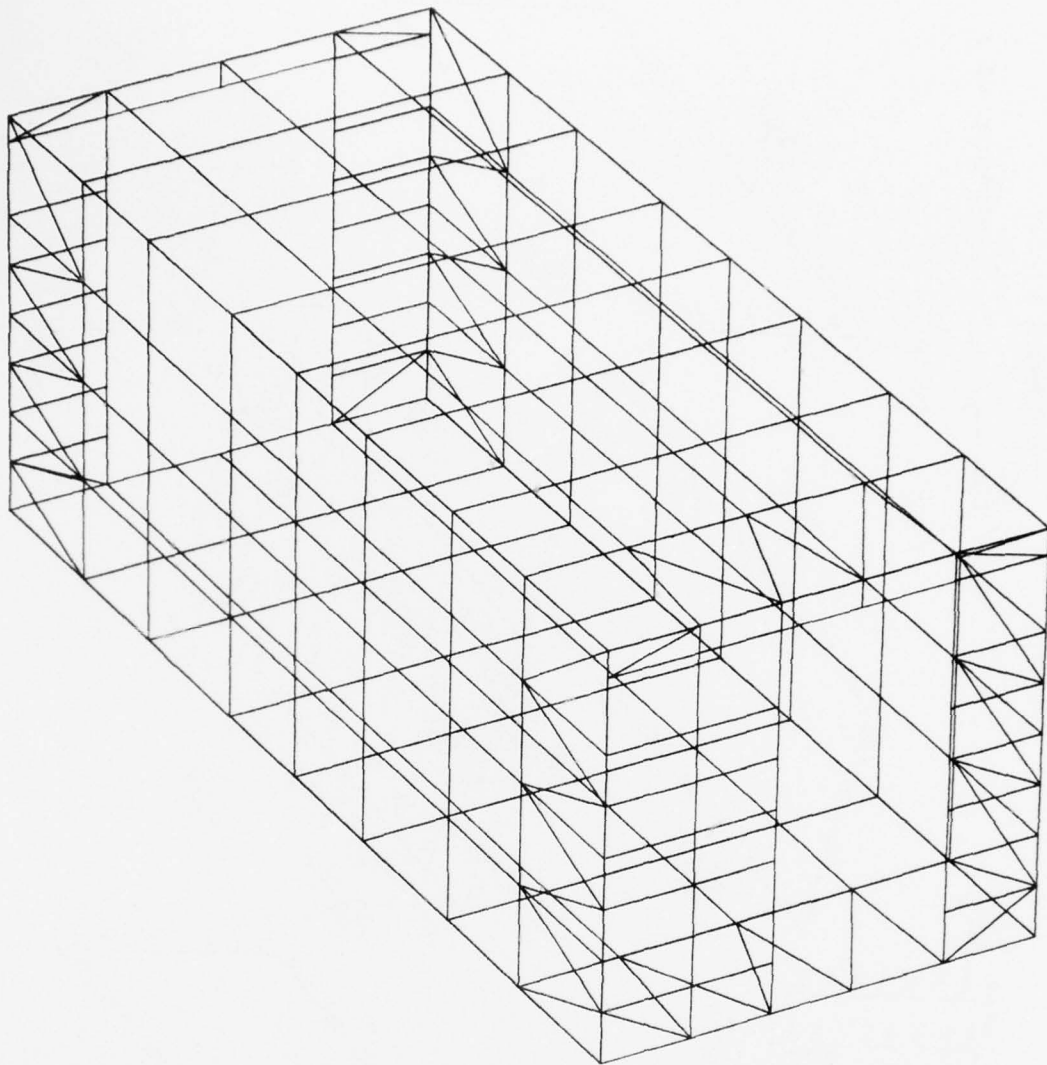


FIGURE 11. THREE DIMENSIONAL PLOT OF FINITE ELEMENT MODEL.

Figure 10 identifies the location of all beam elements used in the analysis. This figure also indicates the two orthogonal bending planes for the elements. The planes are indicated at end A of the beam element. (Note: Data is output for both ends of beam elements, hence the identification of end A and end B in the form given in Figure 8 is important for interpretation of the output data.) The properties referred to in Figure 10 are explained below in section d.

The three-dimensional plot given in Figure 11 is useful for two reasons. First, this plot (made by the computer from the input data deck) is a check on the data deck. Finite element data decks tend to be large and hard to check. A plot of this type indicates that at least the element and grid point data has been input in a form that represents the geometry of the structure. Second, the output data can be compared with the mesh size (in more detailed studies) to evaluate the approximate solution obtained (this process requires mesh refinement).

d. Computation of Structural Properties

One of the objectives of this study is to determine if the panels act as major load-carrying members (or can act as such) when the shelter is statically loaded or if the frame actually supports the load with little help from the panels. A major mechanism for load sharing between the panels and the frame is a load transfer from the frame to the panel in the plane of the panel. Thus, good stiffness properties for the inplane behavior of the panel are required. Since the mesh was sized on the basis of predicting bending behavior a computational study was necessary to verify that the mesh chosen for this analysis was not too stiff to describe the membrane behavior of the panels. The errors associated with using a coarse mesh on membrane problems was clearly shown by Felippa.³ These errors are typically associated both with discretization errors and with improperly chosen mesh layouts.^{4,5} The objective of this computational study on the mesh was to determine a scale factor which could be used to adjust the panel stiffness for the mesh chosen here to be near the panel stiffness of a properly refined mesh. It is assumed that the magnitude of the errors associated with any inconsistencies from the mesh layout are smaller than the errors associated with modeling the shelter as an assembly of beams and panels.

³C. A. Felippa, "Refined Finite Element Analysis of Linear and Nonlinear Two-Dimensional Structures," Department of Civil Engineering, University of California, Berkeley, Report 66-22, October 1966.

⁴V. Dunder and S. Ridlon, "Practical Applications of Finite Element Method," Vol 104, No. ST1, ASCE Structural Division, January 1978, pp 9-21.

⁵J. E. Walz, R. E. Fulton, and N. J. Cyrus, "Accuracy and Convergence of Finite Element Approximations," Proceedings of the Second Conference on Matrix Methods in Structural Mechanics, NTIS, December 1968.

The computational mesh study considered a 2.4 m x 2.4 m honeycomb panel. This panel represents an end wall. The objective was to determine the mesh size necessary to obtain good deflection data for a racking load applied in the form of a parabolic shear load at the top of the panel, as shown in Figure 12, and to use this information to adjust the inplane stiffness of the plate elements to compensate for the coarse mesh. This case was chosen because it closely represents the type of inplane deformation which the beam elements can approximate well but the inplane constant strain plate elements cannot approximate well. The panel used was 6.35 cm thick with 0.102 cm thick aluminum skin and 56 kg/m³ paper honeycomb core. A computer program was written to automatically generate a data deck for NASTRAN. The program was general enough so that any number of divisions along the width and height could be chosen. The program also computed the consistent load vector associated with the parabolic shear load for the given mesh. A systematic variation of the mesh was then used to obtain the data shown in Figure 13 and Table 1.

The actual mesh is nonuniform and has cut-out areas for doors. A detailed analysis of the problems associated with scaling the nonuniform mesh and treating strain singularities at the cut-out corners is considered beyond the scope of this effort. Further, since other modeling problems cause the analysis to be approximate (lumping the structure to plates and beams) an approximate scale factor which is the average of that associated with nearly uniform meshes will be used. The end wall mesh is about 5 horizontal elements by 7 vertical elements. This mesh falls between the 4 x 6 and 6 x 8 cases in Table 1. The scale factor chosen was 1.2 which is the average of the four values in Table 1 for the 4 x 6 and 6 x 8 cases. Thus, the inplane stiffness of the plates was multiplied by $1.0/1.2 = 0.83$ to compensate for the too stiff coarse mesh.

It is important to note that the scaling of the membrane properties requires some extra work when the stress data output by NASTRAN for the plate elements is being used. The procedure for modifying the output stress data can be explained as follows. The output stress data at two points on the plate cross section represents the superposition of bending stresses and a membrane stress. The membrane stress value is incorrect due to the scaled value of the membrane thickness (scaling was done to obtain better stiffness, displacements, and element loads). The bending stresses and the scaled membrane stress must then be separated. The scaled membrane stress should then be corrected by dividing it by the scale factor used above to improve the element's membrane stiffness. Adding the correct membrane stress and the bending stresses yields the desired plate stress data.

There were three different types of sandwich panels used in the shelter. The required structural properties were the membrane thickness of the panel, the transverse shear thickness of the panel associated with the transverse shear modulus, and the moment of inertia of the panel skins associated with bending. These properties were computed by hand and are given in Table 2.

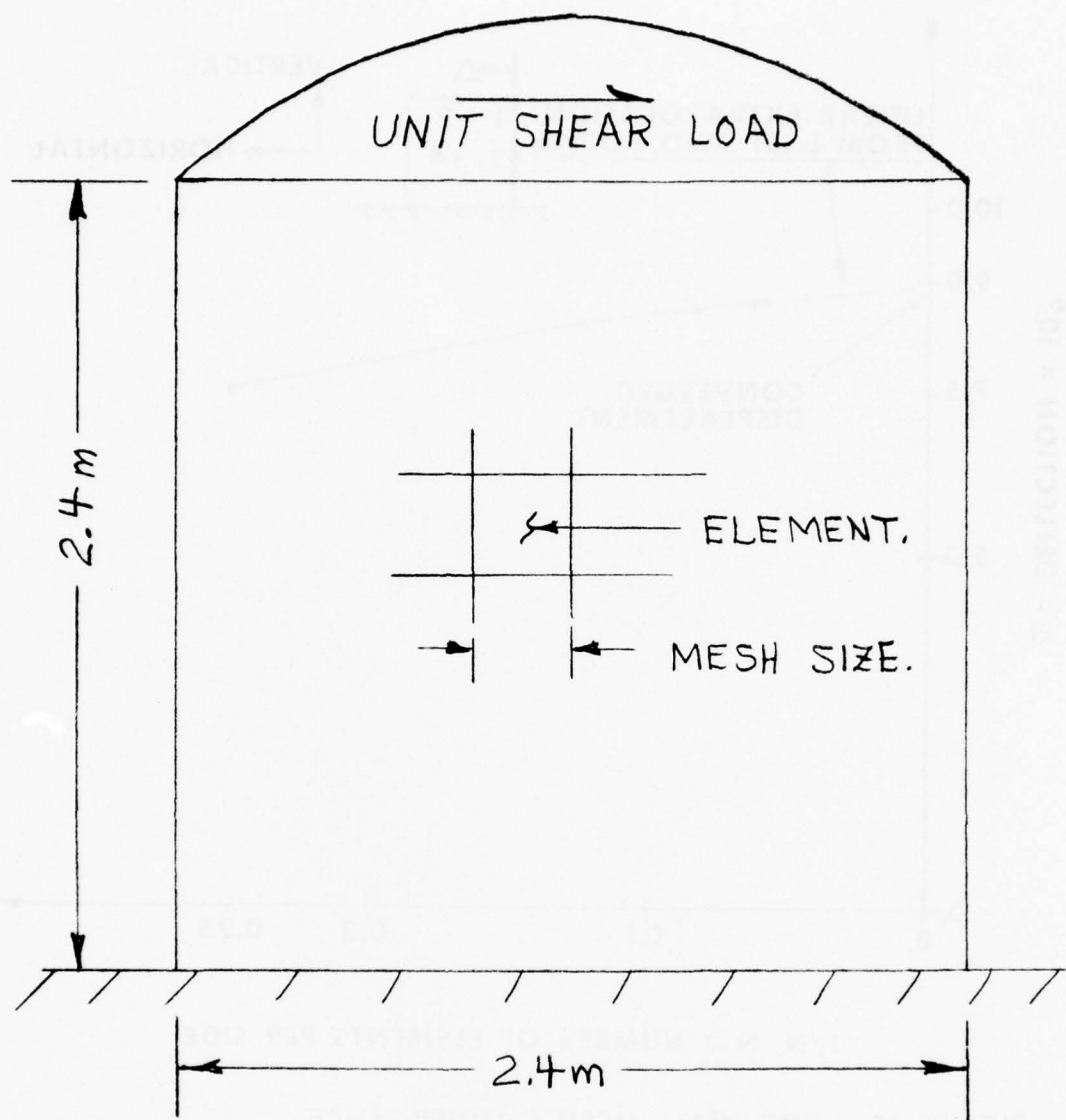


**FIGURE 12. A 2.4m x 2.4m PANEL FIXED AT ONE END
WITH SHEAR LOAD AT OTHER END.**

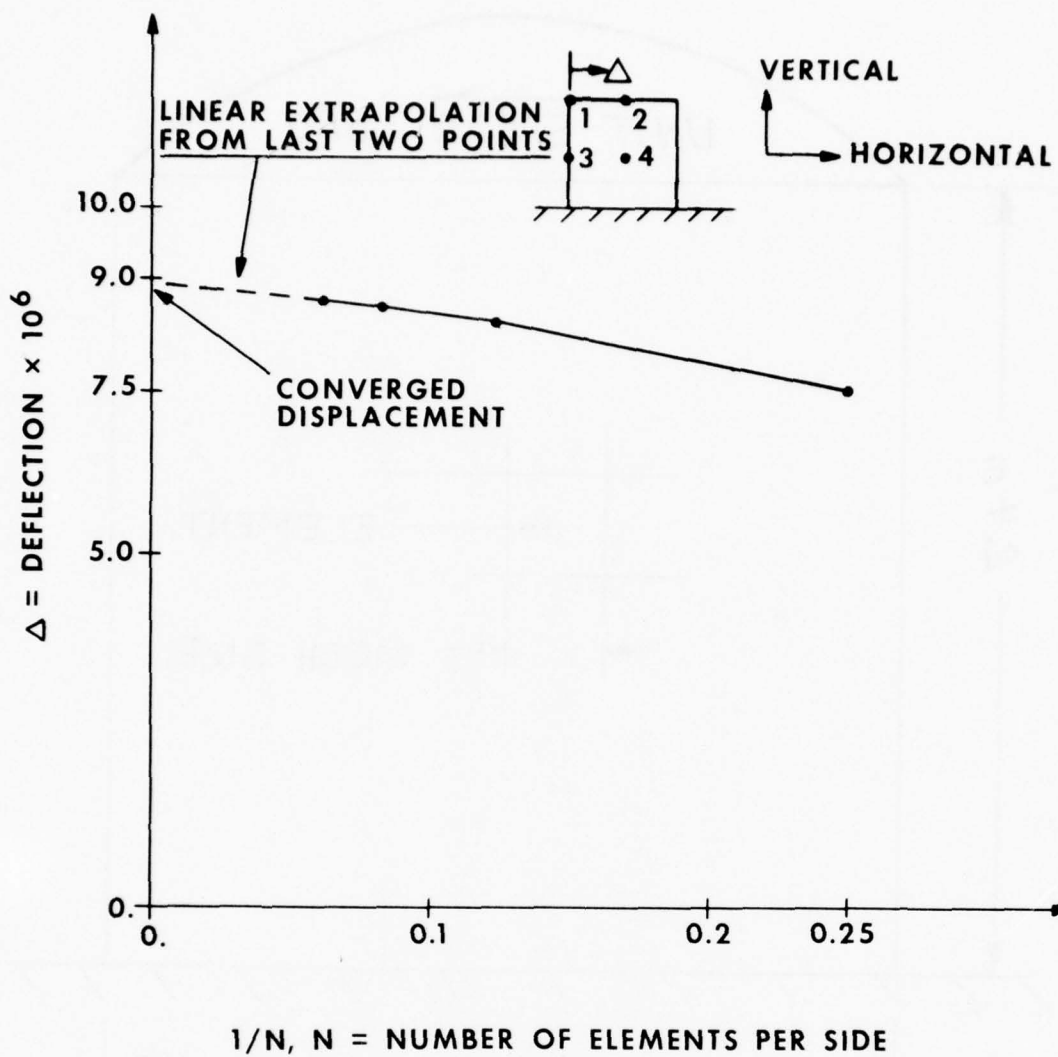


FIGURE 13 END WALL MESH CONVERGENCE
DATA TOP LEFT CORNER ONLY

**TABLE 1. COMPUTED SCALE FACTORS FOR
END WALL IN - PLANE BEHAVIOR.**

MESH SIZE NO. WIDTH × NO. HEIGHT	VERTICAL SCALE FACTOR	HORIZONTAL SCALE FACTOR
4 × 4	1.32	1.20
8 × 8	1.10	1.08
12 × 12	1.06	1.05
16 × 16	1.04	1.03
4 × 6	1.27	1.17
6 × 8	1.14	1.10

$$\text{SCALE FACTOR} = \frac{\text{CONVERGED DISPLACEMENT}}{\text{DISPLACEMENT AT LISTED MESH SIZE}}$$

SCALE FACTORS LISTED ABOVE ARE AVERAGES FOR
POINTS 1 THROUGH 4 SHOWN IN FIGURE 18.

**TABLE 2. PHYSICAL PROPERTIES FOR
PLATE ELEMENTS**

PROPERTY NO. ITEM	1	2	3
MEMBRANE THICK- NESS SCALED CM	0.169	0.169	0.211
MOMENT OF INERTIA CM ⁴	5.37	3.46	9.68
TRANSVERSE SHEAR THICKNESS CM	6.35	5.08	7.62
BENDING AND STRET- CHING MODULUS PA	$6.89 \cdot 10^7$	$6.89 \cdot 10^7$	$6.89 \cdot 10^7$
MODULUS FOR TRANSVERSE SHEAR PA	$1.03 \cdot 10^5$	$1.03 \cdot 10^5$	$1.03 \cdot 10^5$

The extrusions used in the shelter being modeled were special and their geometric properties were not available. Thus it was necessary to compute their properties. Since there were ten combinations of these extrusions and since they were not simple I-beams, a FORTRAN program was written to compute their properties. The program required that the beams be divided into rectangular sections. The length, width, location of center of gravity and angle of inclination was input for each rectangular portion of the beam and a program performed the trivial computations obtaining the location of the neutral axes and the beam geometric properties. The ten beam sections used and their properties are given in Figures 14 through 23. Note: In Figures 14 through 23 the value, I , indicates the moment of inertia about the 1-axis. This value of inertia is used for bending in plane-1 for the beam as indicated in Figure 10. The location of any beam in the structure can be found by using Figure 10, and 14 through 23.

Note: The details of the beams and panels necessary for the above computations were taken from a preliminary set of drawings. These drawings represent the only drawings available for the particular prototype shelter being studied here. The beam properties may be in slight error due to (a) the approximation of the beam cross sections as a group of rectangles (ignoring curved fillets), and (b) the lack of an available complete data package on the beam cross sections at the time when the computations for beam properties were being verified. Furthermore, beam properties 2, 3, and 5 had significant cross products of inertia which were not included in the analysis.

3. STATIC ANALYSIS

The static load tests given in the "Specification for International (ISO) Freight Containers," reference 1, were divided into nine separate cases. A brief description of each of these loading cases is given below; for more detailed information on the tests see either reference 1 or "Experimental Measurement of Strain and Acceleration Levels in a Rigid Wall Shelter Subjected to Environmental Loadings."⁶ All of these load cases were processed by the NASTRAN finite element program. The data obtained on element forces was used to obtain the results on load paths as indicated below. In order to clearly present the data in a form useable to structural design engineers the standard format for displaying bending moments in frames used by civil engineers is used in this report. Thus, the bending moments are plotted adjacent to the frame members with positive bending moments inducing tension in the outer fibers and positive axial load for tension in the member. Although shear and torsional stiffnesses were included in the frame members the loads associated with shear and torsion were not studied here due to the effort necessary to reduce the data to graphical form. In each case the frame loads are studied both with roof and wall panels and without roof and wall panels. The data plots shown below

⁶F. Barca. "Experimental Measurement of Strain and Acceleration Levels in a Rigid Wall Shelter Subjected to Environmental Loadings," Technical Report TR-79/024-AMEL, US Army Natick Research and Development Command, Natick, MA, 1978.

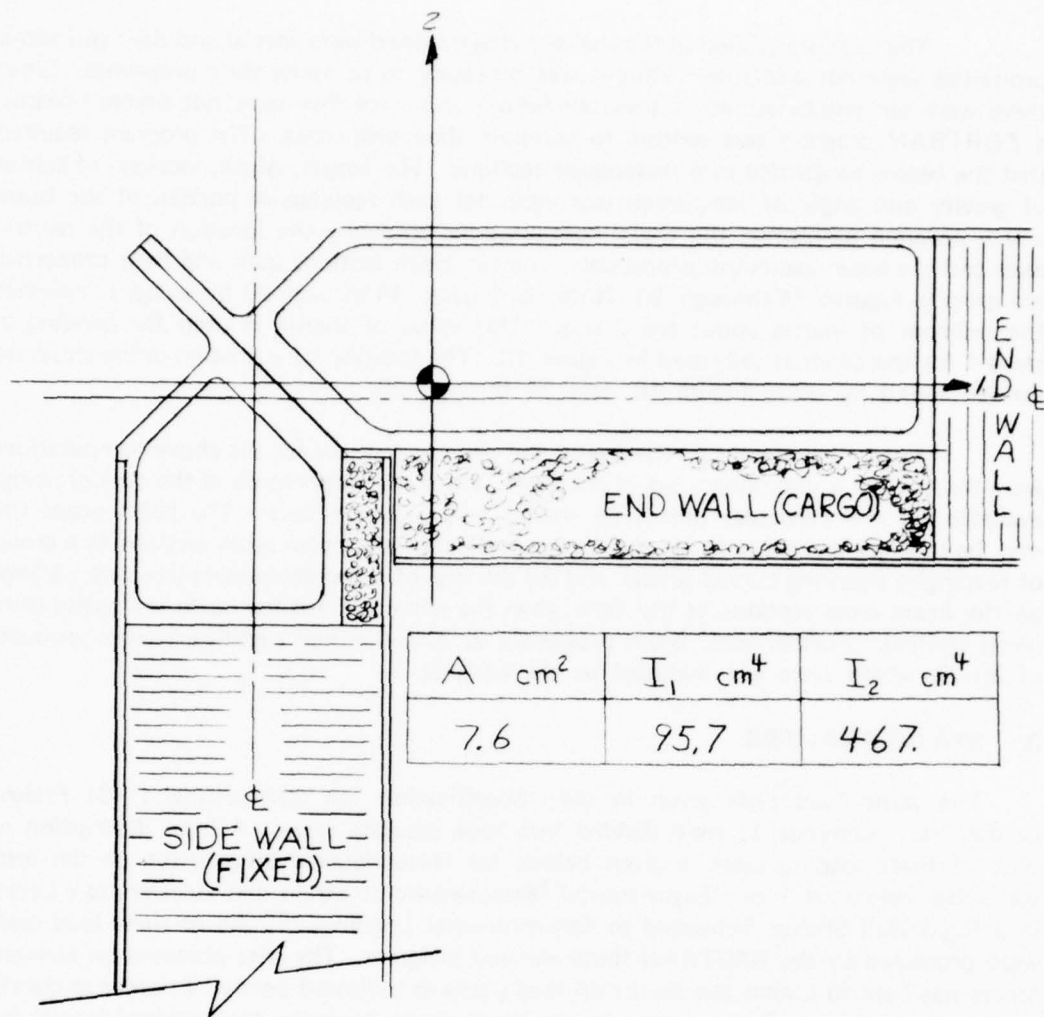
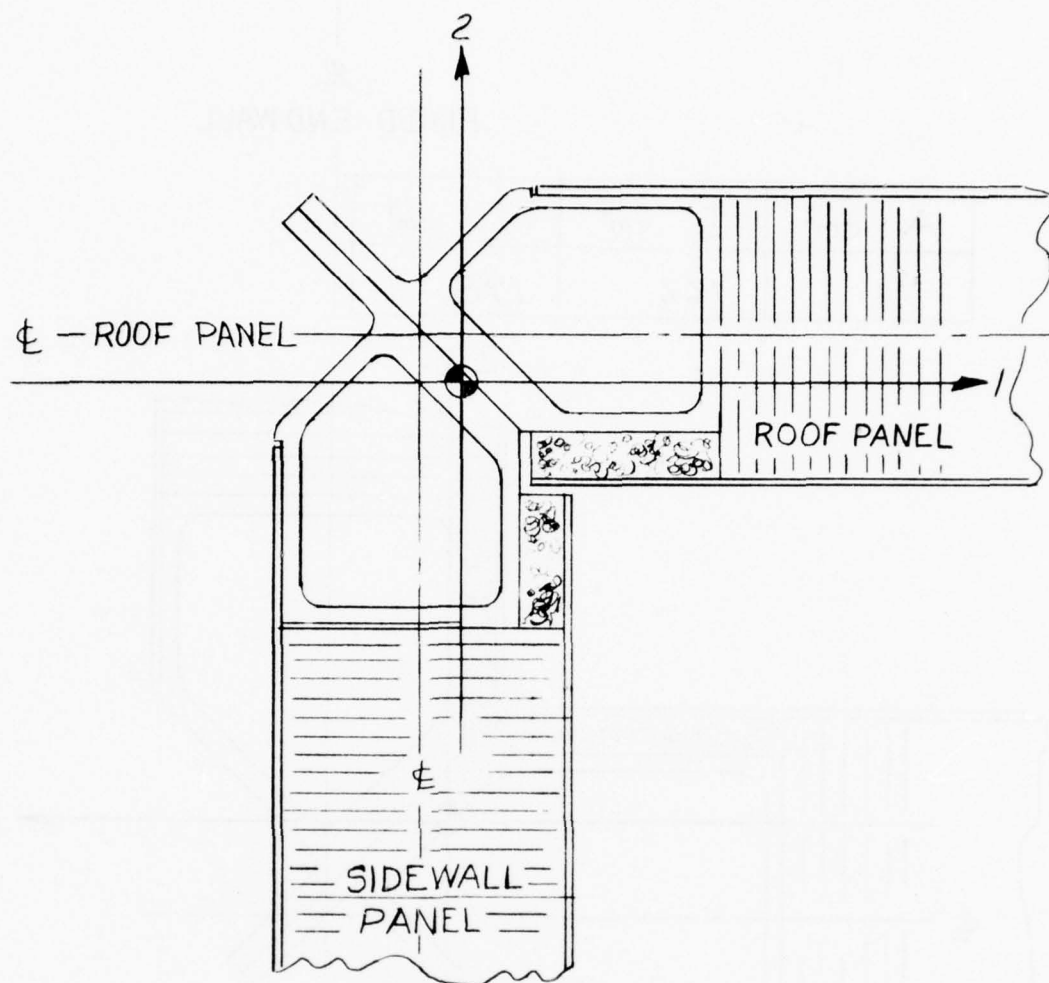


FIGURE 14. BEAM NUMBER 1 PROPERTIES.



$A \text{ cm}^2$	$I_1 \text{ cm}^4$	$I_2 \text{ cm}^4$
5.6	69.9	69.9

FIGURE 15. BEAM NUMBER 2 PROPERTIES.

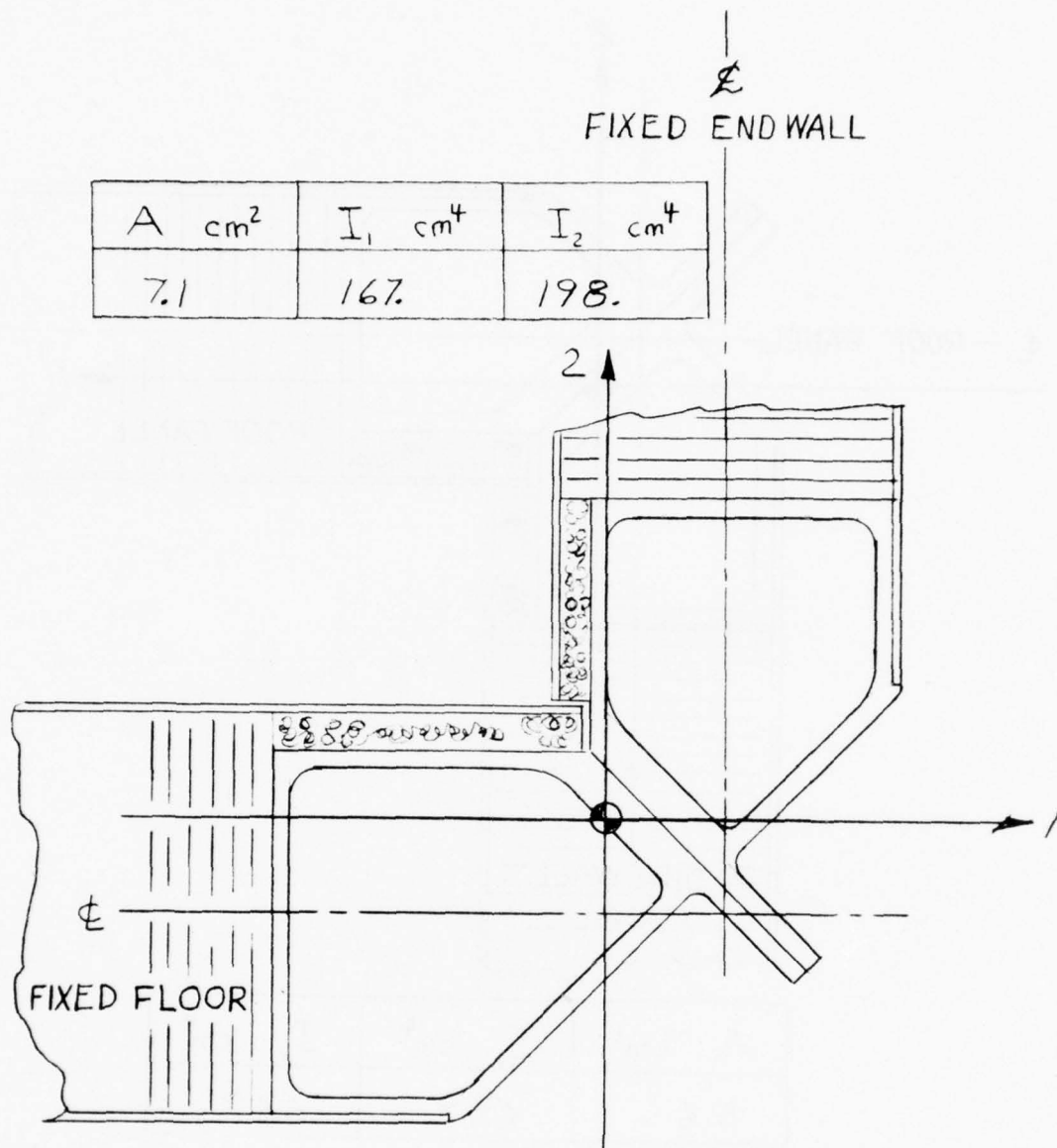
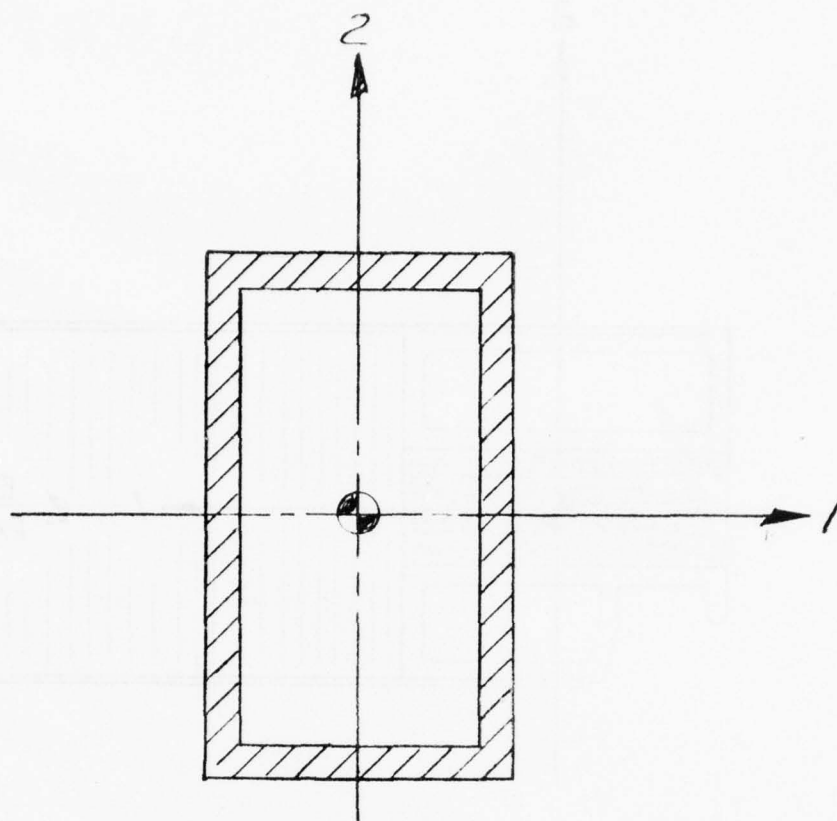
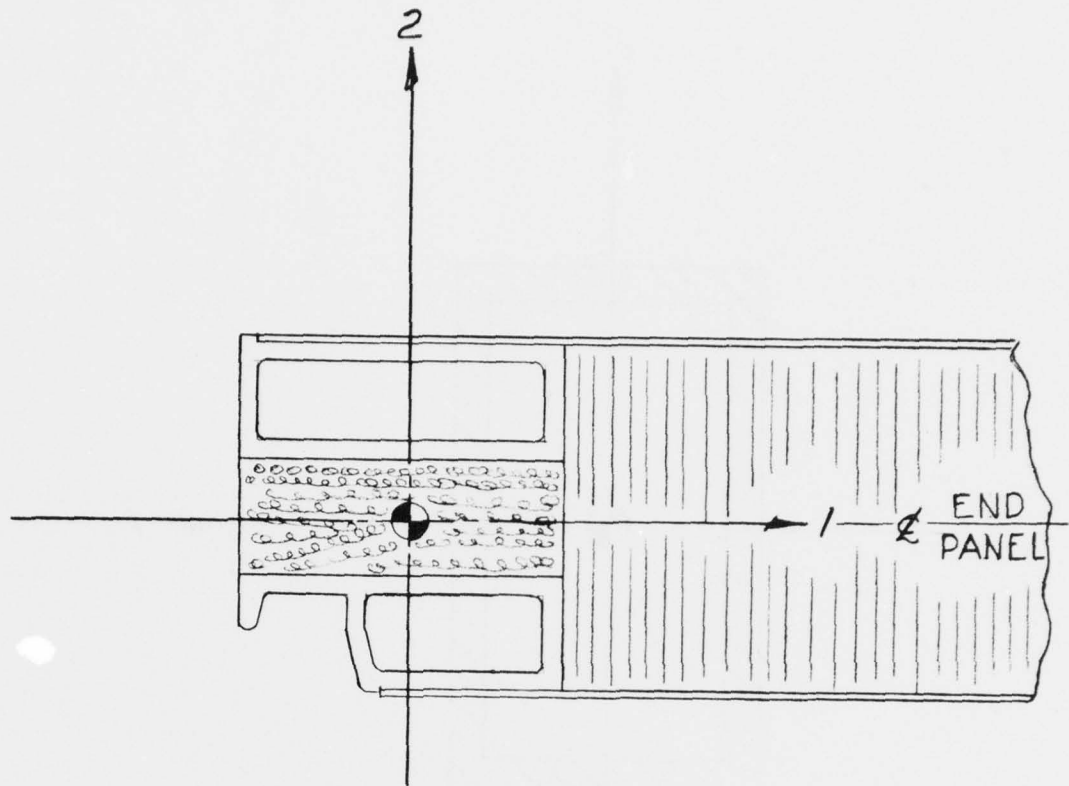


FIGURE 16. BEAM NUMBER 3 PROPERTIES.



$A \text{ cm}^2$	$I_1 \text{ cm}^4$	$I_2 \text{ cm}^4$
4.1	76.6	31.2

FIGURE 17. BEAM NUMBER 4 PROPERTIES.



$A \text{ cm}^2$	$I_1 \text{ cm}^4$	$I_2 \text{ cm}^4$
3.6	45.4	37.5

FIGURE 18. BEAM NUMBER 5 PROPERTIES.

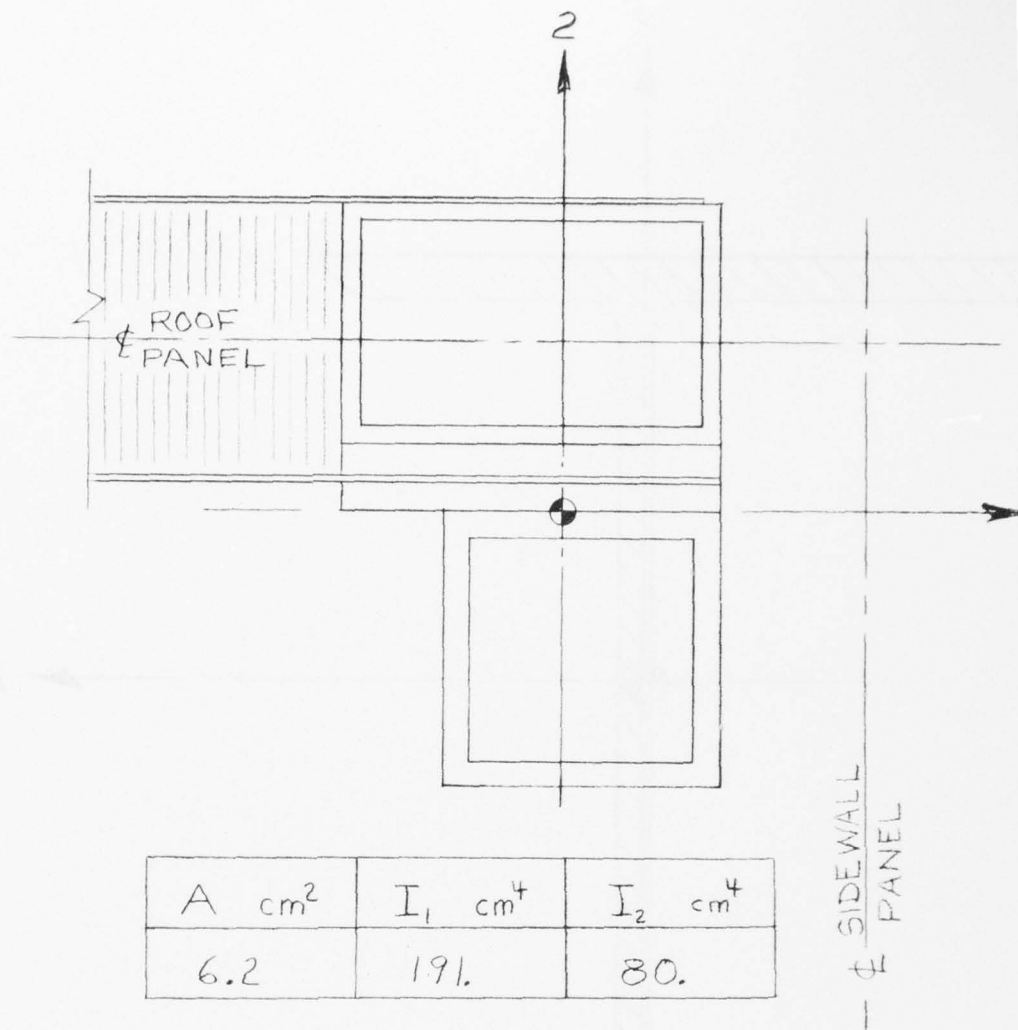
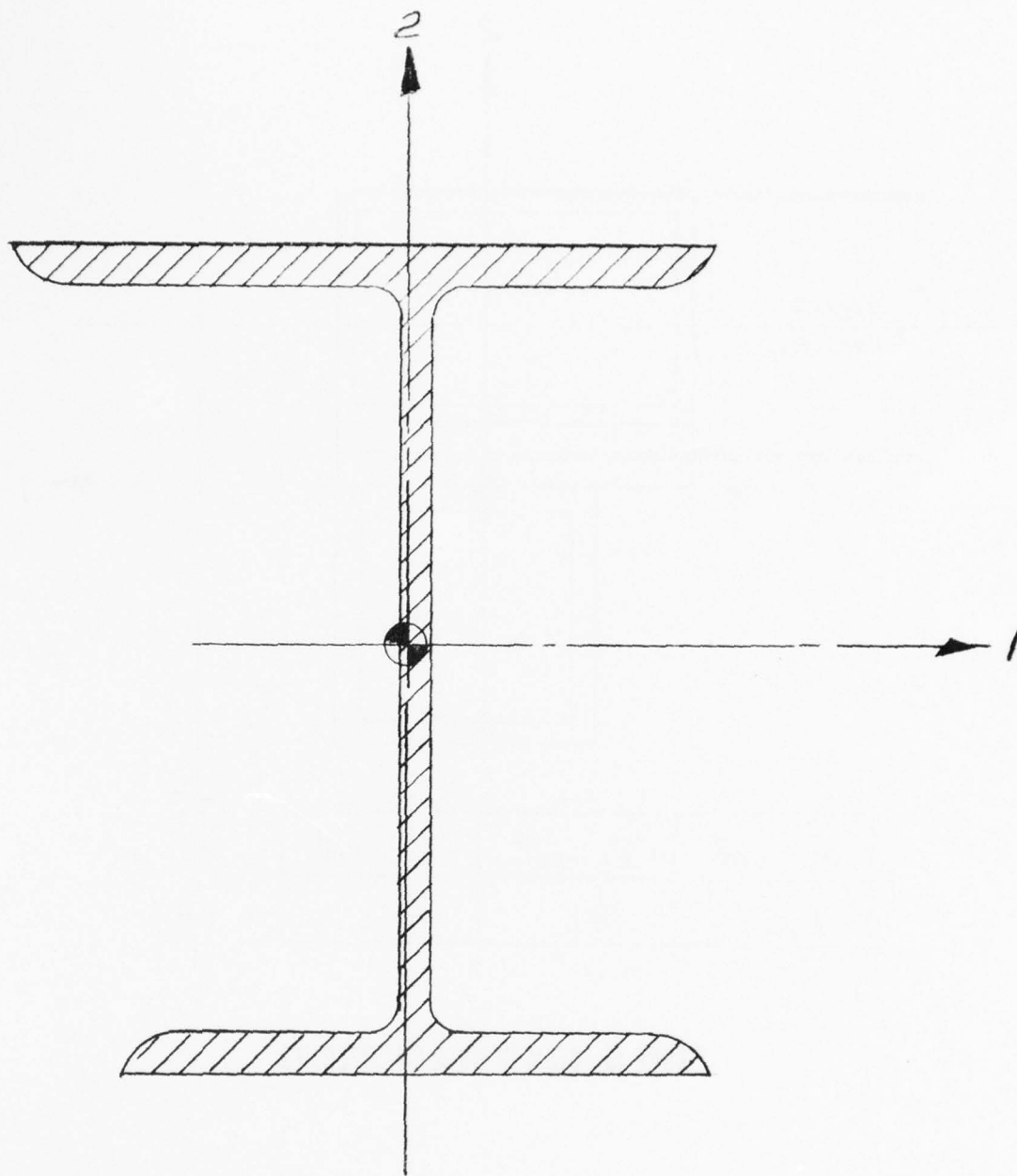
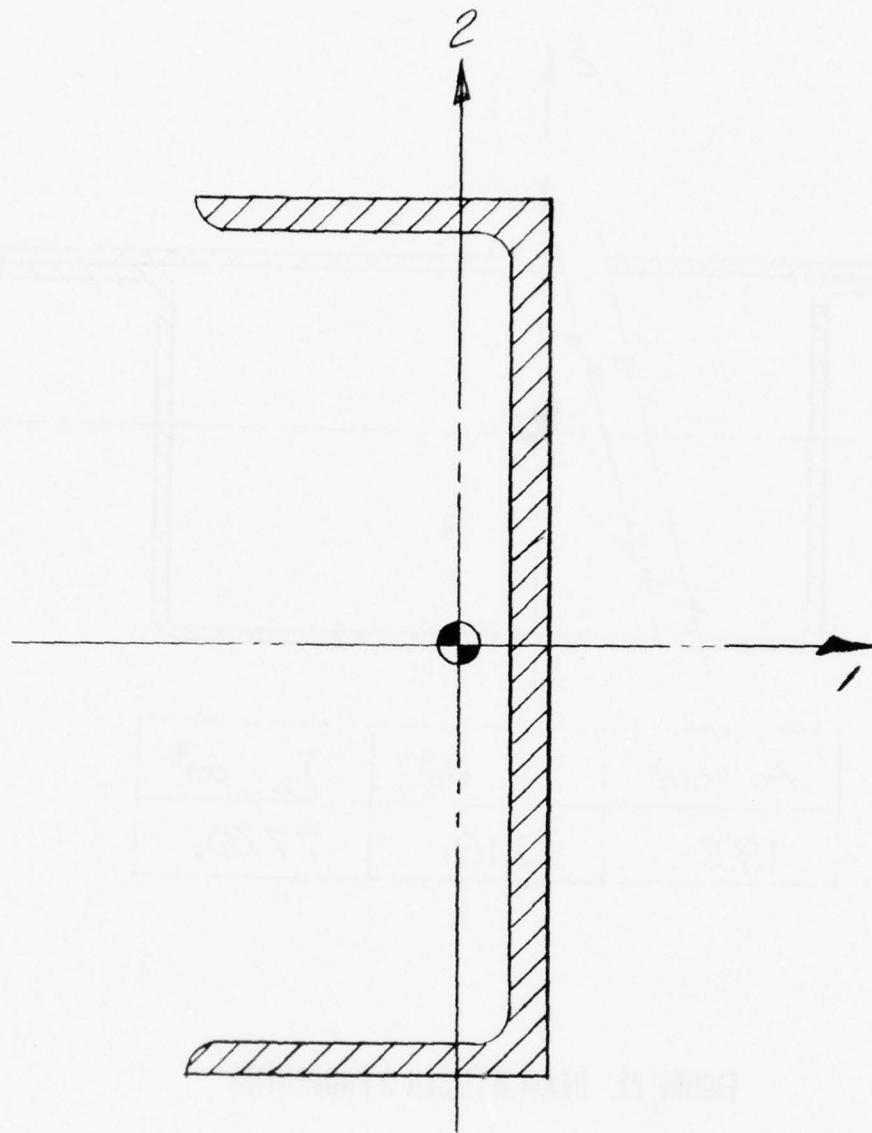


FIGURE 19. BEAM NUMBER 6 PROPERTIES.



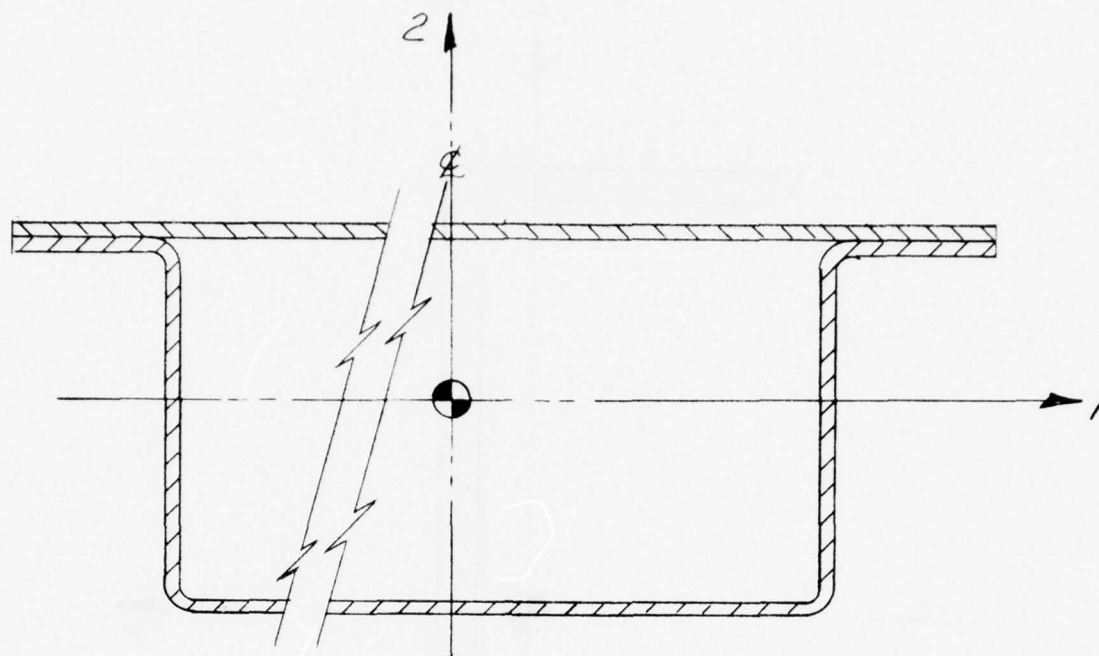
$A \text{ cm}^2$	$I_1 \text{ cm}^4$	$I_2 \text{ cm}^4$
6.8	503.	104.

FIGURE 20. BEAM NUMBER 7 PROPERTIES



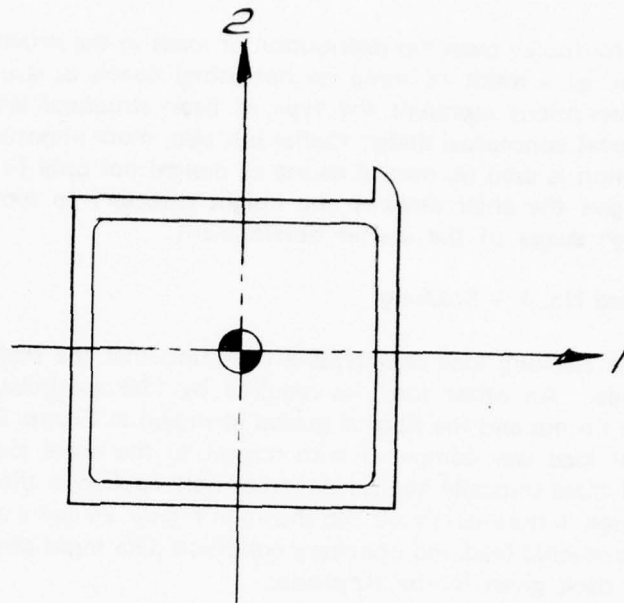
$A \text{ cm}^2$	$I_1 \text{ cm}^4$	$I_2 \text{ cm}^4$
4.1	245.	24.2

FIGURE 21. BEAM NUMBER 8 PROPERTIES



$A \text{ cm}^2$	$I_1 \text{ cm}^4$	$I_2 \text{ cm}^4$
19.5	1330.	7770.

FIGURE 22. BEAM NUMBER 9 PROPERTIES



$A \text{ cm}^2$	$I_1 \text{ cm}^4$	$I_2 \text{ cm}^4$
2.0	16.6	16.6

FIGURE 23. BEAM NUMBER 10 PROPERTIES

are intended to display both the distribution of loads in the structure as well as the change in distribution as a result of using (or not using) panels as structural members. These load path descriptions represent the type of basic structural information necessary not only for rational conceptual design studies but also, more importantly, for actual designs. This information is used (in normal course of design) not only to size structural members but also to give the chief designer the insight necessary to spot weak links during the detailed design stages of the shelter development.

a. Load No. 1 — Stacking

The stacking load represents a condition that the shelter is exposed to in the shipping mode. An offset load (as required by ISO specifications) is applied through the top ISO fittings and the floor is loaded as shown in Figure 24. The static equivalent of the offset load was computed with respect to the nodal locations at the corners of the roof and these statically equivalent forces were applied in the analysis. The boundary conditions used in the analysis are also shown in Figure 24 along with the global coordinate system. The specific load and boundary condition data input can be found in the printout of the data deck given in the Appendix.

Figure 25 shows superimposed deformed and undeformed structure plots for the beams only. The maximum deflection was scaled from 0.0392 m to 0.381 m to more clearly display the form of the deformation. The largest deformations occurred in the floor. It is interesting to note that in the true structure the floor is attached to a foldout floor by a nonstructural hinge. The foldout floor stands vertically in the shipping mode and presents a very stiff interface (in the vertical direction) with the permanent floor. Failure of the nonstructural hinge has been a problem and the plot in Figure 25 indicates this could be due to the high flexibility of the floor. Figure 26 is the deformed body plot of the complete finite element model with the maximum deformation again scaled to 0.381 m.

It would not be practical or useful to simply present tables which give the output values of bending moments, axial forces, etc., from the finite element analysis for each load case. Instead, data was extracted from several hundred pages of output and processed to obtain the plots shown in Figures 27 through 30. These plots show the bending moment and axial force distributions in some of the major load-carrying frame members. The distribution of these forces is shown for two model cases. As stated above, one case includes the wall and roof panels as load-carrying members and the other case does not include wall and roof panels. The benefit of using panels as structural members is clearly shown in these plots. The bending moment in the vertical frame members is reduced significantly except at the point of application of the moment. A design using lighter frame members could overcome the high moment near the ISO fitting by including stiffener plates, as is indeed done for other reasons in most shelters. Figure 28 indicates that the compressional load in the frame members is reduced about 30% when the wall panels are used as structural members.

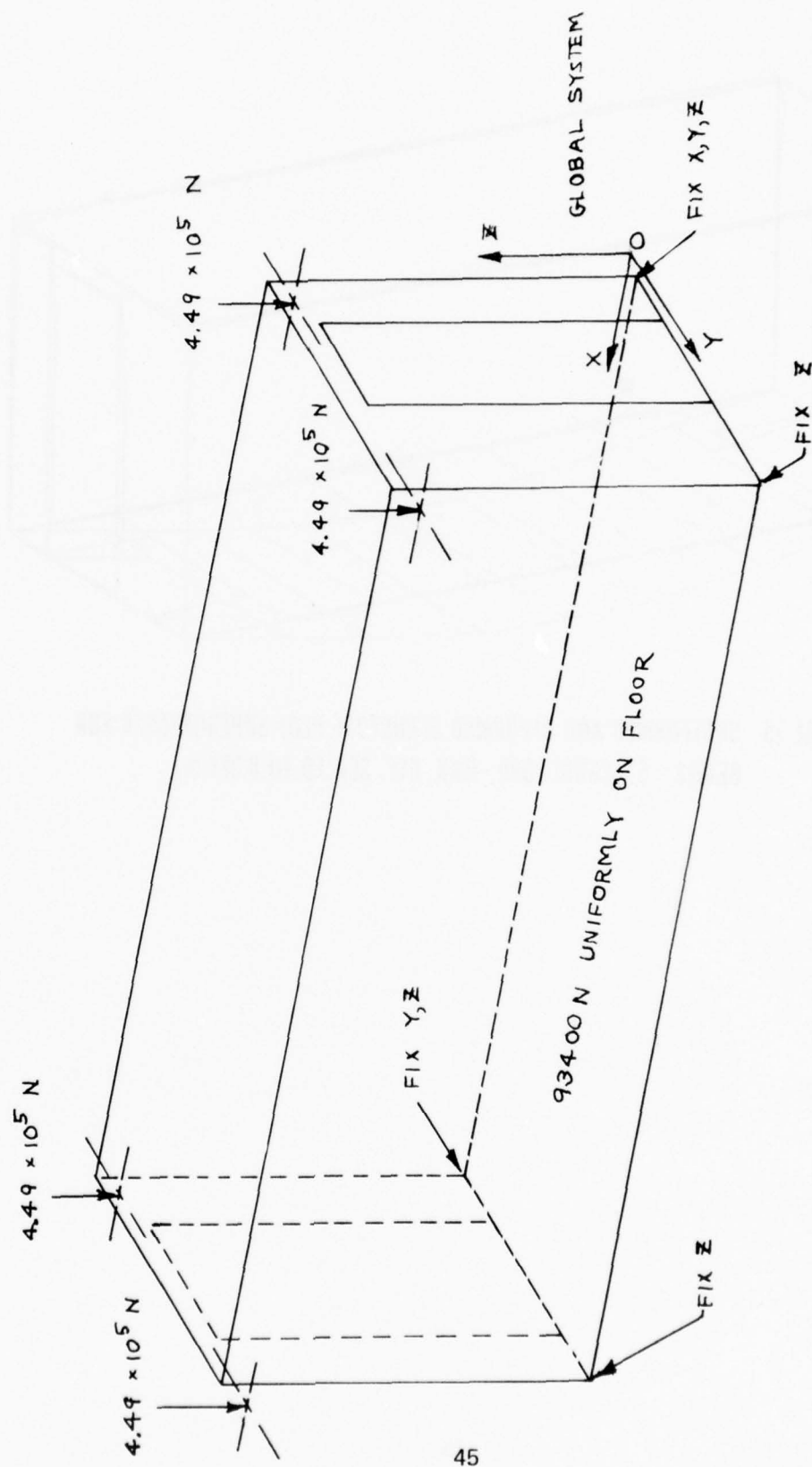
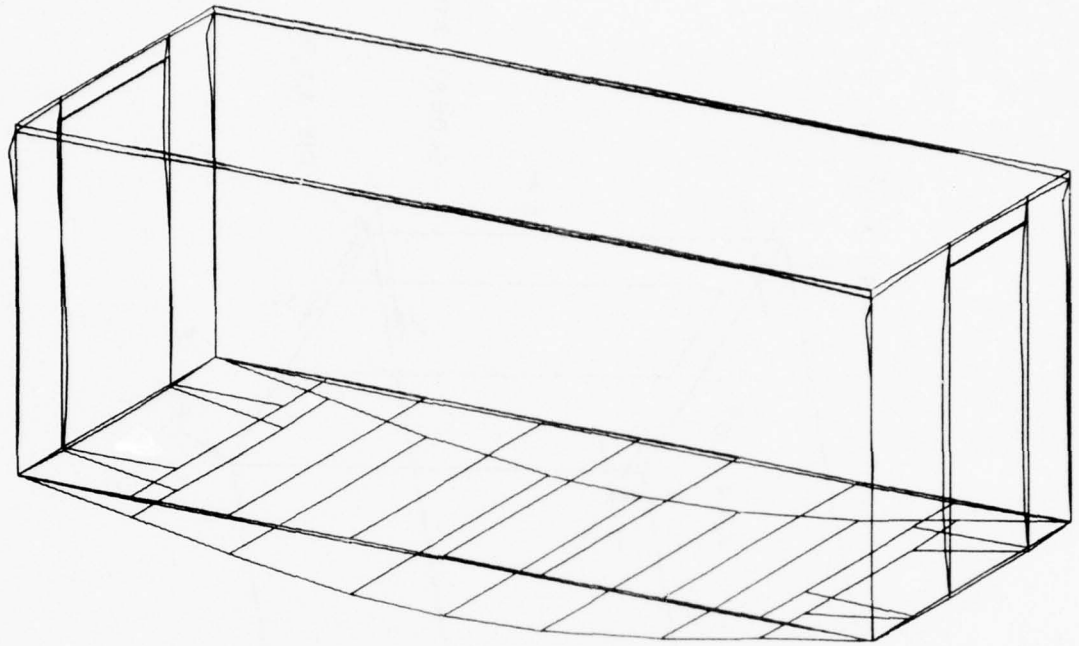


FIGURE 24. TEST NO. 1, STACKING



**FIGURE 25. UNDEFORMED AND DEFORMED STRUCTURE PLOT SUPERIMPOSED FOR
BEAMS - STACKING LOAD. MAX. DEF. SCALED TO 0.381 m.**

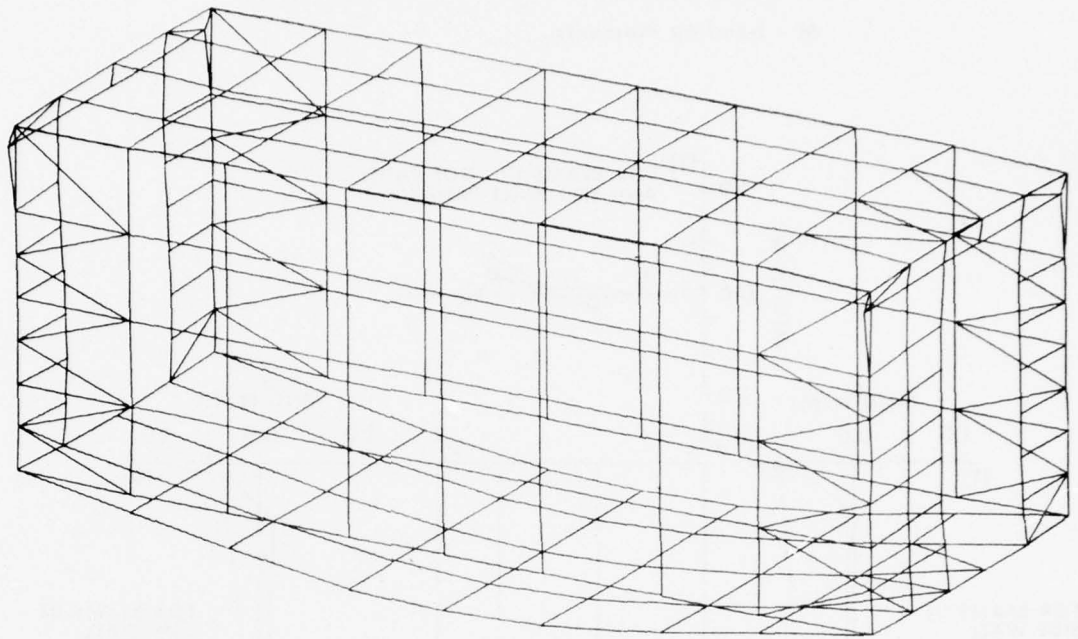


FIGURE 26. DEFORMED STRUCTURE PLOT - STACKING LOAD.

MAXIMUM DEFORMATION SCALED TO 0.381 m.

(T) - Implies bending moments of this sign induce tension in the outside of the shelter.

M - bending moments

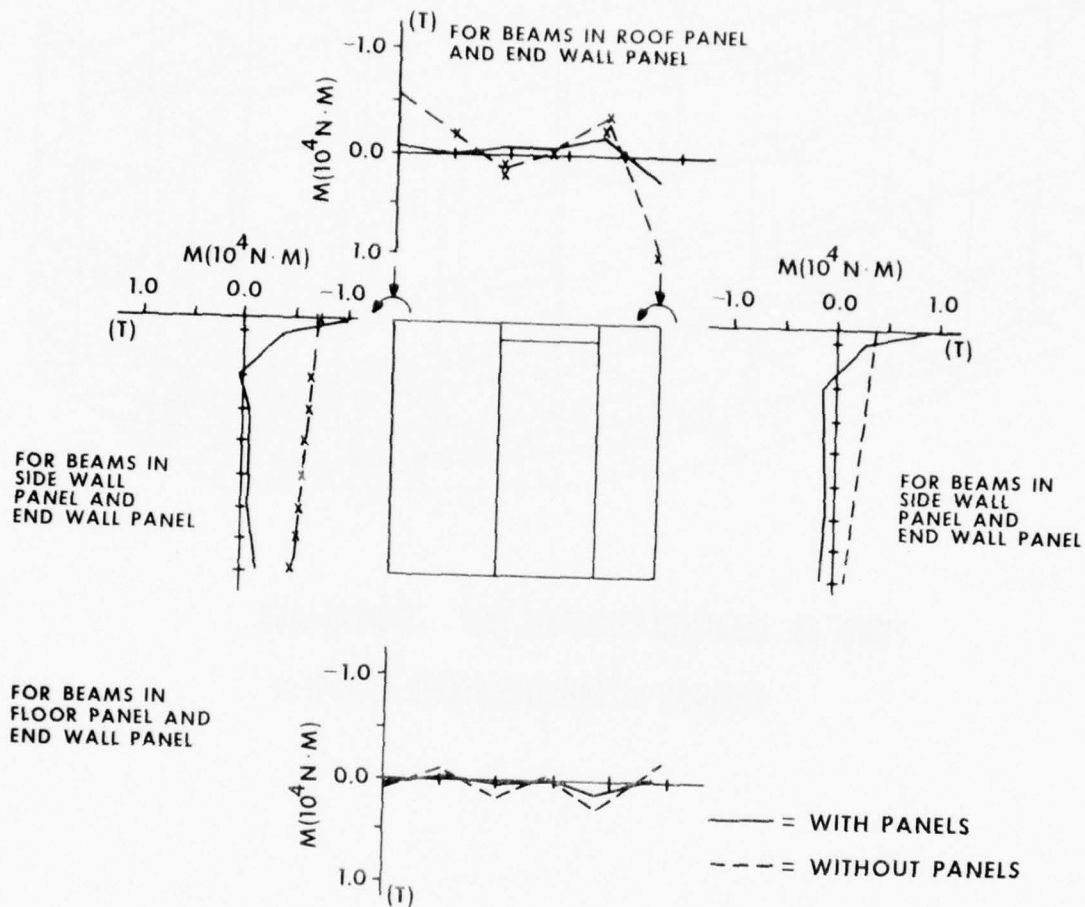


FIGURE 27 PERSONNEL DOOR END. STACKING LOAD. IN PLANE BENDING MOMENTS IN OUTER FRAME.

P - axial force in beam, positive values for tension

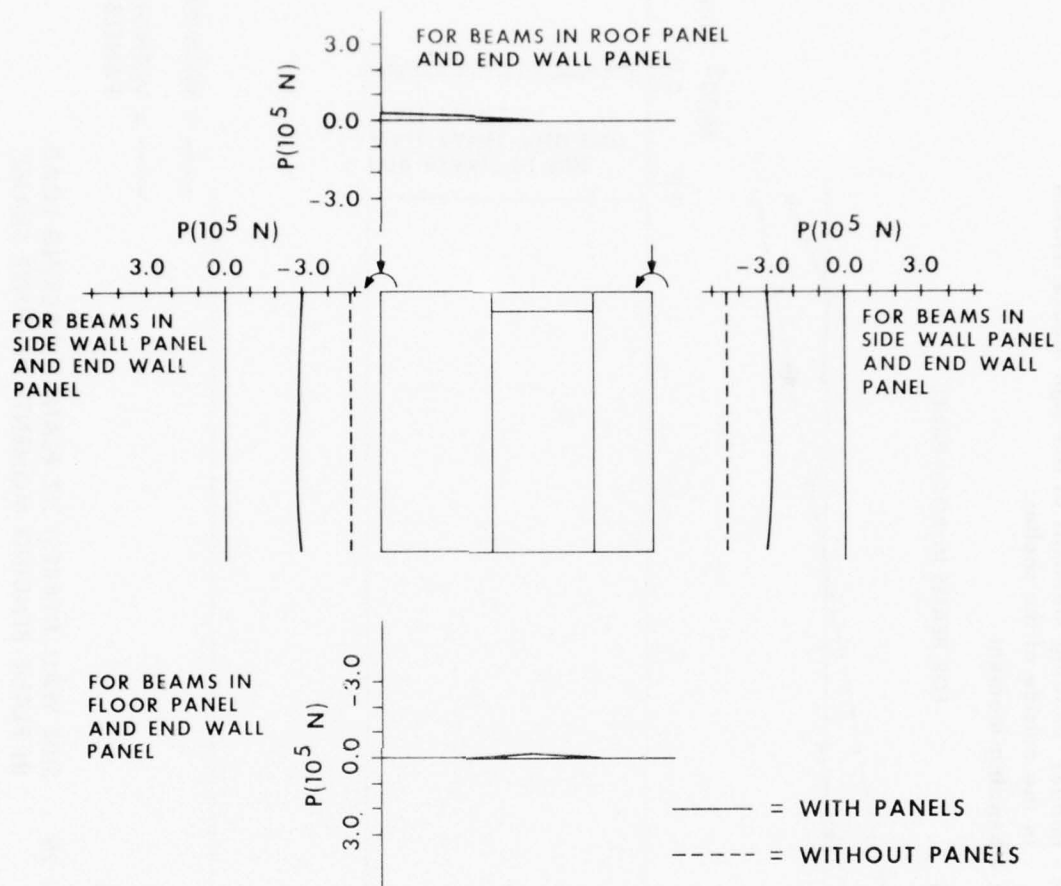


FIGURE 28 PERSONNEL DOOR END. STACKING LOAD. AXIAL LOAD IN OUTER FRAME.

(T) - implies bending moments of this sign induce tension in the outside of the shelter.
M - bending moment.

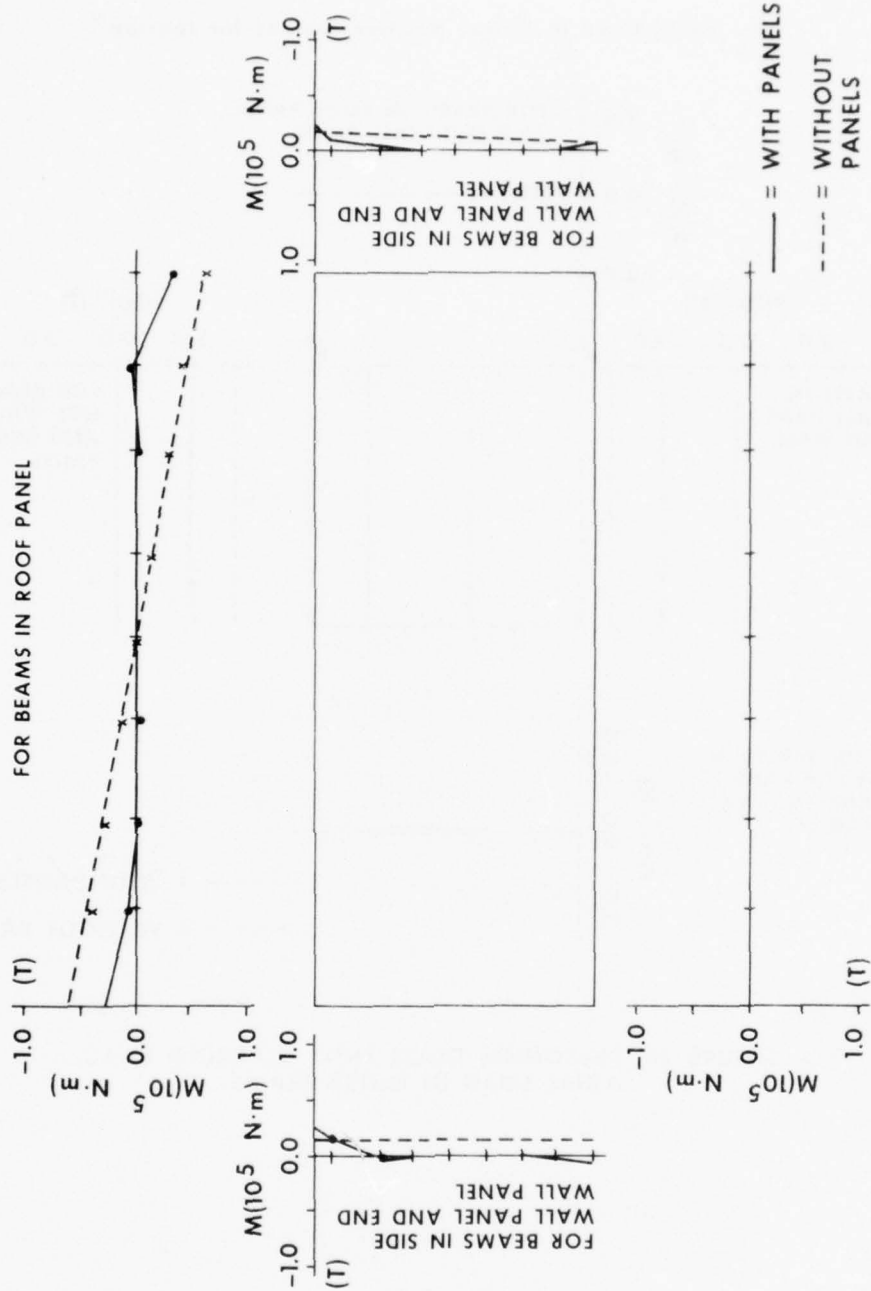
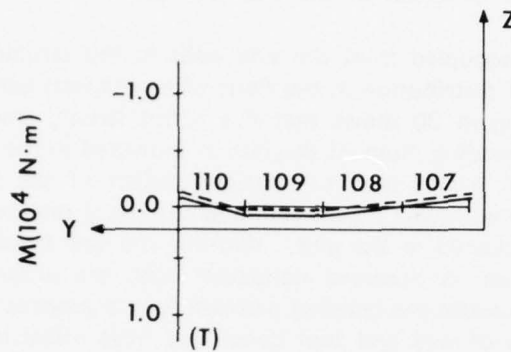


FIGURE 29 SIDE WALL NEAREST XZ PLANE. STACKING LOAD. IN PLANE BENDING MOMENTS IN OUTER FRAME.

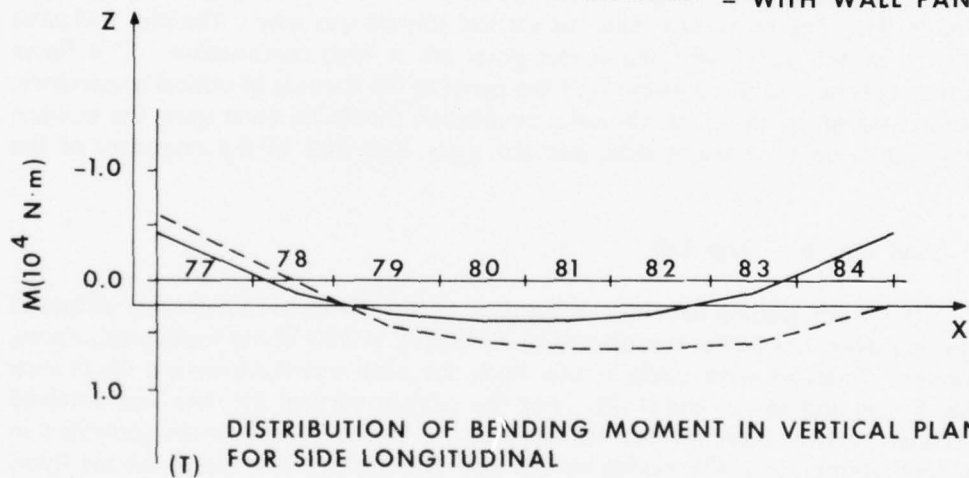
(T) - implies bending moments of this sign induce tension in the bottom of the beam

M - bending moment



DISTRIBUTION OF BENDING MOMENT IN VERTICAL PLANE FOR CENTER CHANNEL

--- = WITHOUT WALL PANELS
 — = WITH WALL PANELS



DISTRIBUTION OF BENDING MOMENT IN VERTICAL PLANE FOR SIDE LONGITUDINAL

FIGURE 30 FLOOR BEAMS. STACKING LOAD.
 BENDING MOMENTS IN VERTICAL PLANE.

In an effort to show that the same general results apply to the bending moments in the plane of the side wall, Figure 29 was made and the same general results were found. However, it should be noted that the bending moments displayed in the side wall plane are much larger than those observed in the end wall plane.

Finally, since the floor is uncoupled from the side walls in this structure one would expect little change in the load distribution in the floor when the wall panels and roof panel were not in the model. Figure 30 shows that this is not strictly true. The major I-beams under the floor have a bending moment diagram as indicated in the bottom set of curves in Figure 30. The wall panels tend to restrict rotation of the floor at the ends. The bending moment curve with wall panels acting as structural members thus takes the more symmetric form as indicated in the plot. Without the wall panels a less symmetric bending moment distribution is observed consistent with the unsymmetric loading. The top plot in Figure 30 indicates the bending moment for a transverse channel near the center of the floor. The use of wall and roof panels has little effect here. In either case the floor design does not appear to be strongly influenced by the structural action of the wall panels.

It was shown above that the wall panels significantly reduce the compressive load in the corner posts. To see the load distribution in the wall the panel stress data for the sidewall nearest the XZ plane was input to a FORTRAN graphics program to obtain Figure 31. The outer skin data for vertical stresses was used. The plot indicated that the ends of the panel near the corner posts are in high compression. This figure indicates that the method of connection of the panel to the frame is of critical importance. The structural design of the panel-to-frame connection should be done using the in-plane stress data, the bending moment data, and the shear load data of the boundary of the panel.

b. Load No. 2 -- Top Lift

The top lift loading condition is designed to test the shelter's ability to withstand loads expected when the shelter is subjected to movement by ISO lifting equipment, cranes, or helicopters. Analyses were made in this study for both a straight vertical lift at each top corner fitting and for a central lift. For the straight vertical lift data was obtained for the shelter hanging from the top fittings and (1) loaded by the forces generated in a vertical gravitational field, (2) loaded by 151,460 N uniformly distributed on the floor, and (3) a superposition of (1) and (2). The central lift case was analyzed with the floor loaded by 151,460 N only. The boundary conditions used and the applied loads (simulating the lifting) are indicated in Figure 32. The deformed body plot for the superimposed straight lift solution is shown in Figure 33. The floor deformations are so large due to the high flexibility of the floor that only the floor appears to have been deformed. The deformed body plot for the central lift is graphically equal to Figure 33. The maximum deformation in Figure 33 was scaled to be 0.381 m from a computed value of 0.0659 m.

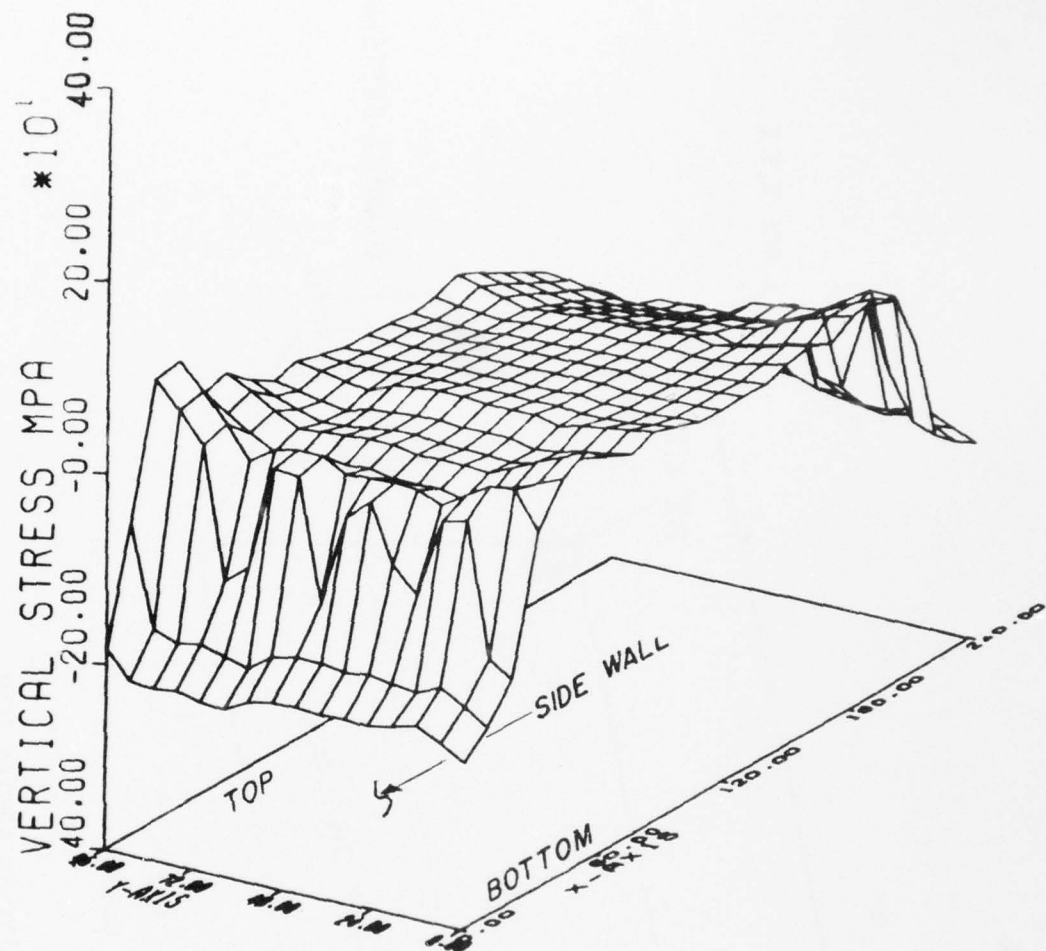
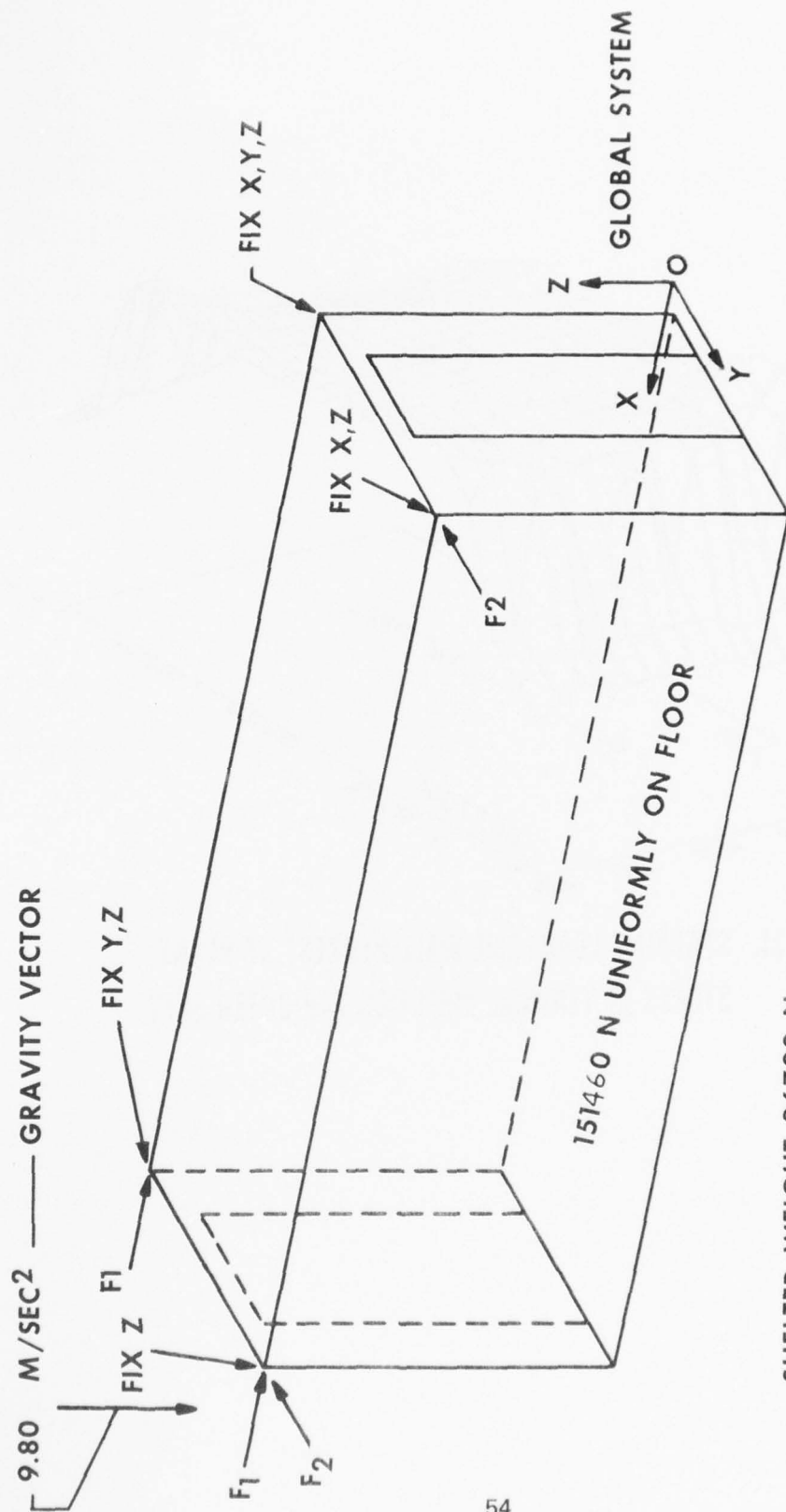
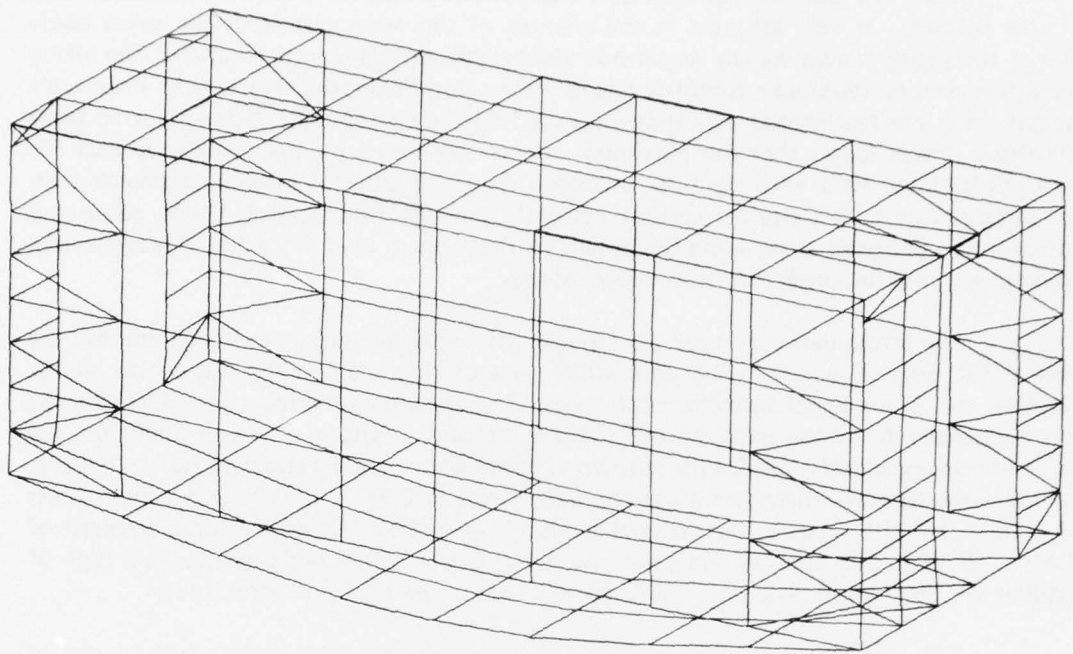


FIGURE 31. STACKING LOAD. SIDE WALL NEAREST XZ PLANE.
STRESS IN VERTICAL DIRECTION FOR OUTER SKIN.



SHELTER WEIGHT 26700 N
 $F_1 = 41,302. \text{ N}$ FOR CENTRAL LIFT CASE
 $F_2 = 16,521. \text{ N}$ FOR CENTRAL LIFT CASE

FIGURE 32 TEST NO. 2, LIFTING FROM TOP



**FIGURE 33. DEFORMED STRUCTURE PLOT - LIFTING FROM TOP.
MAX. DEF. SCALED TO 0.381 m.**

Note, the gravitational load data was collected only for the lifting tests described in this section. It was assumed in the analysis of the other tests that the stress levels due to the shelter's own weight would not yield significant design information. The lifting tests, however, represented a complete change in the load field resulting from the structure's weight since the real shelter was first supported on the bottom and then supported from the top. It was found that the maximum stresses generated by the straight vertical lift in a gravitational field with the floor unloaded were one order of magnitude smaller than the stresses due to the straight vertical lift with only the floor loaded. Thus, additional computation designed at studying the details of the element load fields due to gravitational loading was not in order for this design study.

The stress data for both the straight lift (with gravitational effects) and for the central lift were surveyed. The data which was of significant design value was almost identical in its numerical form for both cases. The specific numerical data which follows was abstracted from the data for the straight lift case. Output values of stress for the floor I-beam indicated a maximum positive extreme fiber bending stress of $2.34 \cdot 10^5$ kPa. At the same location there was a positive axial stress of $0.74 \cdot 10^5$ kPa and a shear stress of $3.08 \cdot 10^5$ kPa. Since the material is aluminum (6061-T6) with a yield strength of $2.41 \cdot 10^5$ kPa, this analysis indicates the floor is not safely designed for this type of loading (if the hinged fold-out floors do not act as part of the structure).

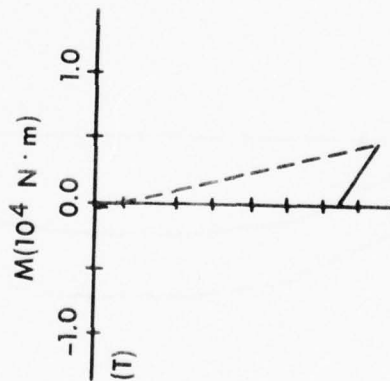
The load distribution data was investigated for the corner post and for one of the longitudinal I-beams under the floor. It was found that the use of wall panels as structural members has a great effect on the magnitude of the load distribution in the shelter. Figure 34 indicates the bending moment distribution in the XZ plane for the corner post nearest the XZ plane on the personnel door end. Except for the point at which the end wall and floor interact, the bending moments in the corner post reduce to insignificant values over the length of the member. Thus, use of the wall panels as load-carrying members and special design attention at the bottom end of the corner post would lead to optimum design of the corner post for this load condition. Although the bending moment patterns are identical for the straight lift and central lift cases, the axial load patterns are much different. However, the stresses resulting from the axial loads were small, and thus a graphical study of the difference in the axial load paths was not made.

Figure 35 indicates the bending moments in the XZ plane for one of the longitudinal I-beams under the floor. The shape of the bending moment curve was not changed when the wall panels were considered as part of the structure but the curve was shifted in a favorable direction as the maximum bending moment was reduced by a factor of about 0.6. The shifted curve takes the form expected when the ends of the I-beam are restricted from rotation. In this case the wall panels provide this rotational interaction at the ends of the I-beam. It should be noted that this bending moment pattern (Figure 35) would be different if the floor was structurally attached to the fold-out floors.

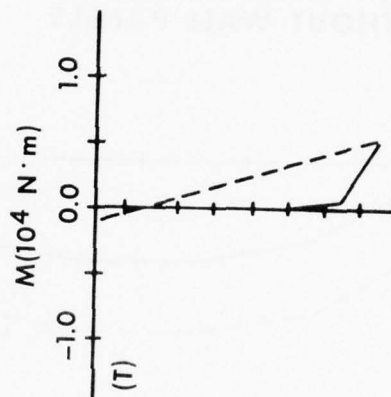
(T) - implies bending moments of this sign induce tension on the outside of the shelter

M - bending moments

CENTRAL LIFT
WITHOUT GRAVITY LOAD



STRAIGHT LIFT
WITH GRAVITY LOAD



— = WITH PANELS
--- = WITHOUT PANELS

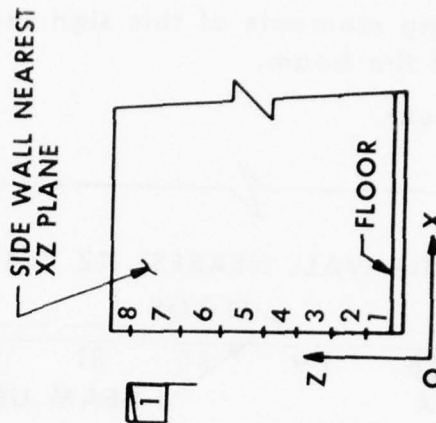


FIGURE 34 LIFTING FROM TOP BENDING MOMENTS IN XZ PLANE FOR CORNER POST

(T) - implies bending moments of this sign induce tension in the bottom of the beam.

M - bending moment.

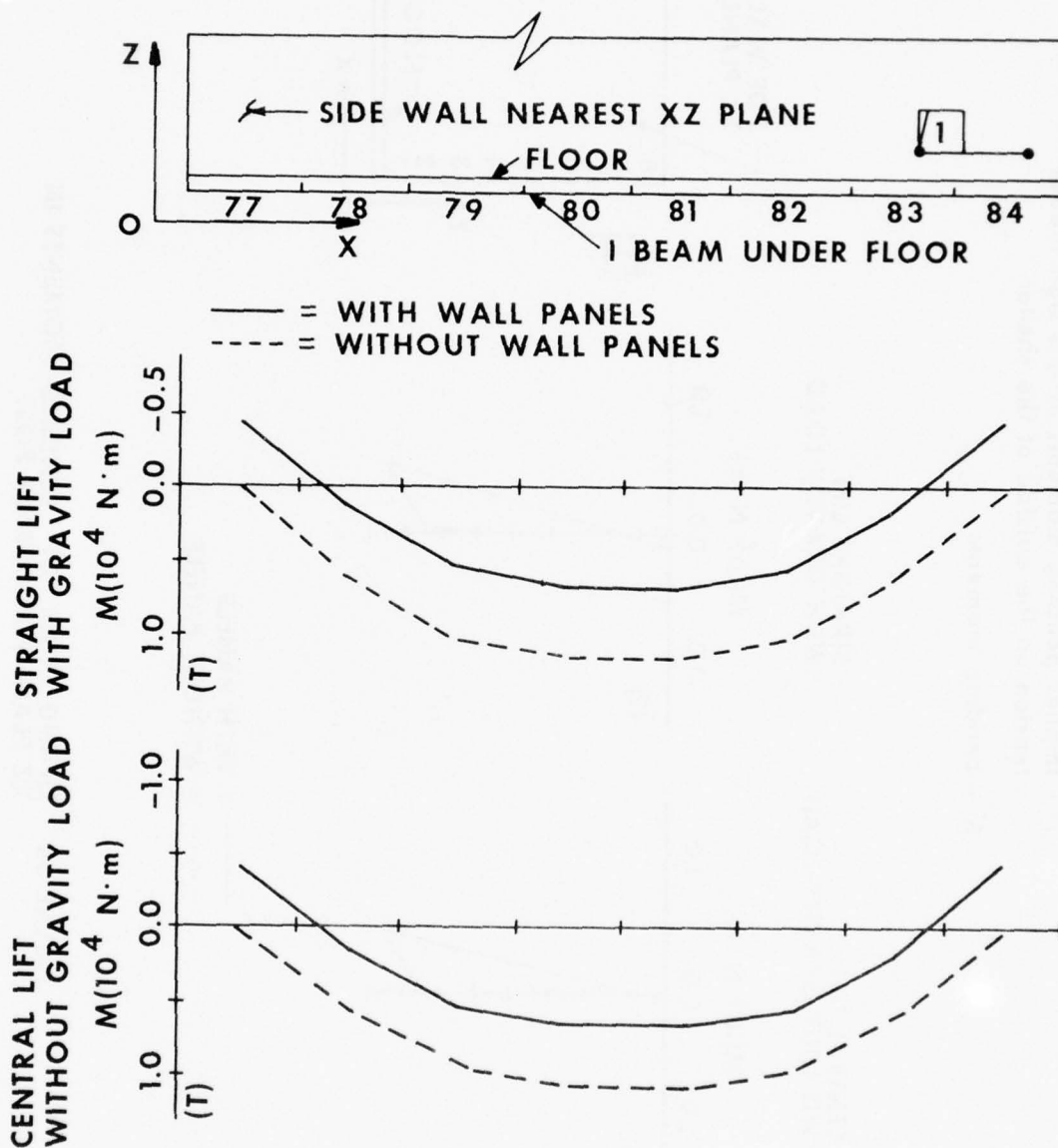


FIGURE 35 LIFTING FROM TOP. BENDING MOMENTS IN XZ PLANE FOR I-BEAM UNDER FLOOR.

Further investigation of the stress data indicated that the floor plate was highly stressed. The longitudinal and transverse stresses were both large and near the yield value for the floor skin. To see the distribution of the floor's top skin stresses in a form that would help the designer know where the worst conditions are, a three-dimensional plot of the Hencky-von Mises stresses in the top skin of the floor plate was made. This plot is shown in Figure 36. The highest stressed area is in the central region of the floor. The corners of the floor plate are also highly stressed. Thus, in this case, the designer can concentrate his efforts on satisfying stress requirements in the central region of the floor, while giving attention to the connection methods used at the corners of the floor.

c. Load No. 3 - Bottom Lift

The bottom lift loading condition is similar to the case of top lifting. As for load No. 2, above, the purpose of load No. 3 is to test the shelter's ability to withstand loads expected from lifting it from the bottom ISO fittings. Analyses were made in this study for both a straight vertical lift at each bottom corner fitting and for a central lift by cables attached between the bottom ISO fittings on each side and one spreader bar over the center of the shelter. For the straight vertical lift, data was obtained for the shelter hanging from the bottom fittings and (1) loaded by the forces generated in a vertical gravitational field, (2) loaded by 151,460 N only. The boundary conditions used and the applied loads are indicated in Figure 37. The deformed body plot for the structural model with wall panels was graphically identical to Figure 33 due to large floor deformations. Thus, the deformed body plot for the case when the wall and roof panels were not considered as part of the structure was included as Figure 38. A close look at Figure 38 indicates that the end columns had large deformations due to their interaction with the floor which is tending to rotate at each end.

As for load No. 2, above, the stresses due to the gravitational loading were one order of magnitude less than those generated from loading the floor. Also, the load distribution data of significant design value was almost identical in its numerical form for both the straight lift and the central lift cases. In particular, the stress data indicated that the corner posts were highly stressed at the bottom. A plot of the bending moments in the corner posts was made and the bending moment distribution was found to be identical to the distribution shown in Figure 34. This indicates that the floor loading governed the moment distribution in the outer framework for this particular structure.

The personnel door frame behaved the same way as the end column. It was highly stressed at the bottom. A bending moment plot for the vertical door frame member (at the personnel door end and nearest the XZ plane) is given in Figure 39. The resulting pattern was similar to the pattern for the corner post. That is, when the wall panels were used as part of the structure the panels carried a significant portion of the load.

The stress data for the longitudinal I-beam under the floor indicated that this member was highly stressed. The bending moment pattern for the I-beam was similar

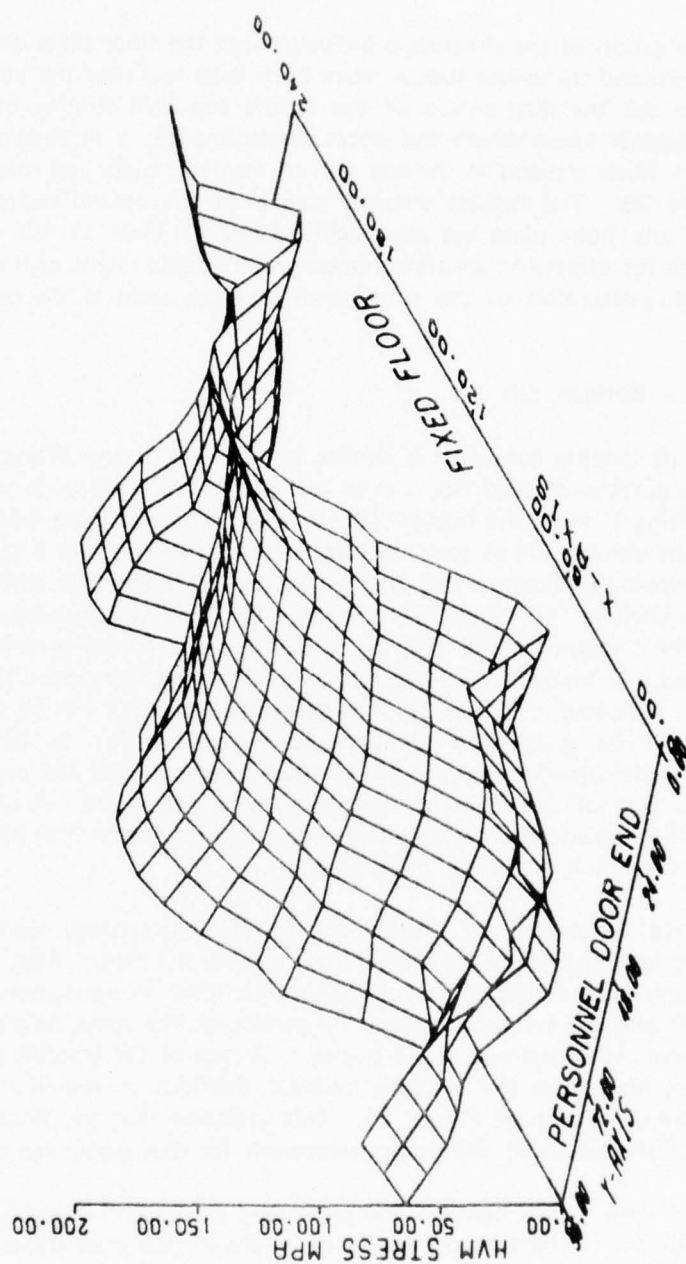


FIGURE 36. LIFTING FROM TOP. HENCKY-VON MISES STRESS IN TOP SKIN OF FLOOR PLATE.

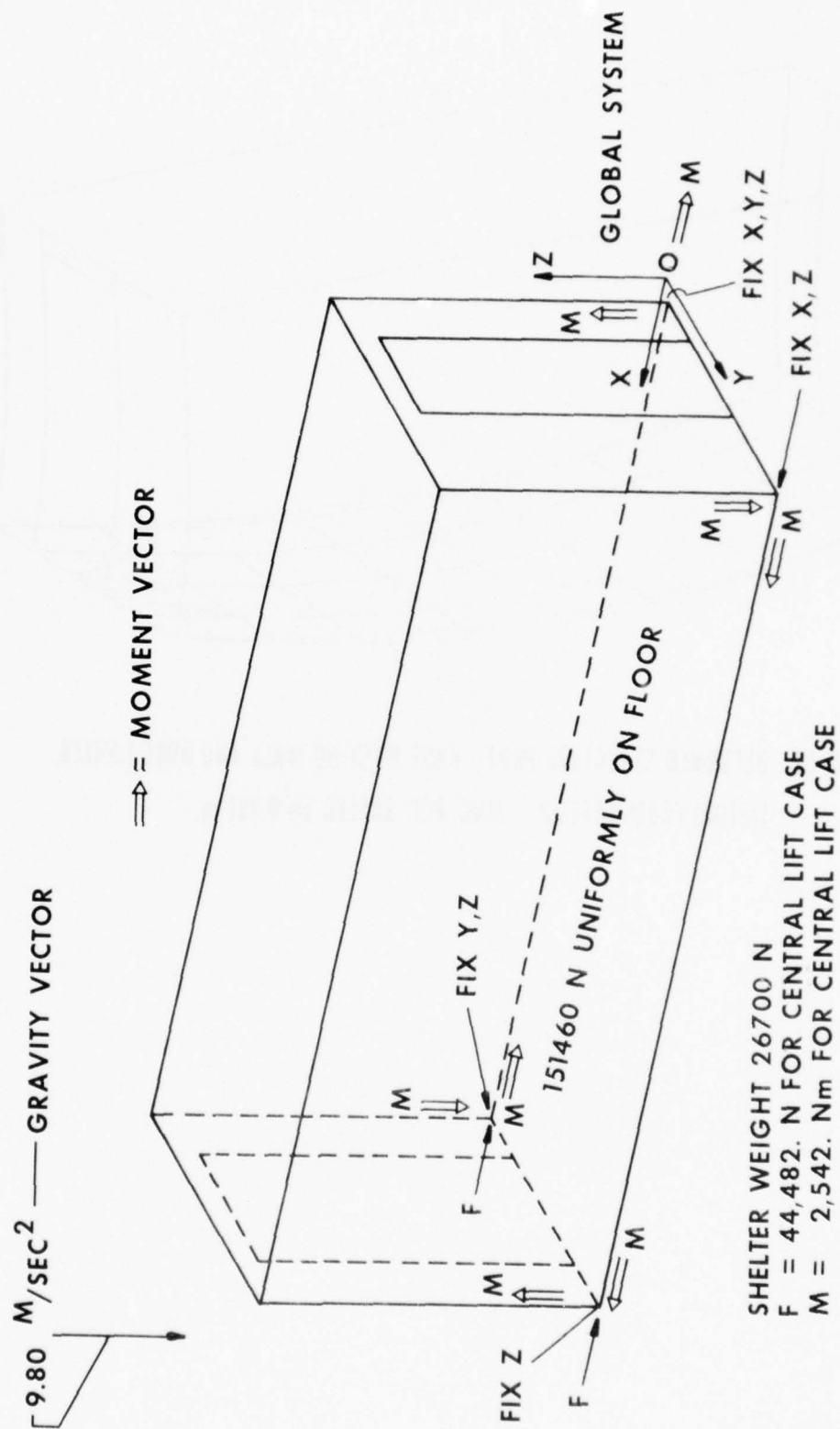


FIGURE 37 TEST NO. 3, LIFTING FROM BOTTOM.

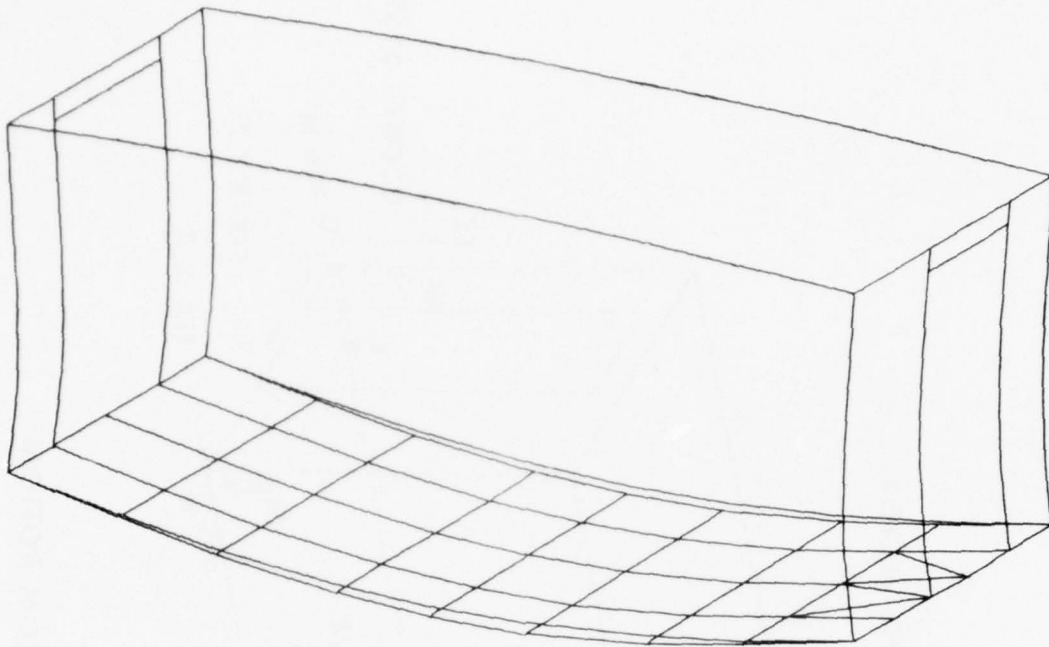
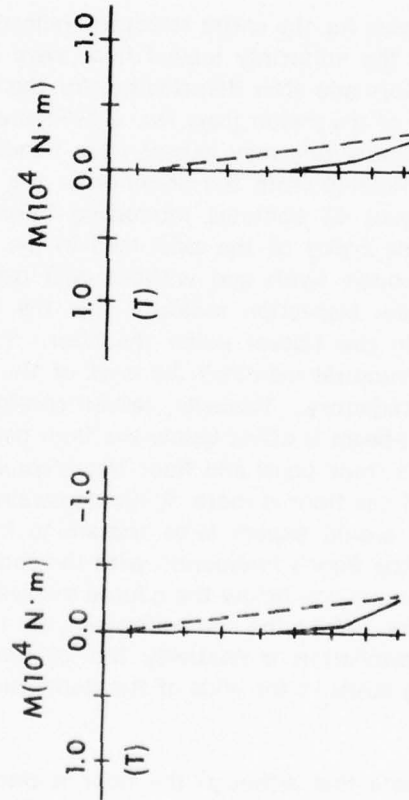


FIGURE 38. DEFORMED STRUCTURE PLOT - CASE WITH NO WALL AND ROOF PANELS.
LIFTING FROM BOTTOM. MAX. DEF. SCALED TO 0.381 m.

(T) - implies bending moments of this sign induce tension on the outside of the shelter.

M - bending moment

CENTRAL LIFT WITHOUT GRAVITY LOAD STRAIGHT LIFT WITH GRAVITY LOAD



— = WITH PANELS
 - - - = WITHOUT PANELS

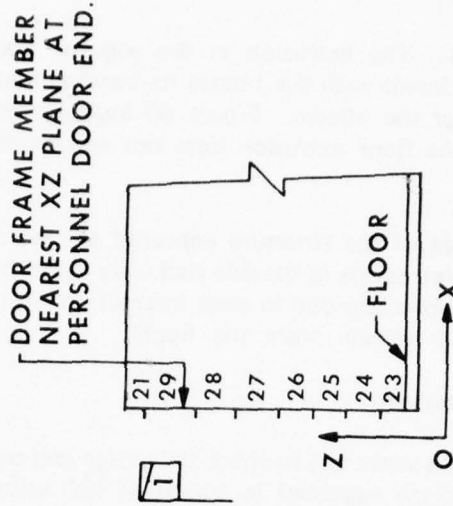


FIGURE 39 LIFTING FROM BOTTOM. BENDING MOMENTS IN XZ PLANE FOR DOOR FRAME MEMBER.

to that shown in Figure 35. The extrusion in the edge of the floor was also highly stressed. Since this member bends with the I-beam its bending moment curve is expected to be similar to the curve for the I-beam. Figure 40 indicates that this is true and also the magnitudes show that the floor extrusion does not add much stiffness to the floor structure.

Only one other area of the structure appeared to have any interesting data for this case. The bottom wall extrusions in the side wall were highly stressed near the bottom corners of the wall. This is obviously due to their interaction with the corner post (which is receiving a rotational load transfer from the floor).

d. Load No. 4 - Restraint

The restraint test is a static test to check the design and construction for exposure to horizontal loading conditions expected in transit of ISO units. The various loading conditions for this test are indicated in Figure 41. There are four possible loadings and each was analyzed.

The deformed body plot for the entire structure indicated that, as in the above loadings, the deformations for the uniformly loaded floor were largest. Figure 42 is a plot of the floor plate both before and after deformation for the case where the restraint load is applied to only one side of the shelter (case No. 3 in Figure 41). This deformation plot indicates that for this structure one may expect floor bending to govern the stress distribution with a small modification from the presence of the tension or compression load on the ISO fitting. Figure 43 contains interesting information supporting this conjecture. The figure contains a plot of the axial load in the I-beam under the floor plate for the two structural models (with and without wall panels) loaded for case 1 as shown in Figure 41. General inspection indicates that the load applied at the ISO fitting induces a tensile load in the I-beam under the floor. Figure 43 indicates that, when the wall panels act as structural members the ends of the I-beam have zero axial load. This appears to be contradictory. However, careful consideration of the structure and the model reveals that the I-beam is offset below the floor panel. That is, the bending axis of the I-beam is below the floor panel and floor frame combined structure's neutral surface. Noting that the end of the floor is more rigidly constrained when the wall panels are part of the structure, one would expect large restraining bending moments at the ends of the floor (because of the floor's interaction with the end wall). Such restraining moments, of course, induce compression below the neutral surface of the panel and I-beam structure at the ends of the floor. When the end wall panels are not part of the structure, the floor panel and frame combination is relatively free at the ends. Bending in this case results in a lower bending stress at the ends of the floor, thus a lower counteracting axial load from bending.

It is interesting to note that although the floor is responding in many ways, its gross behavior can be rationally explained by analogy to simple bending theory; yet

(T) - implies bending moments of this sign induce tension in the bottom of the beam

M - bending moment

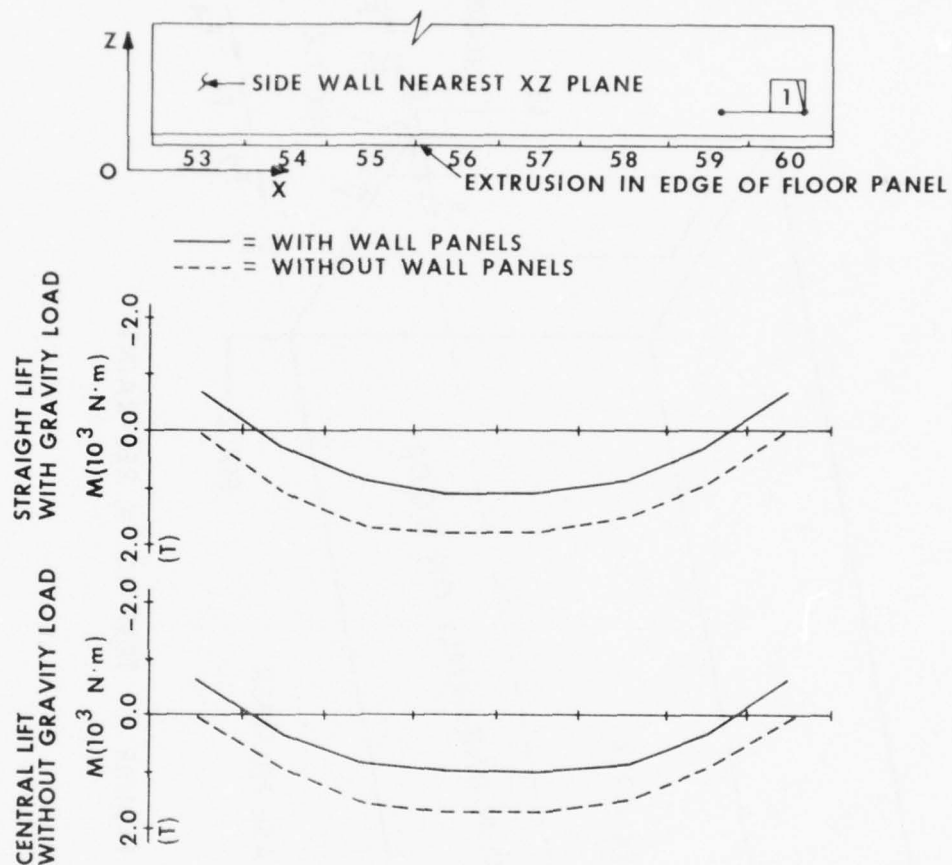


FIGURE 40 LIFTING FROM BOTTOM. BENDING MOMENTS IN XZ PLANE FOR EXTRUSION IN EDGE OF FLOOR PANEL.

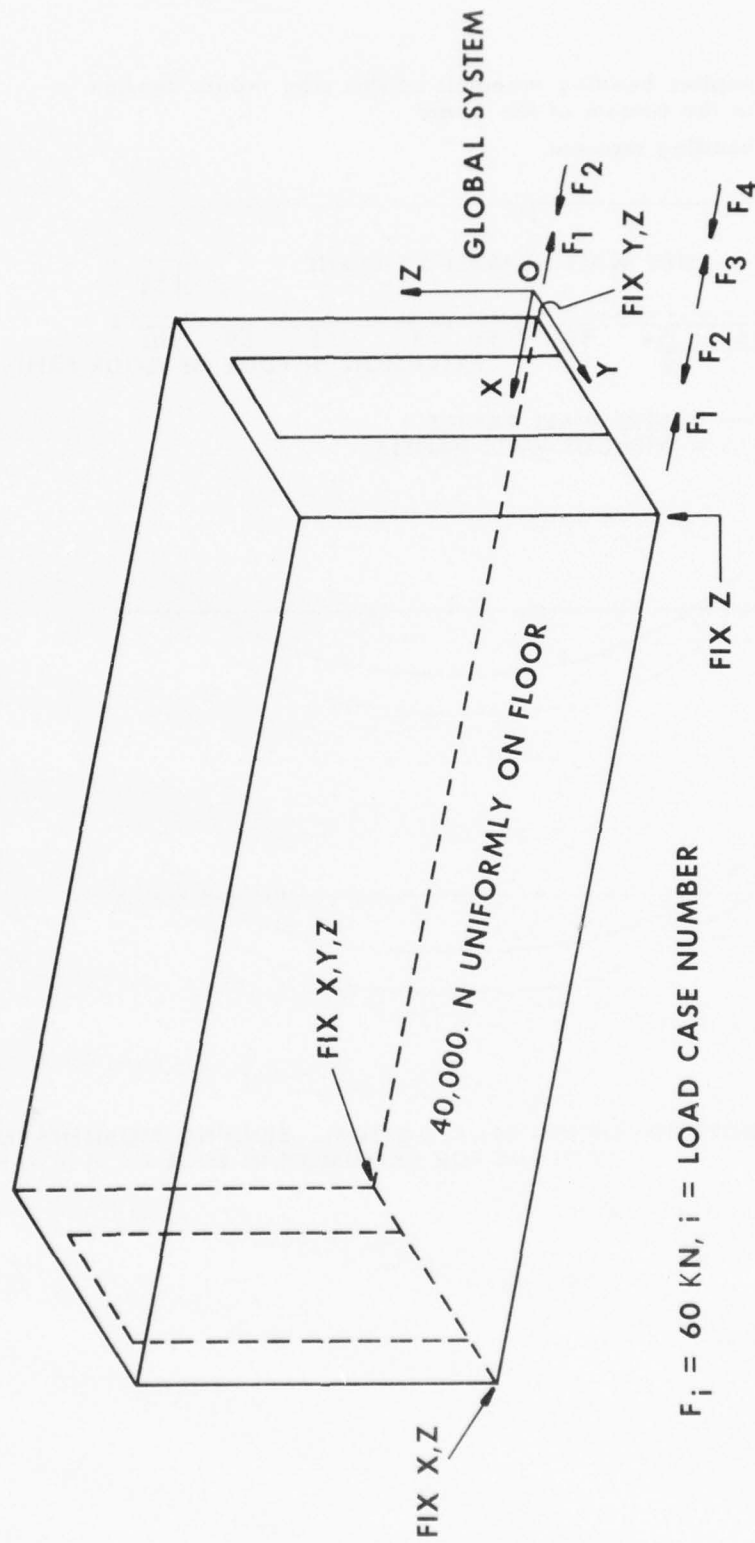


FIGURE 41 TEST NO. 4, RESTRAINT.

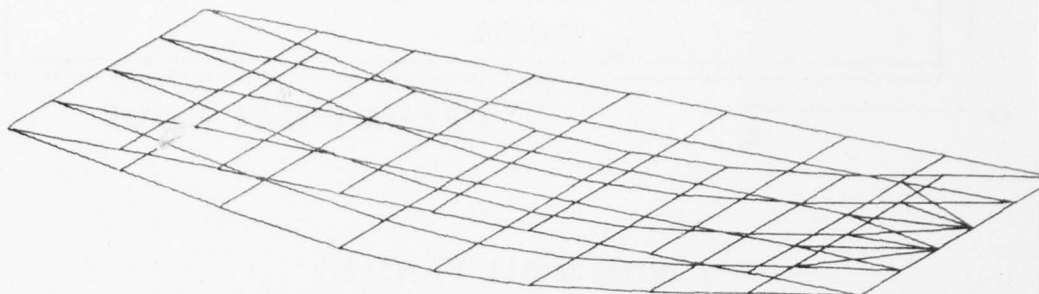


FIGURE 42. RESTRAINT. SUPERIMPOSED PLOT FOR UNDEFORMED
AND DEFORMED FLOOR PANEL.
MAX. DEF. SCALED TO 0.381 m.

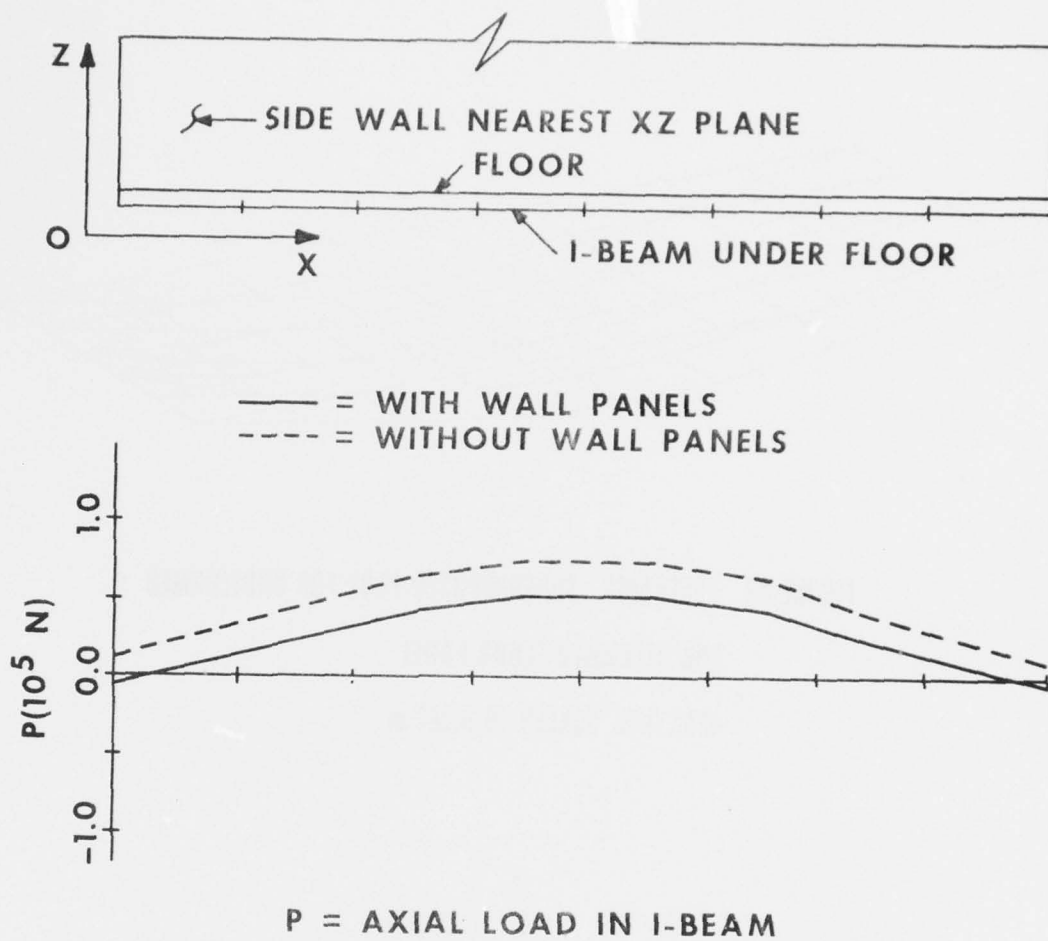


FIGURE 43 RESTRAINT. AXIAL LOAD IN I-BEAM UNDER FLOOR.

simple bending theory is inadequate for determining the numerical data. It is also true that the modeling of the structure and the analysis data have enlightened the designer in the area of understanding how this complex structure works.

Further study of the analysis data for the structural model containing the wall and roof panels brings out the following general design guidance information. The I-beam under the floor was stressed to about $\frac{1}{4}$ of its yield value. The stresses for the entire shelter were, in general, small compared to the previous cases of stacking and lifting. The stress levels did reach about $\frac{1}{2}$ yield value at the bottom of the corner posts where the restraint load was applied. This area is stressed from both the applied restraint load and the uniform loading of the floor and is thus understandably an area of concern. To see how the side wall panel responds to this loading, its outside skin stresses were plotted in Figure 44. This figure serves to visually demonstrate that the panel is stressed significantly only in the bottom corners of the panel near where the restraint load is applied.

When the wall and the roof panels were not considered as part of the structural model the stress level at the bottom of the corner posts reduced to about $\frac{1}{3}$ the value it had when wall panels were part of the structure. However, the stress level remained high in the remainder of the corner post. There was very little change in the stress data for the floor panel and support frame; that is, the floor stress levels were still far from the yield value.

e. Load No. 5 - Racking

The racking test is designed to test the shelter for its longitudinal and lateral strength to resist towing, pushing, and similar shipping loads. Figure 45 contains the details of the four loads and the boundary conditions used in this analysis to represent the actual test. This test is the first of the nine tests studied in this report which did not have a uniform load on the floor and thus contains information about load distributions in the end wall when the end wall is not affected by the floor bending.

Figure 46 is the deformed body plot for the entire structure exposed to the first load indicated in Figure 45. The maximum deflection was scaled to 0.254 m, and thus the figure is not as exaggerated as past figures. A better indication of the troubled area is given in Figure 47 where a straight-on view of the personnel door end is given in the deformed state. The actual deformation at the corner in the direction of the load was 0.018 m when wall and roof panels acted as part of the structure and 0.435 m when the panels were not part of the structure. Thus, the wall panels are extremely important in keeping the structure intact when the shelter is subjected to racking loads.

After a survey of the load distribution data was made it was determined that a plot of the inplane bending moment distribution in the outer frame of the personnel door end wall would yield interesting information. Figure 48 contains this plot. The

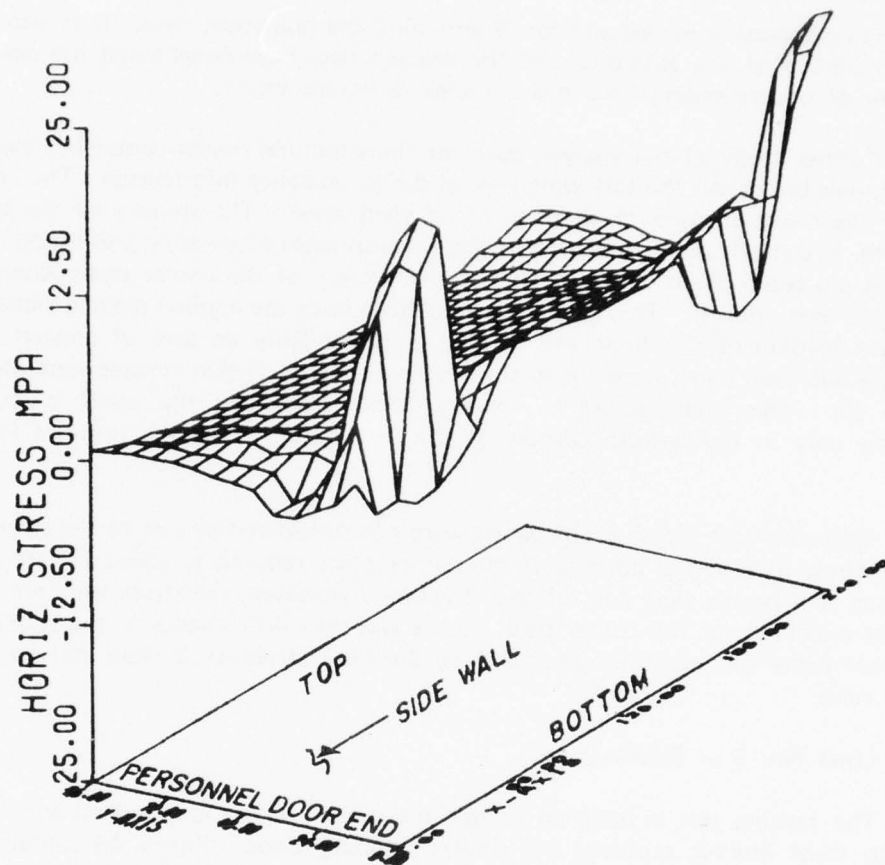
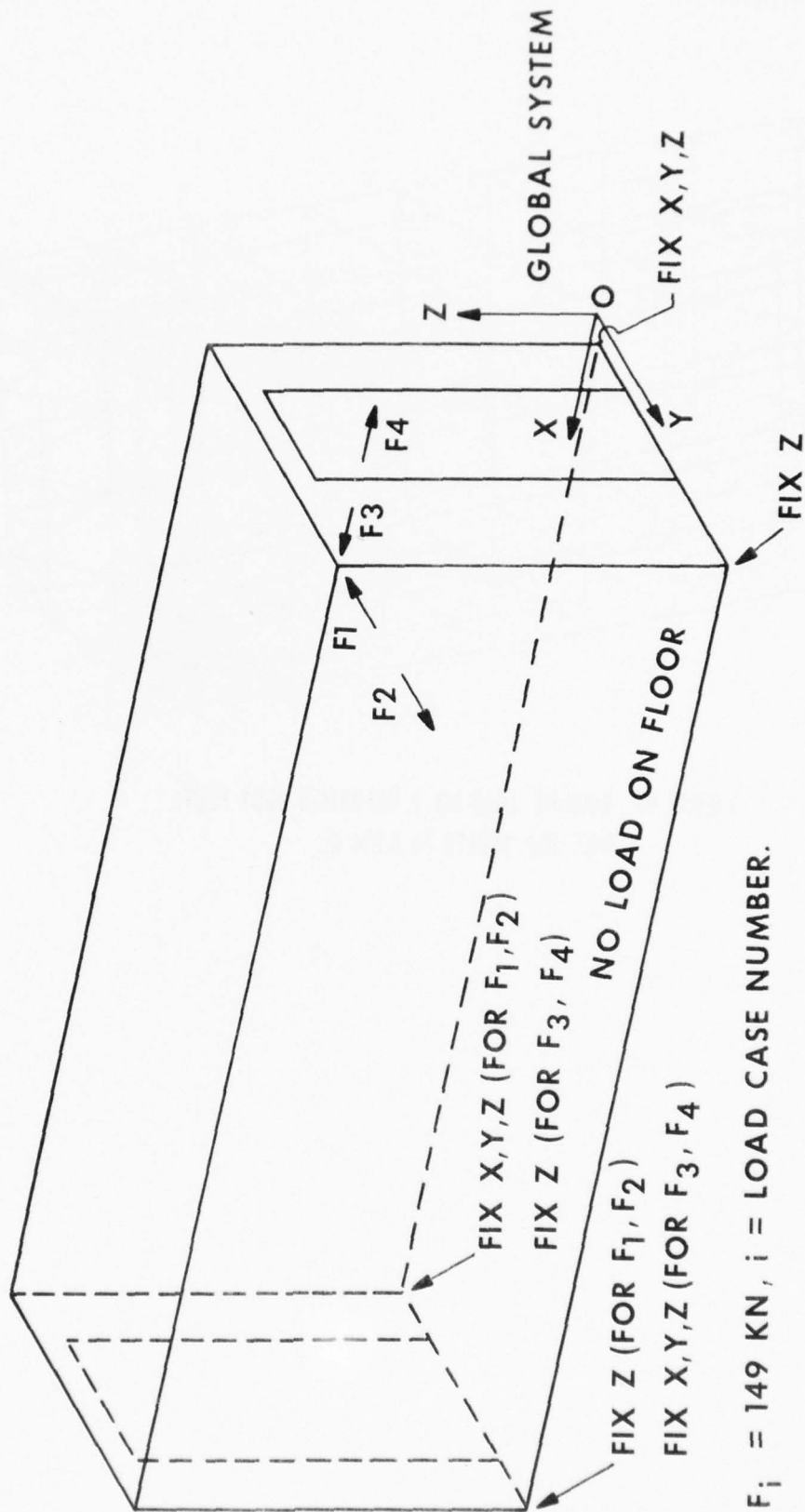


FIGURE 44. RESTRAINT. SIDE WALL FARTEST FROM XZ PLANE.
HORIZONTAL STRESS DISTRIBUTION.



$F_i = 149 \text{ KN}, i = \text{LOAD CASE NUMBER.}$

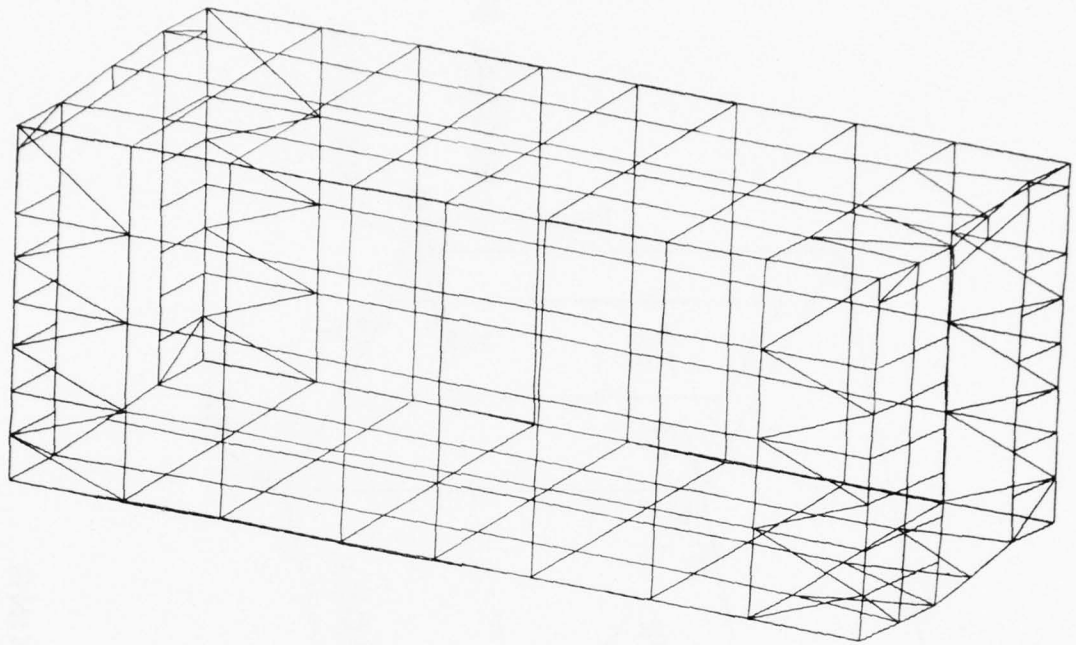
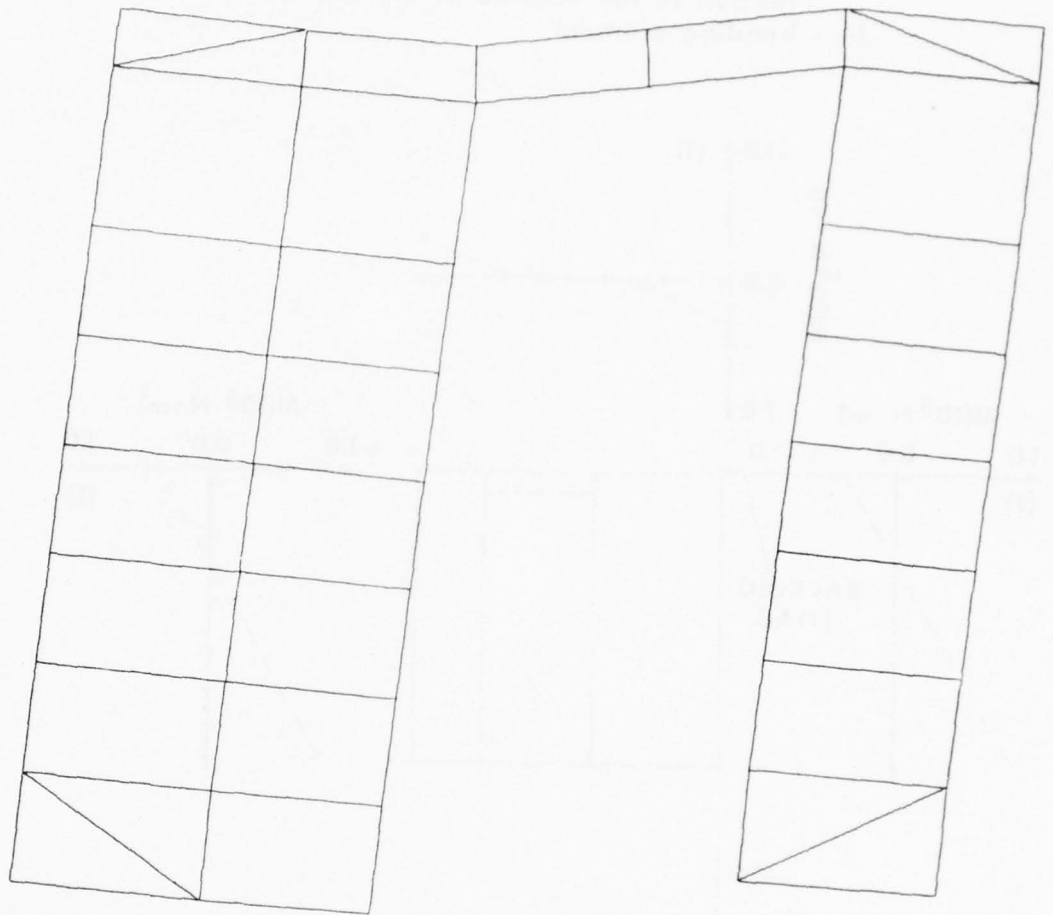


FIGURE 46. RACKING. LOAD NO. 1, DEFORMED BODY PLOT.
MAX. DEF. SCALED TO 0.254 m.



**FIGURE 47. RACKING. LOAD NO. 1, DEFORMED BODY PLOT
PERSONNEL DOOR END. MAX. DEF. SCALED TO 0.254 m.**

(T) - implies bending moments of this sign induce tension in the outside of the shelter.
M - bending moment.

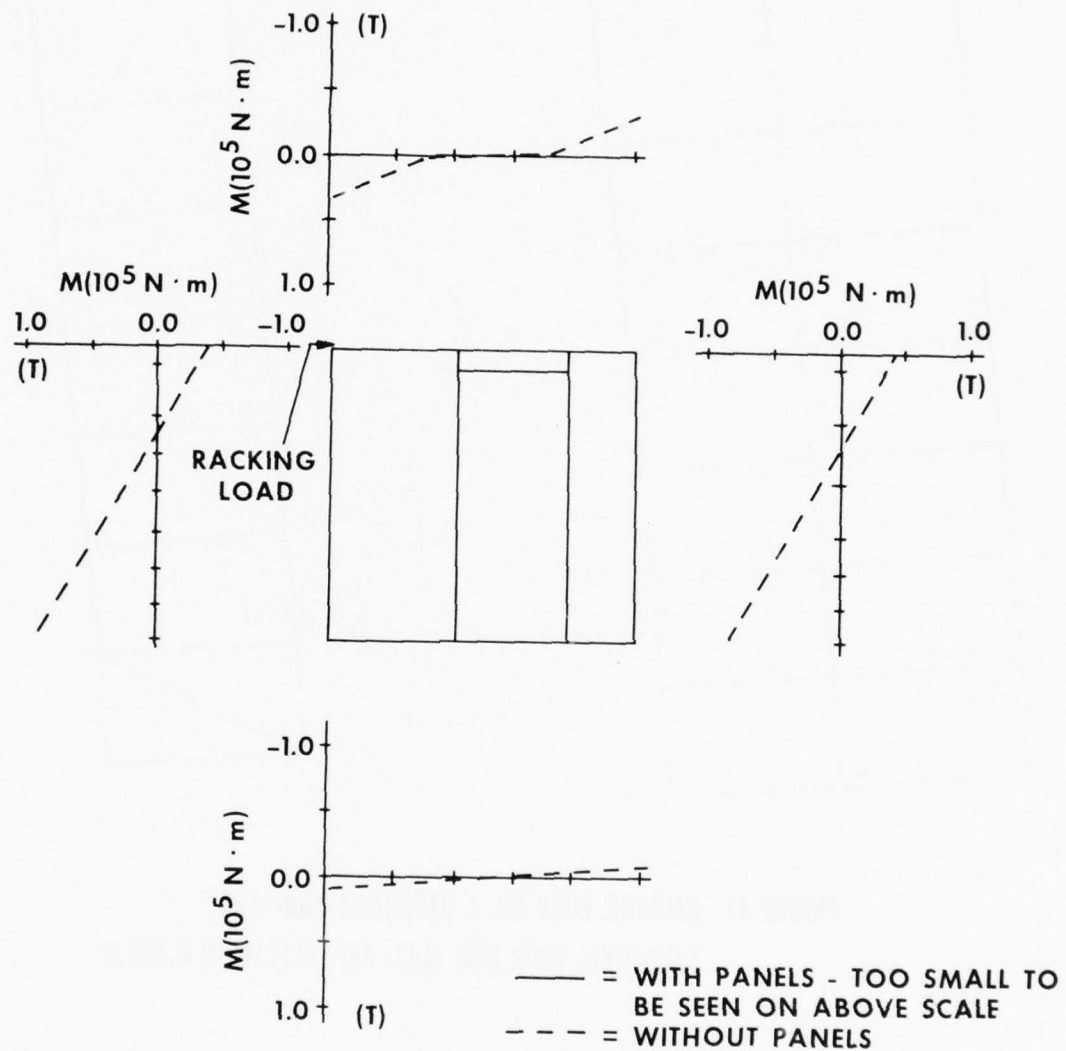


FIGURE 48 RACKING. PERSONNEL DOOR END. IN PLANE BENDING MOMENTS IN OUTER FRAME.

bending moments in the frame were large when the panels did not act as part of the structure. These bending moments reduced to a value too small to plot on the same scale when the wall and roof panels acted as load-carrying members. Figure 48 indicates that the corners of the end wall may be the problem area for design.

The stress data for the structural model with panels was surveyed and the following general results obtained. Transverse racking caused the panel elements in the corners of the end wall to have high inplane principal stresses. These stresses were also high along the entire top of the end wall. The corner posts were found to be highly stressed near the corners of the end wall, and the door frame members were stressed to yield in some locations. Longitudinal racking caused a behavior in the side wall similar to that found in the end wall above for transverse racking except that the stress magnitude were well below yield.

Data for the model without panels and loaded in transverse racking indicated high stresses in the corners of the floor panel at the loaded end of the structure. The stresses in the frame at the personnel door end exceeded yield and some values were at least twice the ultimate strength of 6061-T6 aluminum. Longitudinal racking also caused high stresses in the corners of the floor plate at the loaded side of the structure. The calculated floor skin stresses actually reached yield. The stresses in the frame members near the load were again at least twice yield.

f. Load No. 6 — Lashing

The lashing test loads are intended to expose the shelter to conditions expected when the shelter is secured on ships. The boundary conditions and loads used to obtain the analysis data for lashing are indicated in Figure 49. There are five separate lashing tests in which opposing compressive and tensile loads are sequentially applied. Since the forces are opposing each other it was expected that the bending moments and deflections found would be small relative to those found for stacking, lifting, and other tests in which the forces were not opposing each other.

The floor is not loaded in this test so the deformed body plots are more interesting than in the past cases where the floor was loaded (floor deformations being so large that they obscured the remaining deformations). Figures 50, 51, and 52 are views of the personnel door end as it is successively loaded by F_1 , F_3 , and F_5 indicated in Figure 49. The maximum deformations were scaled from the computed values of 5.93×10^{-4} m, 1.24×10^{-3} m, and 2.83×10^{-3} m to 0.254 m, respectively in Figures 50 to 52. Figure 53 is a deformed body plot of the entire structure when it is loaded by F_8 . Figure 54 singles out the side wall loaded by F_8 and shows a superposition of the undeformed and deformed scaled body plots.

Since the significant effects of each loading were restricted to the region surrounding the particular frame member loaded, it was decided to plot the results of several loading conditions on one figure. Figure 55 shows the axial loads picked up by

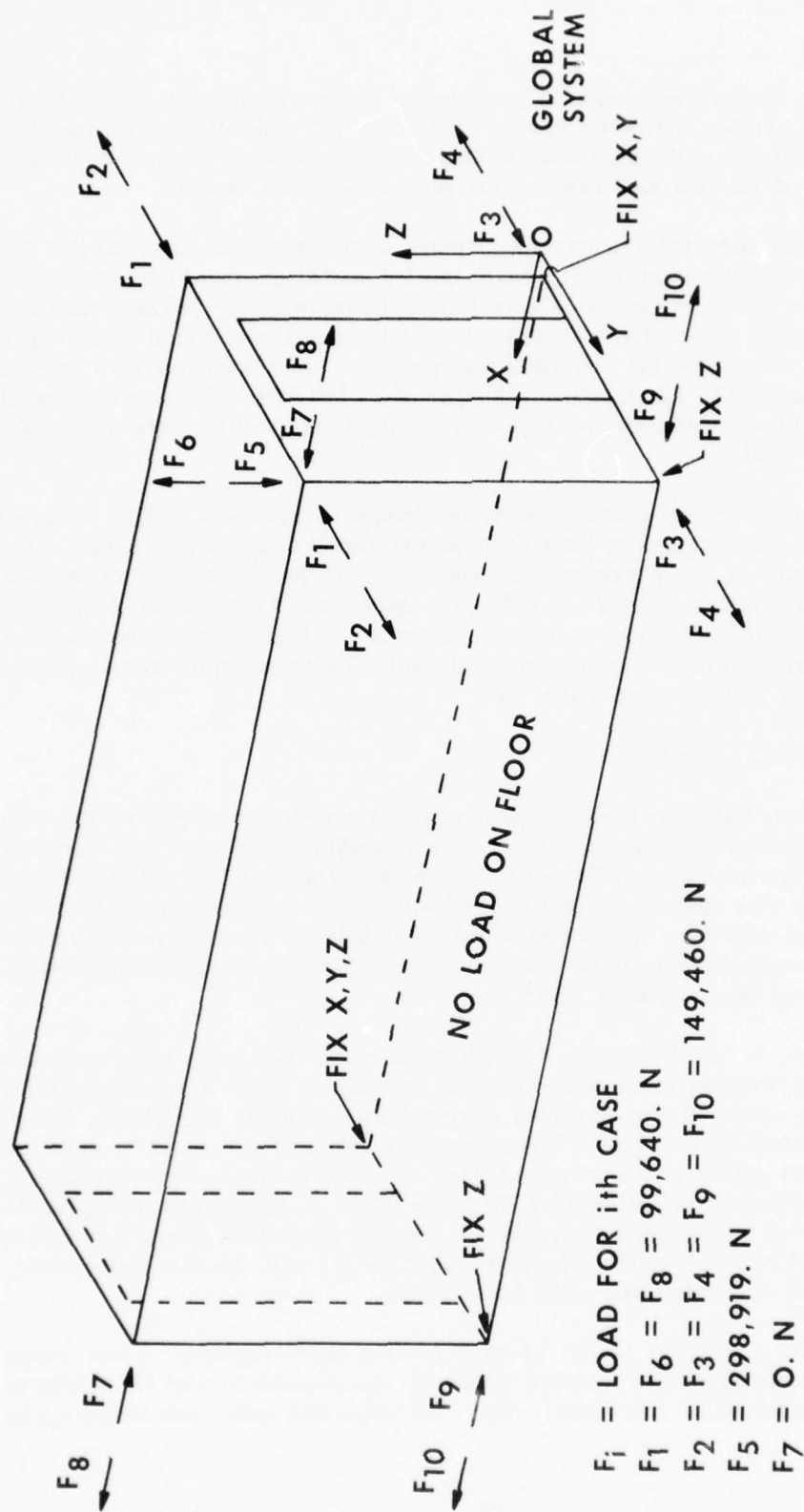
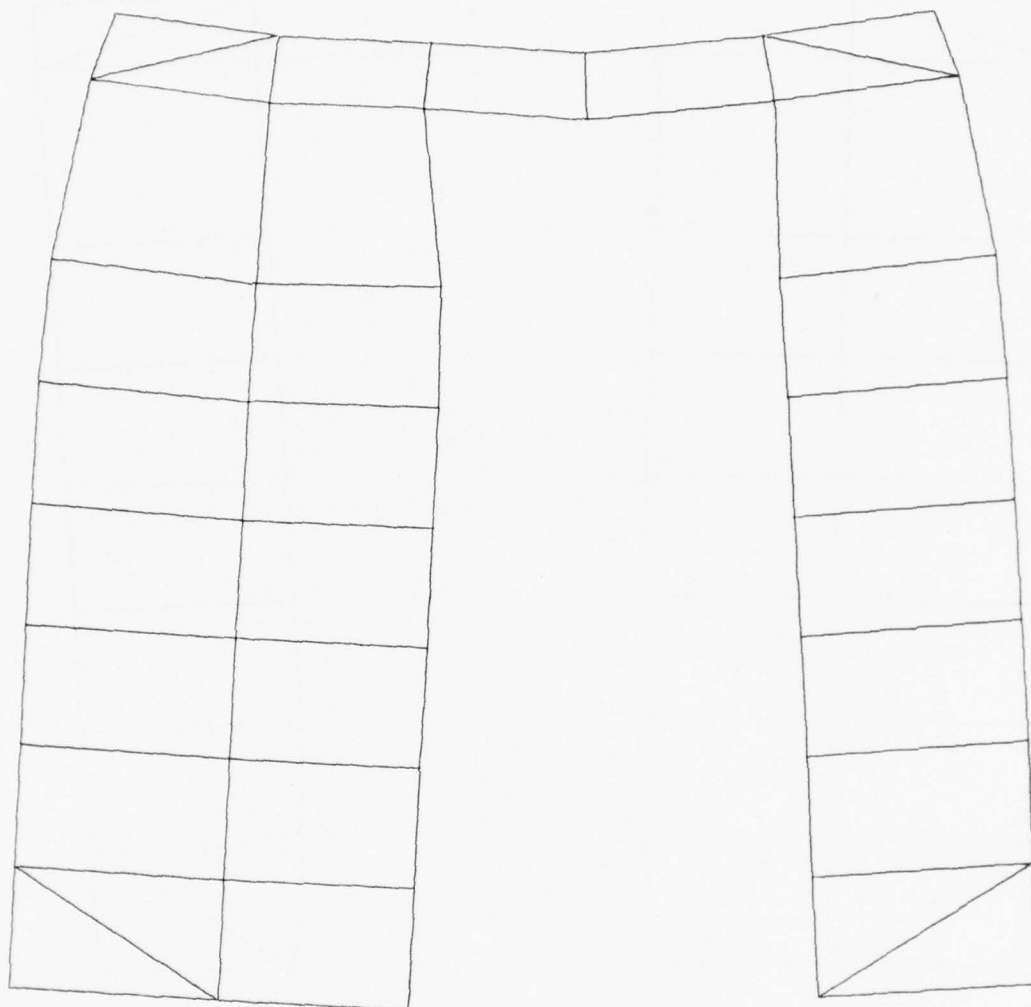


FIGURE 49 TEST NO. 6, LASHING.



**FIGURE 50. LASHING. LOAD NO. 1, DEFORMED BODY PLOT
PERSONNEL DOOR END. MAX. DEF. SCALED TO 0.254 m.**

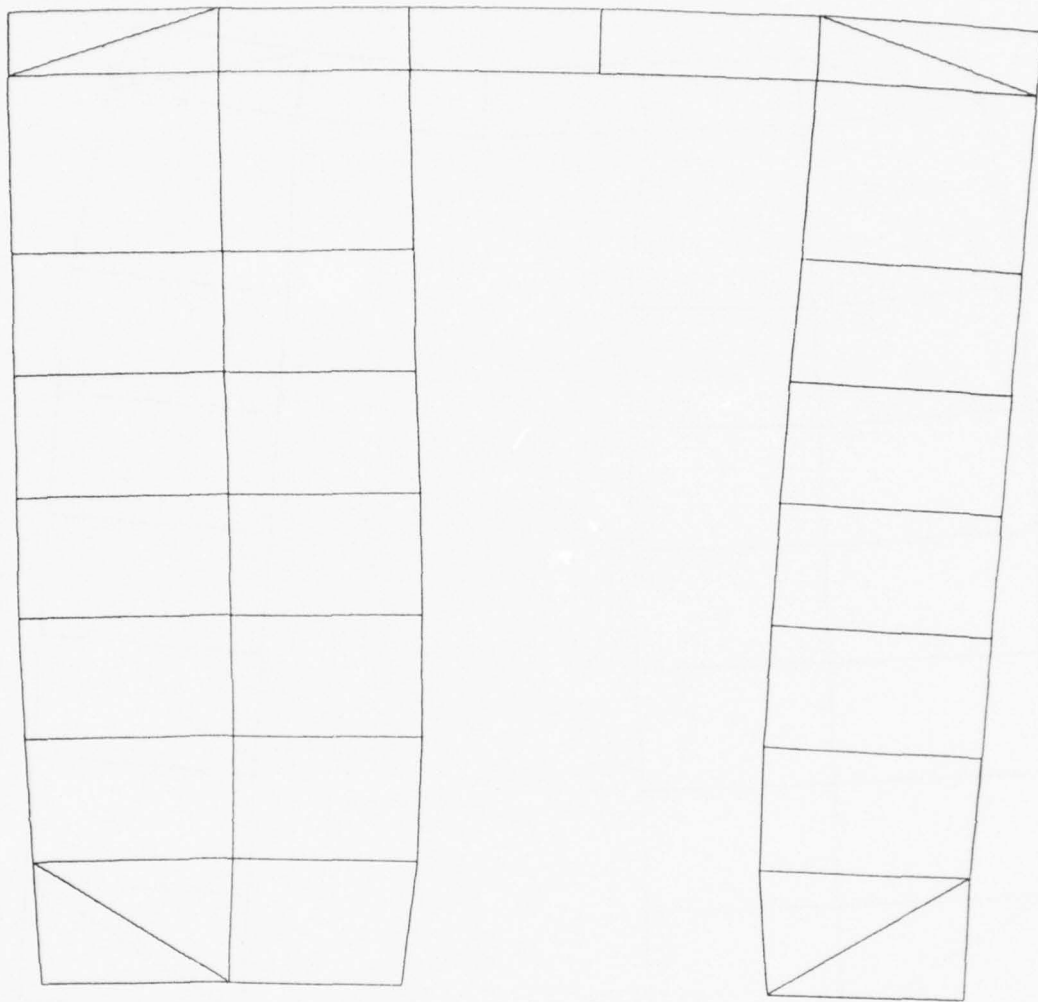


FIGURE 51. LASHING. LOAD NO. 3, DEFORMED BODY PLOT PERSONNEL DOOR END.
MAX. DEF. SCALED TO 0.254 m.

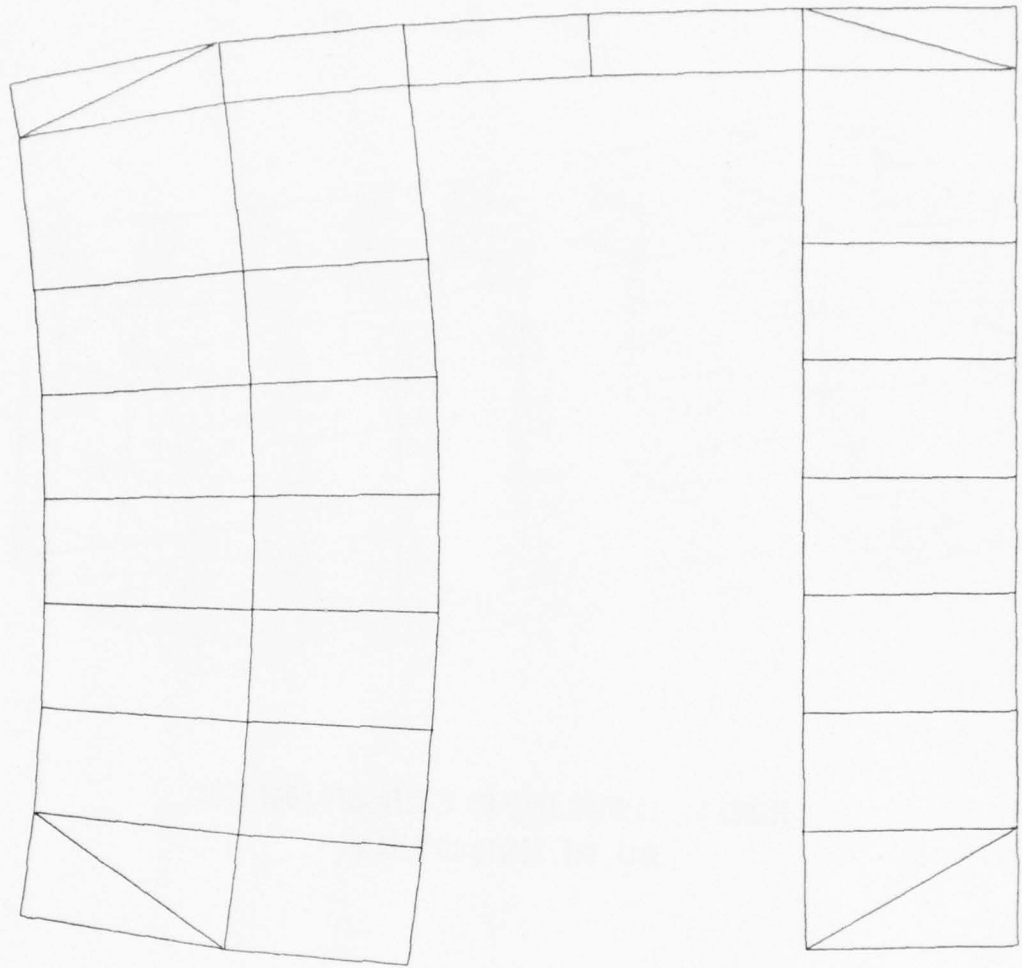


FIGURE 52. LASHING. LOAD NO. 5, DEFORMED BODY PLOT
PERSONNEL DOOR END. MAX. DEF. SCALED TO 0.254 m.

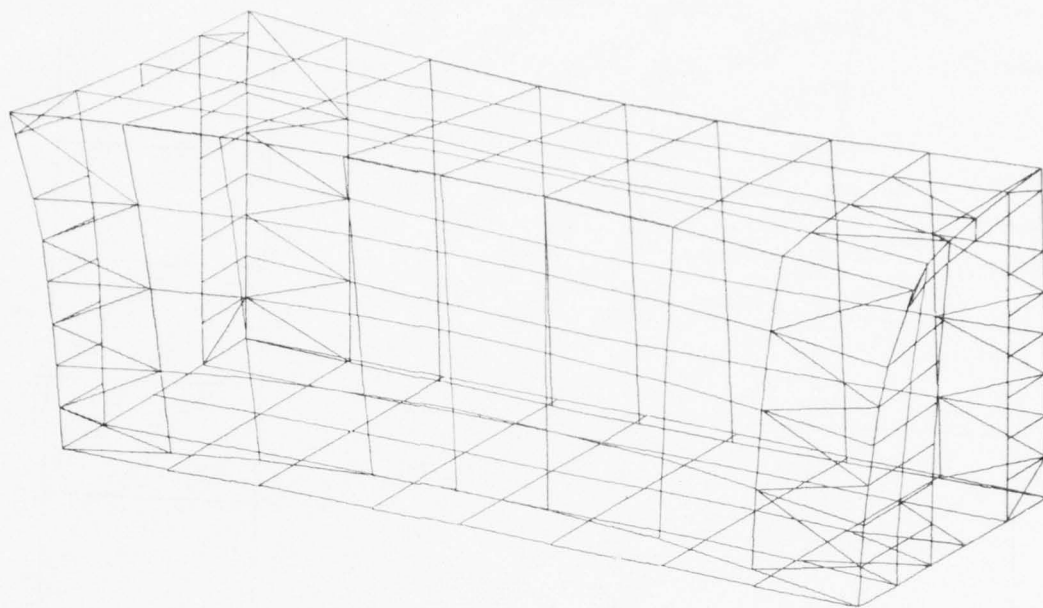


FIGURE 53. LASHING. LOAD NO. 8, DEFORMED BODY PLOT.
MAX. DEF. SCALED TO 0.381 m.

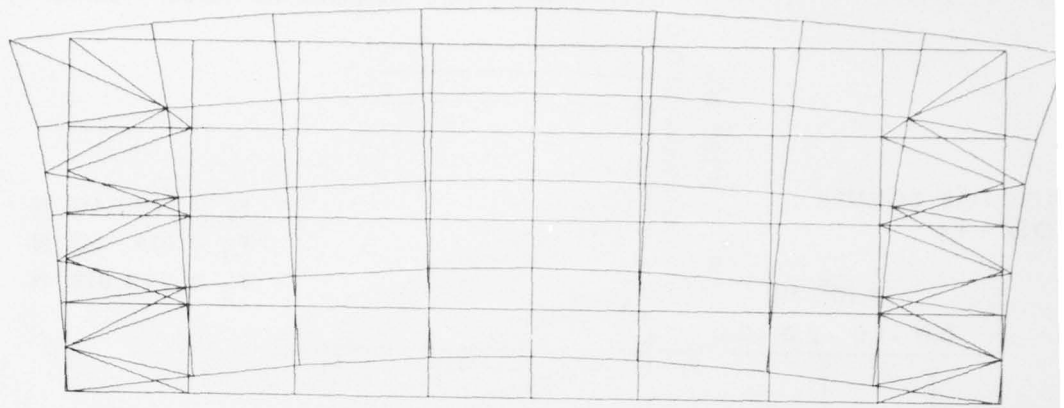


FIGURE 54. LASHING. LOAD NO. 8, DEFORMED BODY PLOT SIDE WALL
FARTHEST FROM XZ PLANE. MAX. DEF. SCALED TO 0.381 m.

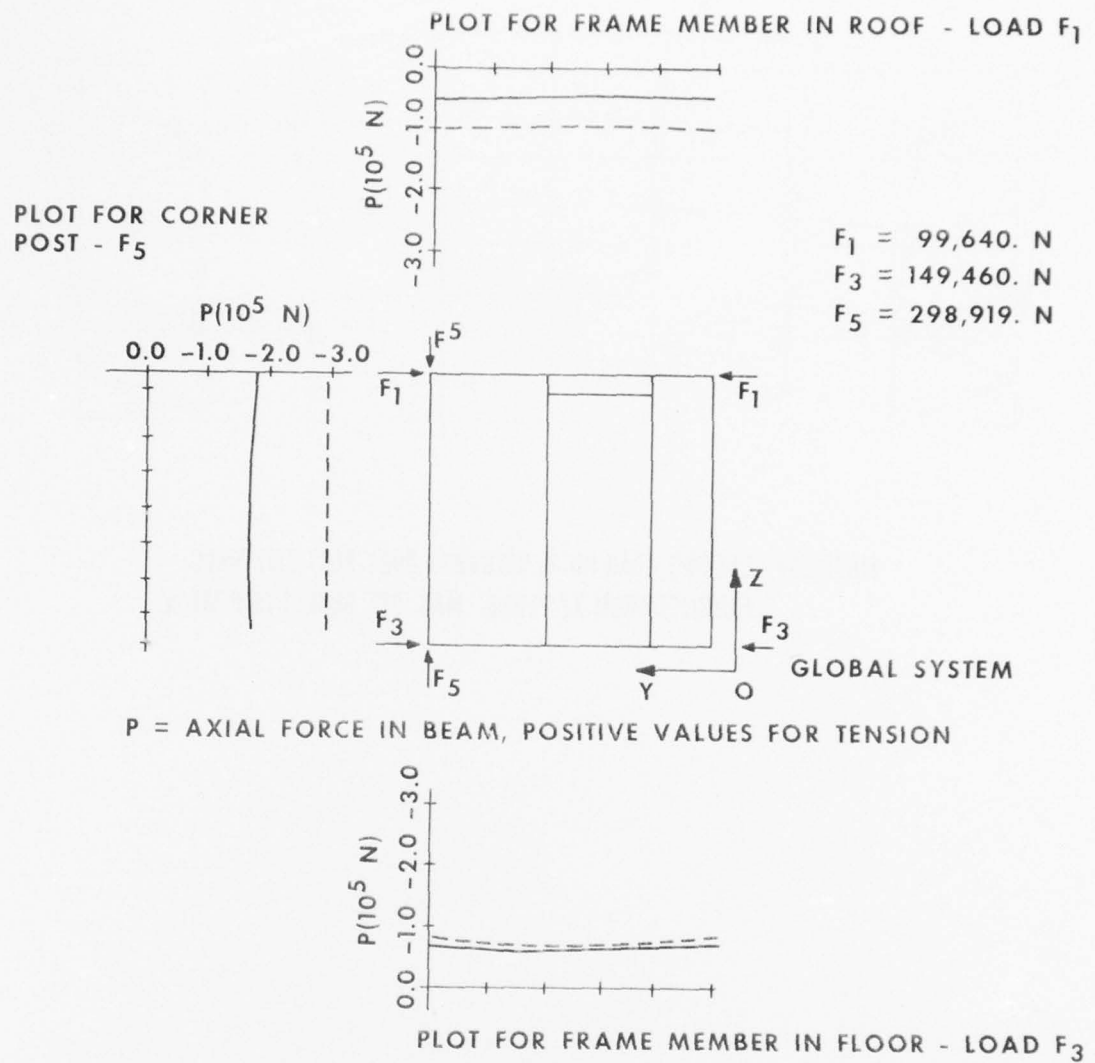


FIGURE 55 LASHING. AXIAL LOADS IN END WALL FRAME.

the major frame members (indicated in the figure) for load conditions F_1 , F_3 , and F_5 . Figure 56 shows similar results for loadings F_8 and F_9 . These figures indicate that when the panels do not act as part of the structure most of the load is carried by the beam between the opposed loads and very little, if any, is carried away by the adjacent framework, the exception being for the cases when frame members attached to the floor plate are loaded (floor plate was always considered part of the structure). In any event, the wall panels are seen to reduce the structural loading by at least $1/3$ if these panels are properly attached to the frame members.

A general survey of the stress levels for load cases F_1 , F_3 , F_5 , F_8 , and F_9 was made for both structural models. The results indicated that the stress levels in the panel's skins near the loaded frame member were about the same as the axial stress levels in the frame member. The results can be summarized as follows:

Load F_1 . For the structural model with wall panels the end wall panel's skins near the applied load were stressed to about $1/5$ yield, as was the loaded roof beam at the top of the end wall. Stresses at the other locations in the structure were negligible. The model without the wall panels had stress levels in the roof beam up to $1/2$ yield.

Load F_3 . The model with panels had stress levels in the panel skins at the bottom of the end wall of about $1/5$ yield (much higher applied load than F_1 but a strong floor was attached to help carry the load). The transverse beam under the floor and the panel skins near the load application point were also about $1/5$ yield. The model without panels had the stresses about $1/3$ yield in value, which represents a 50% increase over the model with panels.

Load F_5 . The model with panels had stresses in the end wall panel skins and in the corner post near the load application points of about $1/2$ yield in magnitude. The panel skin stresses were only $1/4$ yield midway between the applied loads. (This may just be a result of different distances from the corner post to the stress recovery points in the triangular and quadrilateral elements.) The model without panels had stresses in the corner post of $3/4$ yield. Stresses in the other members, of course, were negligible.

Load F_8 . The model with panels had very small stresses everywhere. The highest stresses in the panel skins and roof beam were $1/7$ yield in value at the locations near the applied loads. The model without wall panels had the stresses in the roof beam increase to $1/4$ yield value, still relatively small.

Load F_9 . This case is similar to the case of load F_3 in that the floor acts as part of both structural models. For the model with wall panels the stresses in the skins of the side wall panel near the load application point were $1/5$ yield as were the stresses in the I-beam under the floor, the extrusions in the side wall panel and floor panel, and the skins of the floor panel near the applied load. The model without the wall panels had the stresses in the same beams and floor panel skin locations increase to about $1/4$ yield.

P - AXIAL FORCE IN BEAM, POSITIVE VALUES FOR TENSION

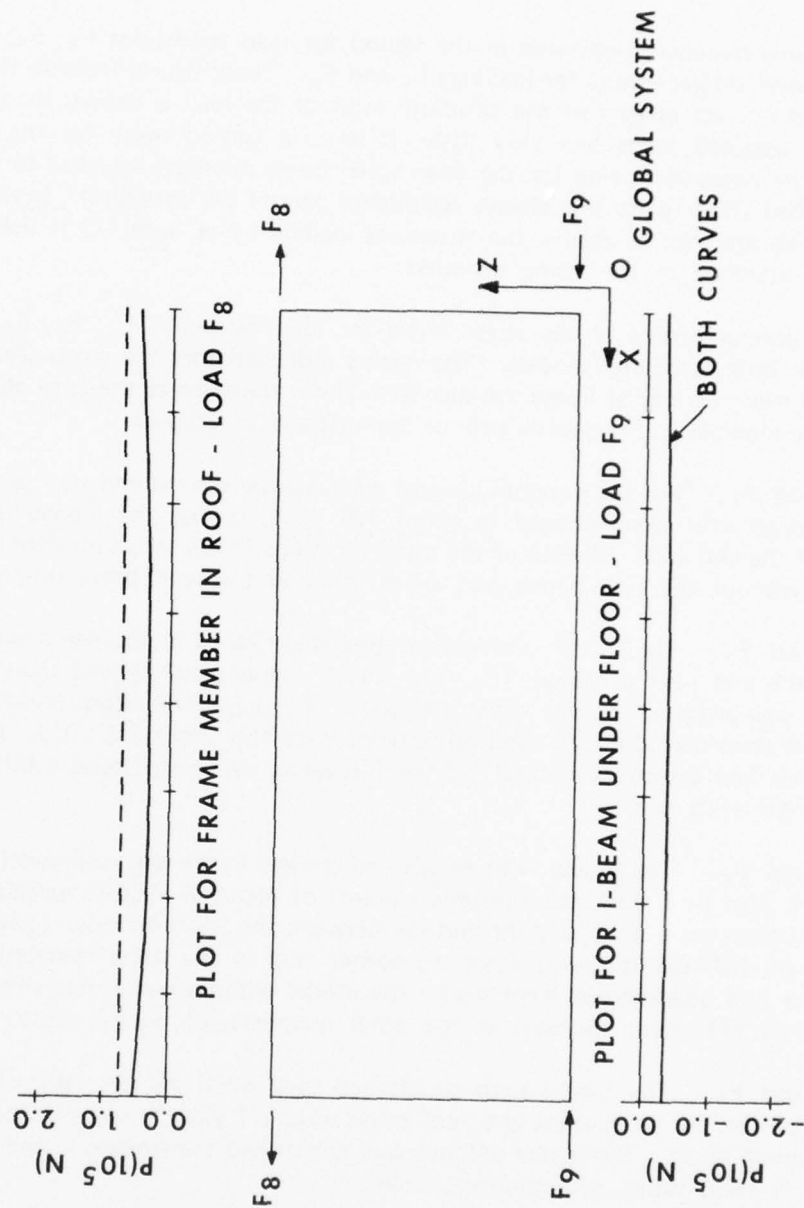


FIGURE 56 LASHING. AXIAL LOADS IN SIDE WALL FRAME FARTHEST FROM XZ PLANE.

g. Load No. 7 — End Wall Uniform Load

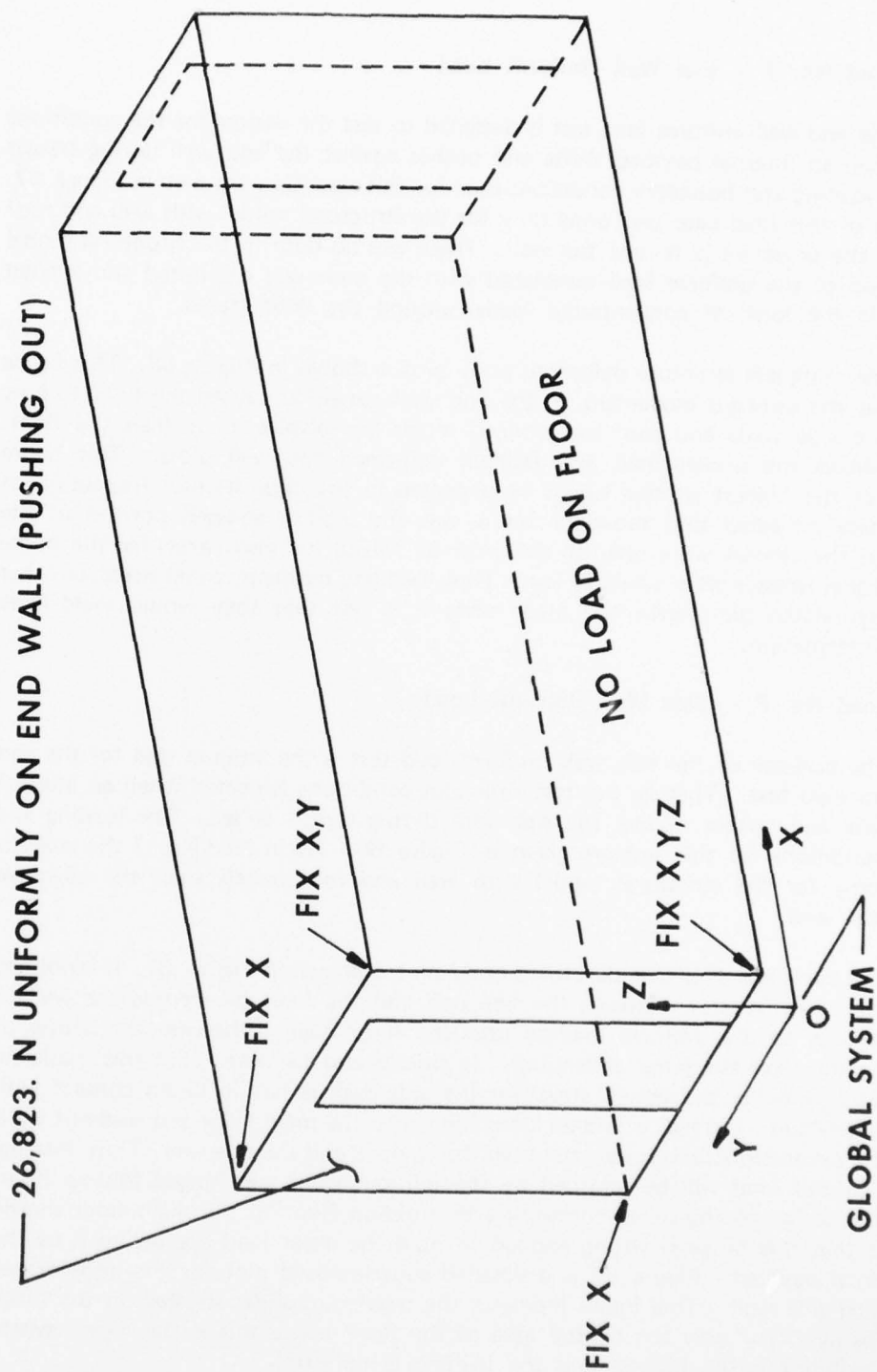
The end wall uniform load test is designed to test the shelter for the conditions expected when an internal payload shifts and pushes against the end wall during transit at sea. The loading and boundary conditions used for this analysis are shown in Figure 57. The analysis of this load case was done only for the structural model with wall and roof panels since the objective is to test the wall. There was no door in the structure, so the portion of the uniform load associated with the door was computed and applied uniformly (in the form of concentrated loads) around the door frame.

The complete structure deformed body plot is shown in Figure 58. This indicates that the outward movement of the end wall panel has caused the floor to rise up while the side walls and roof experienced much less displacement than the floor. Figure 59 shows the undeformed and (scaled) deformed end wall plots. This indicates that the highest stresses would be expected in the door frame. Inspection of the stress data indicated that the door frame was the highest stressed portion of the structure but the stresses were only on the order of 1/10th the yield stress for the members. Panel stresses were similarly low. Thus, bending moment, panel stress, and other typical design-related plots were not made since it is felt that they would yield no significant information.

h. Load No. 8 — Side Wall Uniform Load

The purpose of the side wall uniform load test is the same as that for the end wall uniform load test. That is, the test simulates conditions expected when an internal payload shifts and pushes against the side wall during transit at sea. The loading and boundary conditions for this test are given in Figure 60. As in load No. 7 the analysis was done only for the structural model with wall and roof panels since the objective is to test the wall.

The complete structure deformed body plot is shown in Figure 61. It indicates that the lack of connection between the side wall and the floor has caused the side wall to be quite flexible to the uniform loading near the floor edge (otherwise the deflection of the panel would have been large). It should also be noted that this result is conservative since in the actual structure the side wall is not in direct contact with the internal payload. Instead, a fold-up floor hinged to the main floor and fold-out walls (used for the expanded structure) are between the payload and the side wall. Thus, movement of this load will be retarded by the fold-out walls and hinged fold-up floor. However, the design of the hinge connecting the fold-up floor to the main floor should be made so that this hinge is strong enough to hold the shear load applied to it by the sliding internal payload. Figure 62 is a detailed superimposed plot for the undeformed and deformed side wall. This figure indicates the maximum shear stresses on the side wall would probably occur near the central area of the floor (since this is the region where the wall flexibility is the highest and the loading is uniform).



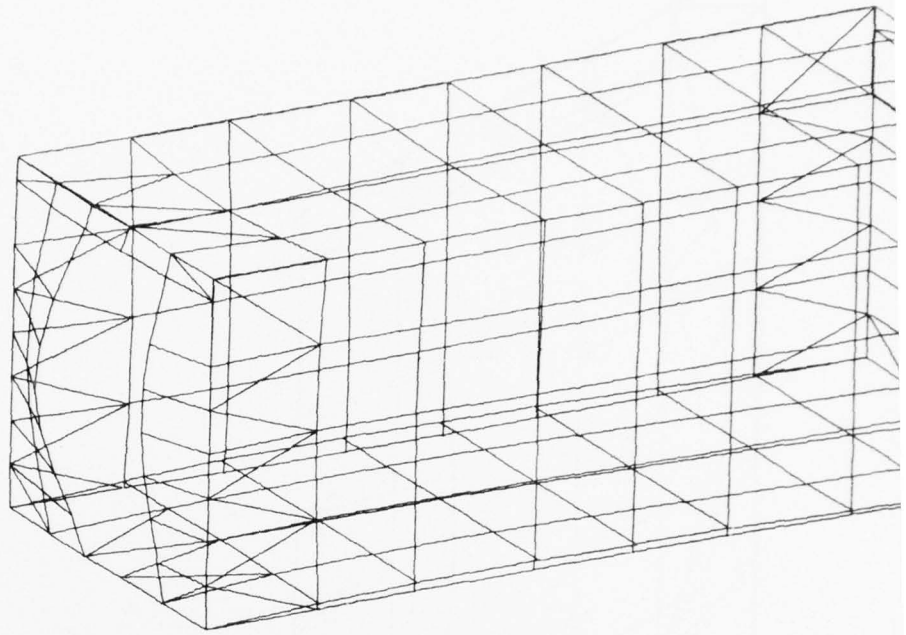


FIGURE 58. DEFORMED STRUCTURE PLOT - UNIFORM LOAD ON END WALL
MAX. DEF. SCALED TO 0.381 m.

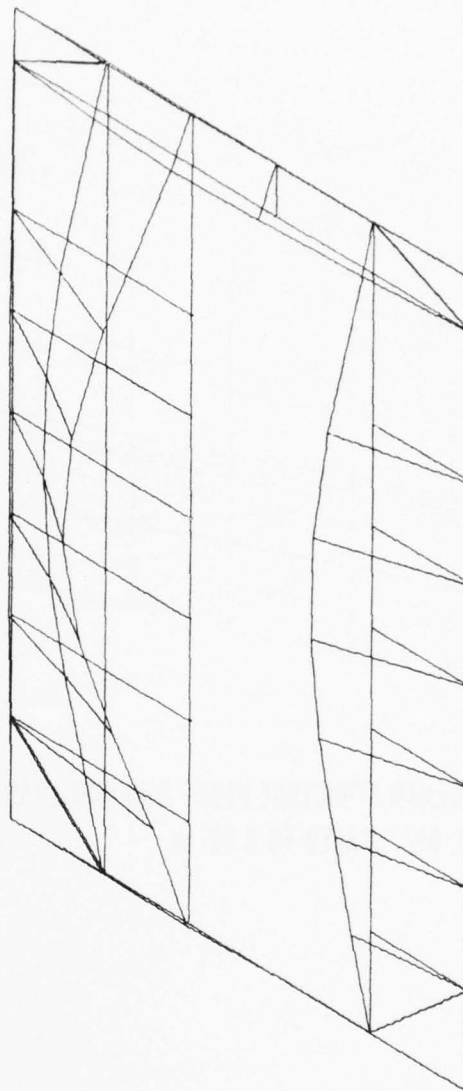
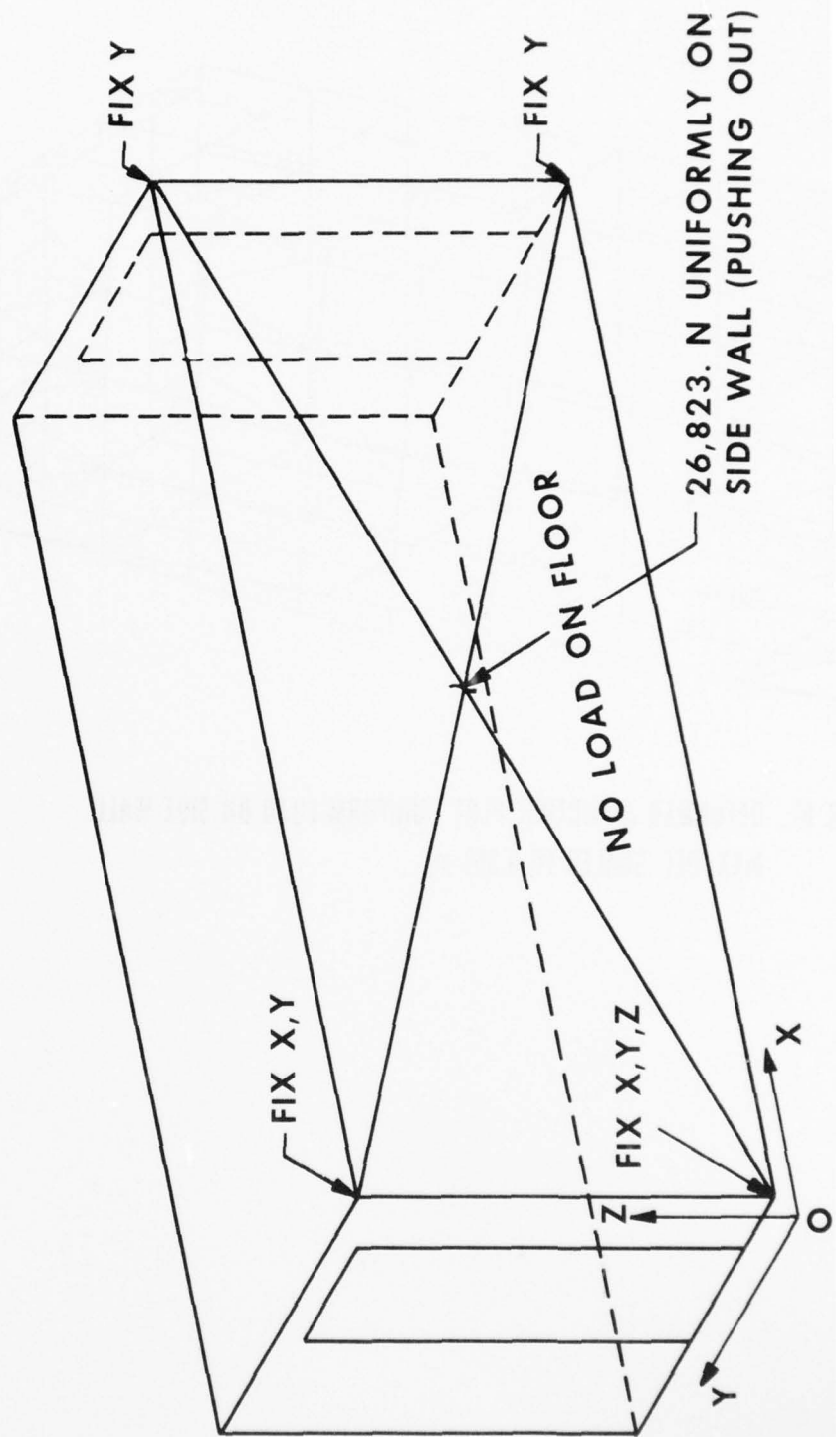
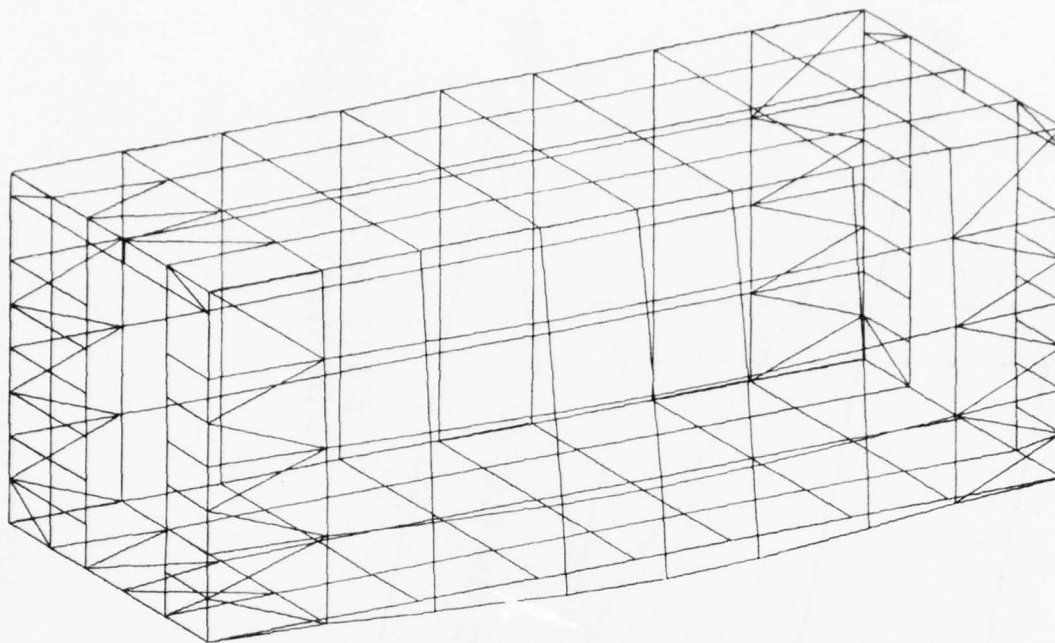


FIGURE 59. UNIFORM LOAD ON END WALL. SUPERIMPOSED PLOT FOR UNDEFORMED AND DEFORMED END WALL.





**FIGURE 61. DEFORMED STRUCTURE PLOT - UNIFORM LOAD ON SIDE WALL.
MAX. DEF. SCALED TO 0.381 m.**

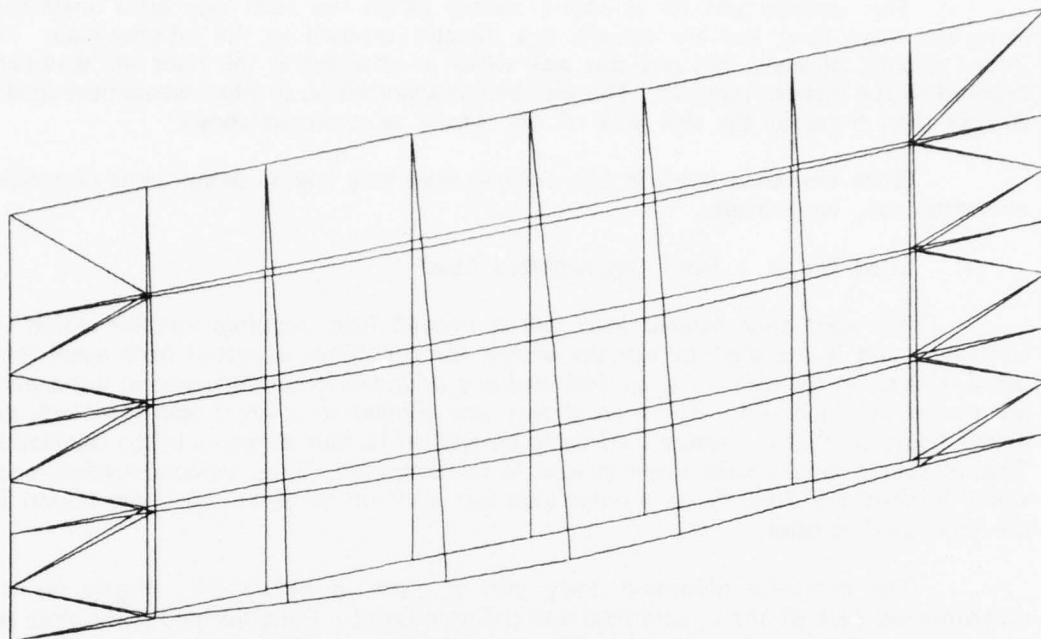


FIGURE 62. UNIFORM LOAD ON SIDE WALL. SUPERIMPOSED PLOT FOR UNDEFORMED AND DEFORMED SIDE WALL.

This analysis was for a 3-for-1 shelter which has both side walls unattached along the main floor but are actually not directly exposed to the internal load. The 2-for-1 shelter, however, has one side wall which is attached to the floor and is directly exposed to the internal payload. This wall being supported on all edges would have smaller stresses than those in the side wall of the 3-for-1 as analyzed above.

Since the stress levels in this analysis were very low no design plots of bending moments, etc., were made.

i. **Load No. 9 - Roof Concentrated Load**

The roof concentrated load test is derived from requirements for closed van containers and is designed to test the shelter for conditions expected from small items being stacked on the roof. The applied load and boundary conditions used in this analysis are shown in Figure 63. The load shown was applied to a larger area than indicated in the figure so that a pressure load could be applied to four elements in the calculation. This, of course, would cause lower stresses to be computed. Thus, a second loading model which applied the 2936 N as a point load was also run to obtain an upper bound for the computed stresses.

The complete deformed body plot is given in Figure 64. Figure 65 is a superimposed plot of the undeformed and deformed roof. The deformed body plots are, of course, scaled for visual effects. The actual maximum deformation in the center of the roof was only 0.7 cm which is very small. The element forces and stresses were also small for both loading models mentioned above, and thus this test required no further study.

4. COMPARISON OF MEASURED DATA AND COMPUTED DATA

A series of tests was performed on the shelter being analyzed in this report. For a detailed description of these tests see "Experimental Measurement of Strain and Acceleration Levels in a Rigid Wall Shelter Subjected to Environmental Loadings", reference 6.

A few comments to make clear the meaning of the computed and measured data is worthwhile at this point. The real structure is different from the model in several ways. The real structure has many fastening holes, corner plates on panels, bolts connecting two extrusions to make them act as one extrusion, fabrication errors, etc. Time was not taken to try and model these items since of most importance to the designer is a complete description of the behavior of all the panels and beams acting together to resist the loads. Trying to model the details of fastening holes, etc., in a complex structure of this type would complicate the analysis to an unjustifiable level. The modeling was thus directed at obtaining the gross behavior of the structure and so the comparison of the measured and computed data must be made with consideration of the details of the real structure. A short discussion of the measured and computed data for each of the tests conducted follows.

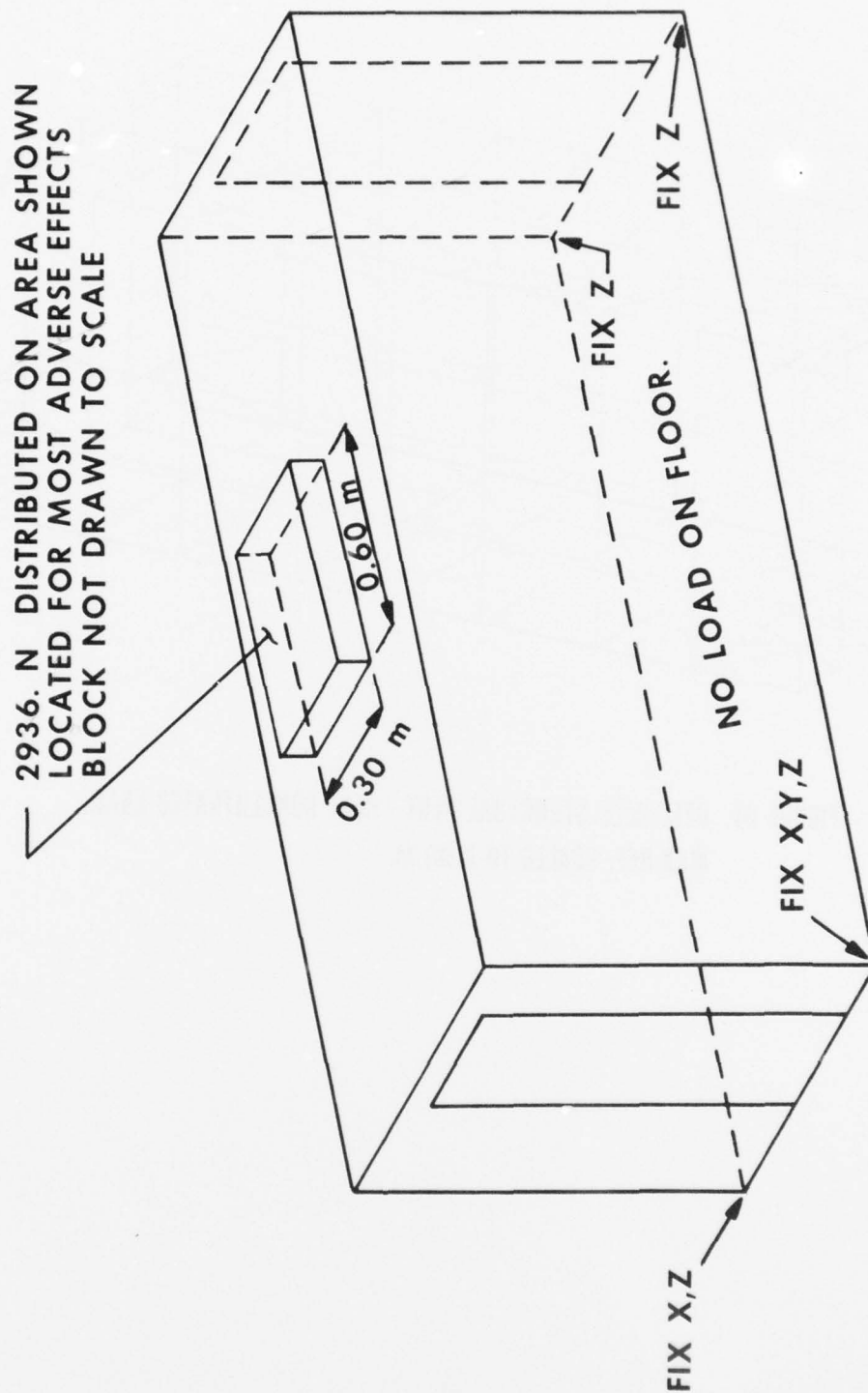
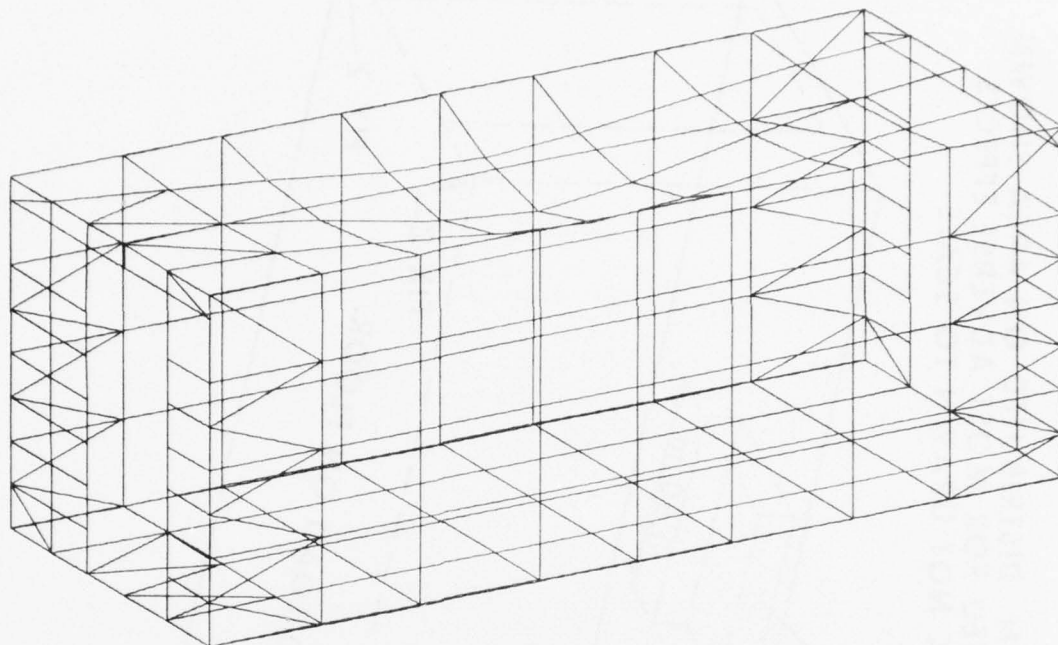


FIGURE 63 TEST NO. 9, ROOF CONCENTRATED LOAD



**FIGURE 64. DEFORMED STRUCTURE PLOT - ROOF CONCENTRATED LOAD.
MAX.DEF. SCALED TO 0.381 m.**

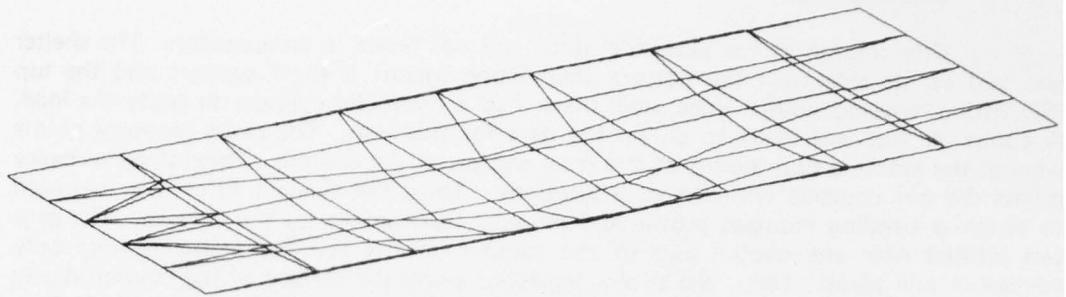


FIGURE 65. ROOF CONCENTRATED LOAD. SUPERIMPOSED PLOT FOR UNDEFORMED AND DEFORMED ROOF.

Stacking Test

One column at the personnel door end was tested in compression. The shelter was laid on its side with the bottom ISO fitting against a fixed support and the top ISO fitting, covered with a thick steel plate, had a hydraulic cylinder to apply the load. A computer run was made to obtain the data for this test. The stress recovery points were at the extreme fiber points of the cross section of the column. These stress recovery points did not coincide with the gage locations. Thus, the element force data was used to obtain a bending moment profile and an axial load profile for the column. The gage was located near one neutral axis of the column, so the bending moments were only needed in one plane. Next, the strains expected along the surface of the column where the gages were mounted, were computed from the bending moment and axial load data.

Figure 66 is a plot of the computed strain distribution and the measured strains from two gages. It should first be noted that the corner post had failed in a test done previous to this one and was not completely secured to the rest of the structure. Thus, higher measured strain data would be expected. The figure shows good agreement near the center of the column but poor agreement near the bottom of the column. Also, poor agreement between computed and measured strain data near the ISO fittings exists for other tests described below. This indicates that the modeling near the corners is not sufficiently detailed to accurately compute strain near the fittings (or corners).

It should be noted, however, that the computation of strain at the top of the column indicate a high strain due to the "offset" applied load. In fact, the computed value due to the "offset" load is close to the measured value found at the bottom end of the column. A close inspection of the column after the test indicated that the fixed support at the bottom of the column did not meet the ISO fitting evenly. In fact, it was an "offset" support. This faulty support may have induced strains similar to those computed for the top. This would then explain why the computed and measured data do not agree near the ISO fitting.

Restraint

The restraint test which requires the floor to be uniformly loaded and the bottom of the shelter to be longitudinally loaded in tension was made. The shelter's ISO fittings were resting on pads allowing the floor to bend under the uniform load which was applied. One end of the shelter was restrained from longitudinal translation and the other end fastened to a cable which supplied the tensile load. The stress (strain) recovery points of interest were along the I-beam under the floor. The gages were located at the neutral axis of the I-beam. Thus, only the computed axial stress data was needed for comparison to the experiment. It should be noted, however, that this axial stress data for the I-beam is a function of the floor bending. Also, the load was resolved into its static equivalent for application in the finite element model.

Figure 67 is a plot of the computed and measured strains in the floor I-beam indicated by its element numbers. The computed data near the ISO fittings is obviously not correct. However, the data agrees well in the region of elements 87 to 90 which represents one-half the length of the I-beam. The computed stress data for the floor

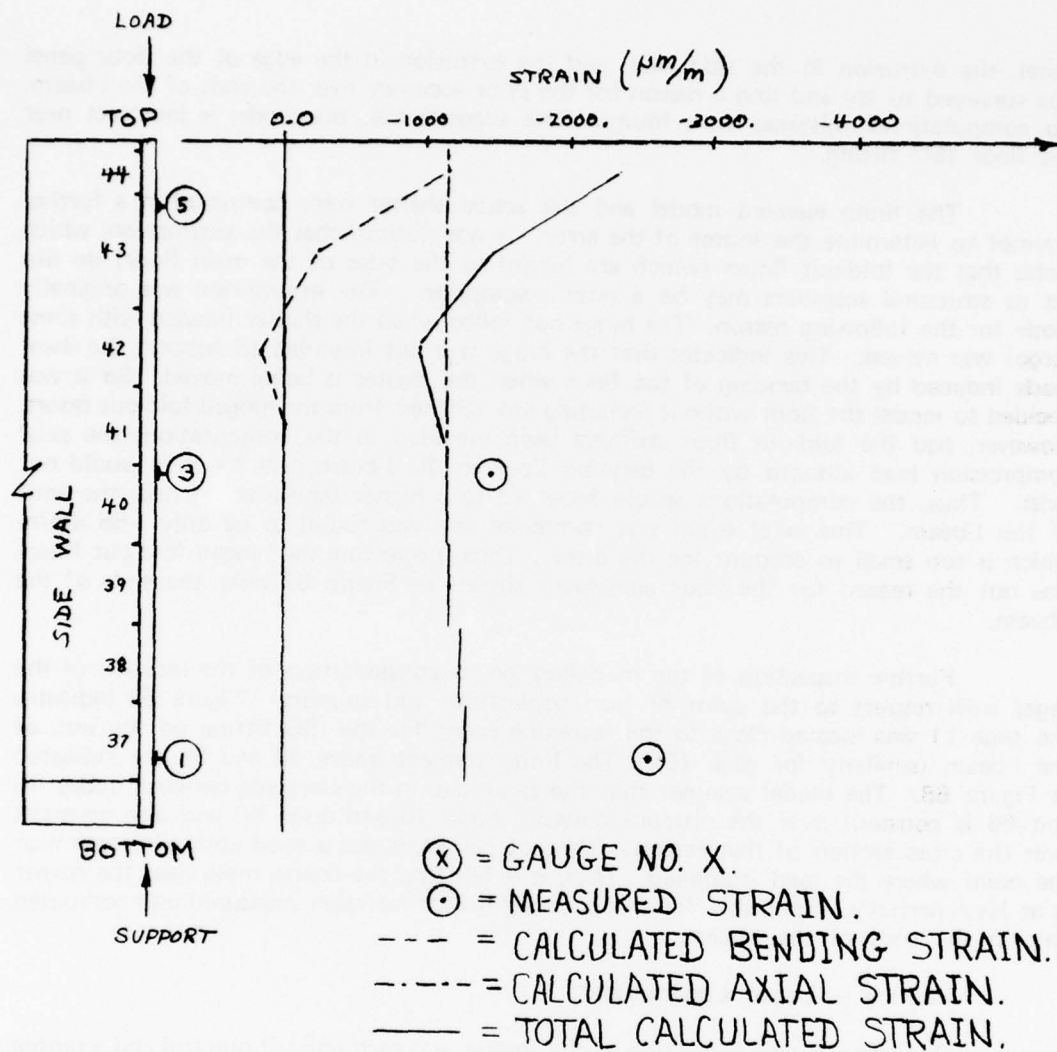


FIGURE 66. STACKING TEST. COMPUTED AND MEASURED STRAINS IN CORNER POST.

panel, the extrusion in the side wall, and the extrusion in the edge of the floor panel was surveyed to try and find a reason for the poor accuracy near the ends of the I-beam. No computational mistakes were found. This suggests that the model is incorrect near the floor ISO fitting.

The finite element model and the actual shelter were compared in a further attempt to determine the source of the error. It was noticed that the assumption, which states that the fold-out floors (which are hinged to the sides of the main floor) do not act as structural members may be a poor assumption. The assumption was originally made for the following reason. The hinge had failed when the shelter (loaded with some cargo) was moved. This indicates that the hinge was not intended to support the shear loads induced by the bending of the floor when the shelter is being moved. So it was decided to model the floor without including any stiffness from the hinged fold-out floors. However, had the fold-out floor stiffness been included in the computations the axial compression load induced by the bending floor in the I-beam near its ends would not exist. Thus, the computations would have led to a higher tensile strain near the ends of the I-beam. This axial strain was computed and was found to be only $-55 \mu\text{m/m}$ which is too small to account for the error. Thus, neglecting the hinged fold-out floors was not the reason for the poor agreement shown in Figure 67 near the ends of the I-beam.

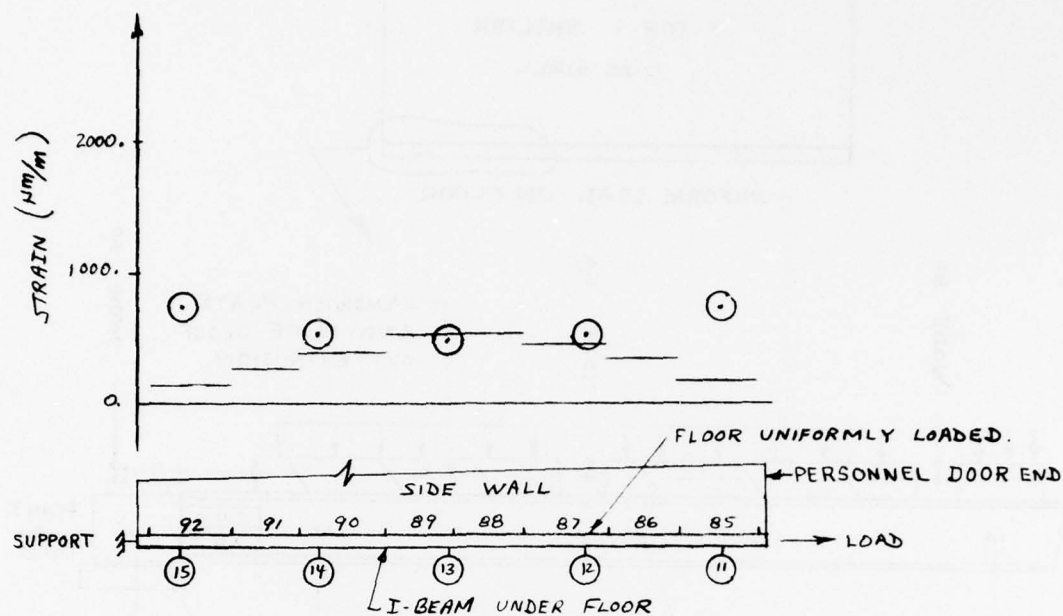
Further inspection of the modeling led to consideration of the location of the gages with respect to the point of load application and support. Figure 68 indicates the gage 11 was located close to the fastening point for the ISO fitting on the web of the I-beam (similarly for gage 15). The finite element nodes 40 and 66 are indicated in Figure 68. The model assumes that the axial load in the elements between nodes 40 and 66 is constant over the distance between node 40 and node 66 and also constant over the cross section of that region. This, of course, is not a good approximation near the point where the load is applied. Thus, it is felt that the coarse mesh near the corner is at least partially responsible for the poor agreement between measured and computed data at the ends of the I-beam.

Lashing — Upper Longitudinal

One upper longitudinal side of the shelter was restrained at one end and a tensile load was applied to the other end. Figure 69 contains the measured and computed strains for this test. Again, the agreement is good except at the ends. Figure 70 is a detailed view of the region near the ISO fitting where the measured strain is much higher than the computed strain. The corner plate indicated in the figure was not in the model and served to concentrate the loading near the end strain gage. Thus, the measured strains are higher than the computed strains near the end, since the model was not designed to approximate the complicated stress fields near the ISO fittings.

Lashing — Corner Post Compression

The corner post that was tested for the stacking load was tested in the lashing compression test. Figure 71 indicates the measured and computed strains. The central region, near gage 3, appears to agree well. However, the difference between the computed and measured strains increases near the ISO fitting.



○ = MEASURED STRAIN.
 — = CALCULATED STRAIN.
 XX = ELEMENT NUMBERS.

FIGURE 67. RESTRAINT. COMPUTED AND MEASURED STRAINS IN FLOOR I-BEAM.

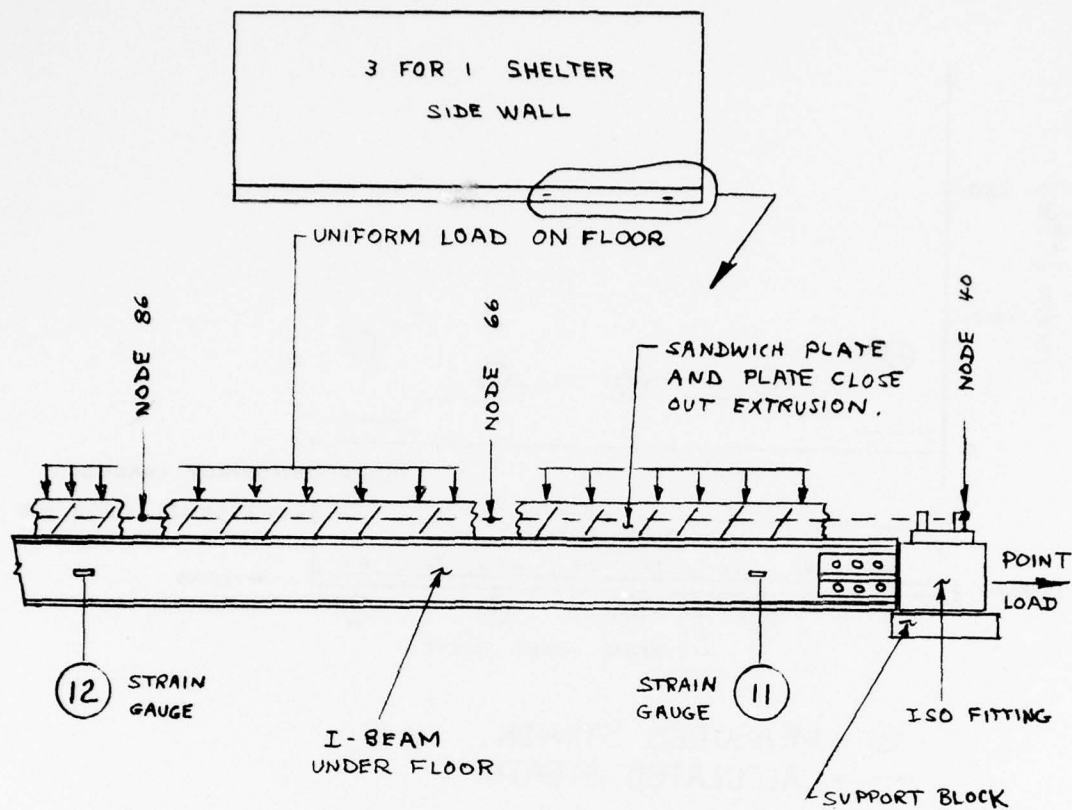


FIGURE 68. RESTRAINT. DETAILED VIEW OF FLOOR FRAME NEAR ISO FITTING.

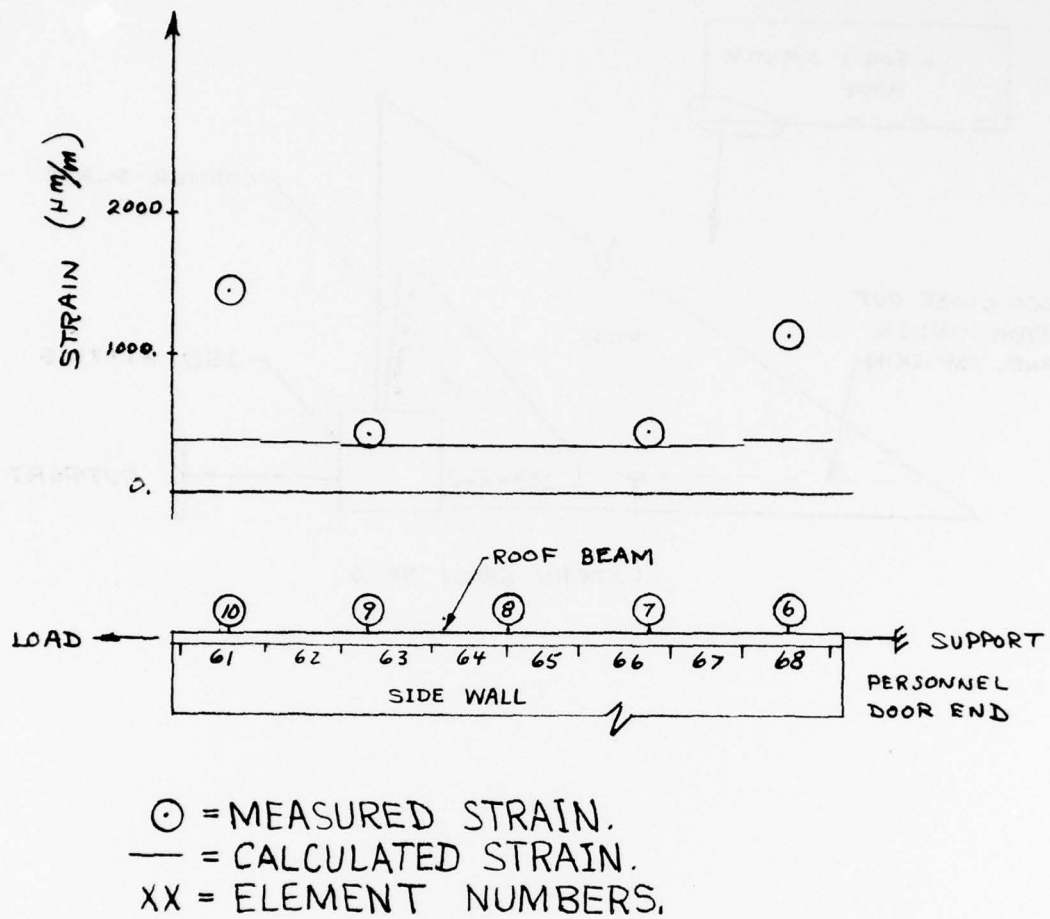


FIGURE 69. LASHING. COMPUTED AND MEASURED STRAINS IN ROOF BEAM.

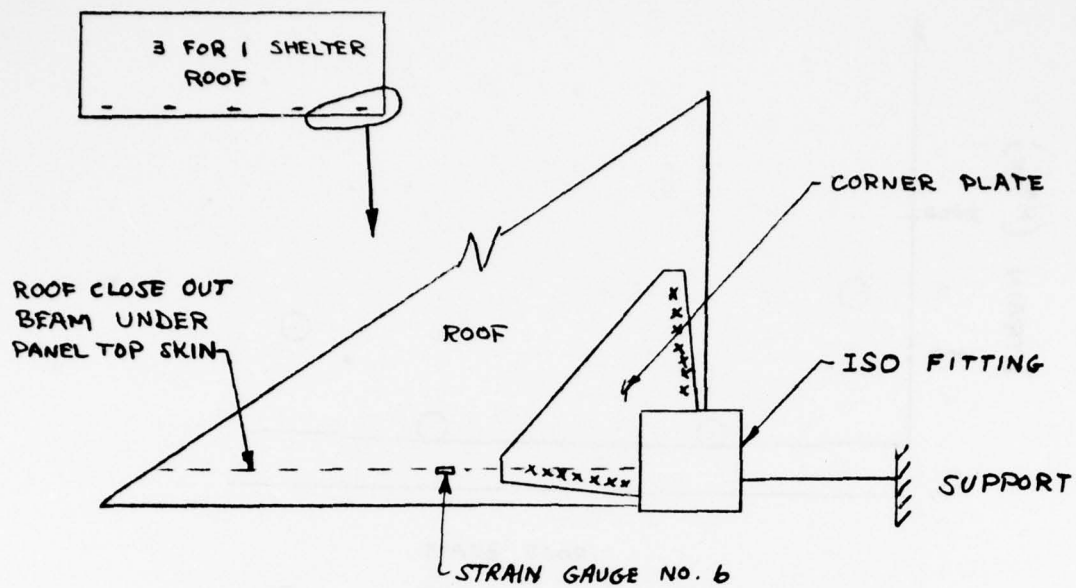


FIGURE 70. LASHING DETAILED VIEW OF ROOF NEAR ISO FITTING.

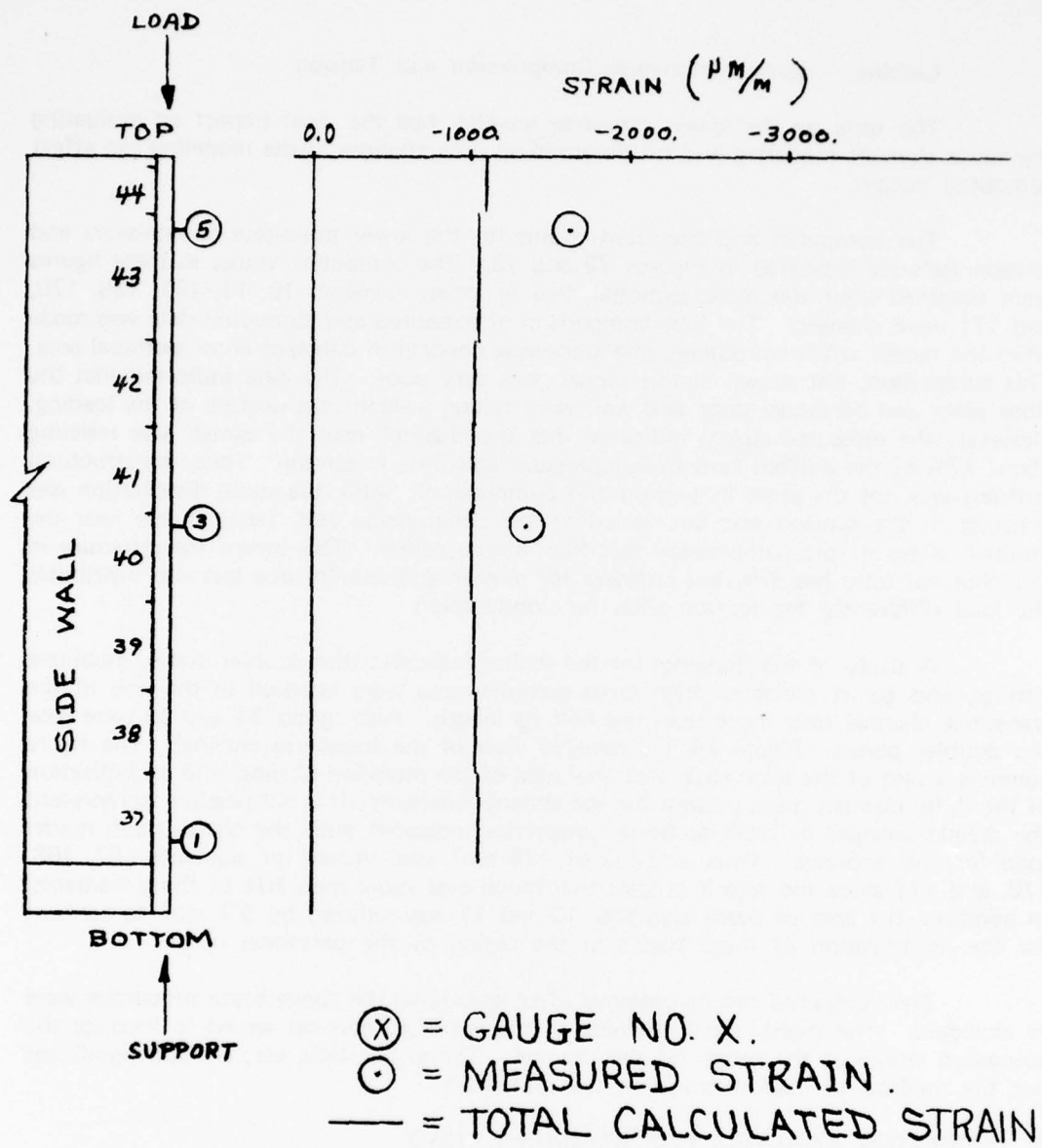


FIGURE 71. LASHING. COMPUTED AND MEASURED STRAINS IN CORNER POST.

Lashing — Lower Transverse Compression and Tension

The tests on the lower transverse member had the most impact on evaluating the finite element modeling and on determining how changes in the modeling can affect computed output.

The computed and measured strains for the lower transverse compression and tension tests are indicated in Figures 72 and 73. The computed results in these figures were obtained after the cross sectional area of beam elements 10, 11, 167, 168, 170, and 171 were changed. The first comparison of measured and computed data was made from the model which considered the transverse channel of constant cross sectional area. This comparison, not shown in this report, was very poor. The data indicated that the floor plate and personnel door end wall were taking a significant portion of the loading. However, the measured strains indicated that the channel, near the center, was resisting about 72% of the applied load in compression and 94% in tension. Thus, the structural stiffness was not the same in tension and compression. Also, the strain distribution was constant in the tension test but varied in the compression test, being higher near the doubler plates in the compression test than at the center. This means the structure in this area not only has different stiffness for tension and compression but also distributes the load differently for tension than for compression.

A study of the drawings for the shelter indicated that doubler plates, mobilizer fittings, and gusset plates of high cross sectional area were fastened to the web of the transverse channel over more than one-half its length. Also, gages 31 and 33 were near the doubler plates. Figure 74 is a detailed view of the transverse channel. The figure contains a plot of the total cross sectional area of the modified channel and an indication of the finite element mesh pattern for the channel elements. It is not possible to represent the drastic changes in cross sectional properties indicated with the coarse mesh model used for this analysis. Thus, a value of 110 cm^2 was chosen for elements 167, 168, 170, and 171 since the area is at least that much over more than 70% of those elements. In addition, the area of beam elements 10 and 11 was reduced by 5.7 cm^2 to account for the modification of these beams in the region of the personnel door.

The computed results obtained after modifying the above beam properties were as expected. The higher axial stiffness of the modified channel served to increase the computed strains at the center of the channel. The errors, however, are still significant but the method of load distribution was predicted.

5. BUCKLING ANALYSIS FOR STACKING LOAD

The design of a structure should always include investigations to determine if the structure could become unstable. The structure could be simply underdesigned for the intended load or components of the structure may not function properly causing an unexpected failure. The buckling analysis described below was made to determine if the complete structure would buckle under the stacking load indicated in Figure 24 and to determine the effects that the wall and roof panels have on the stability of the structure.

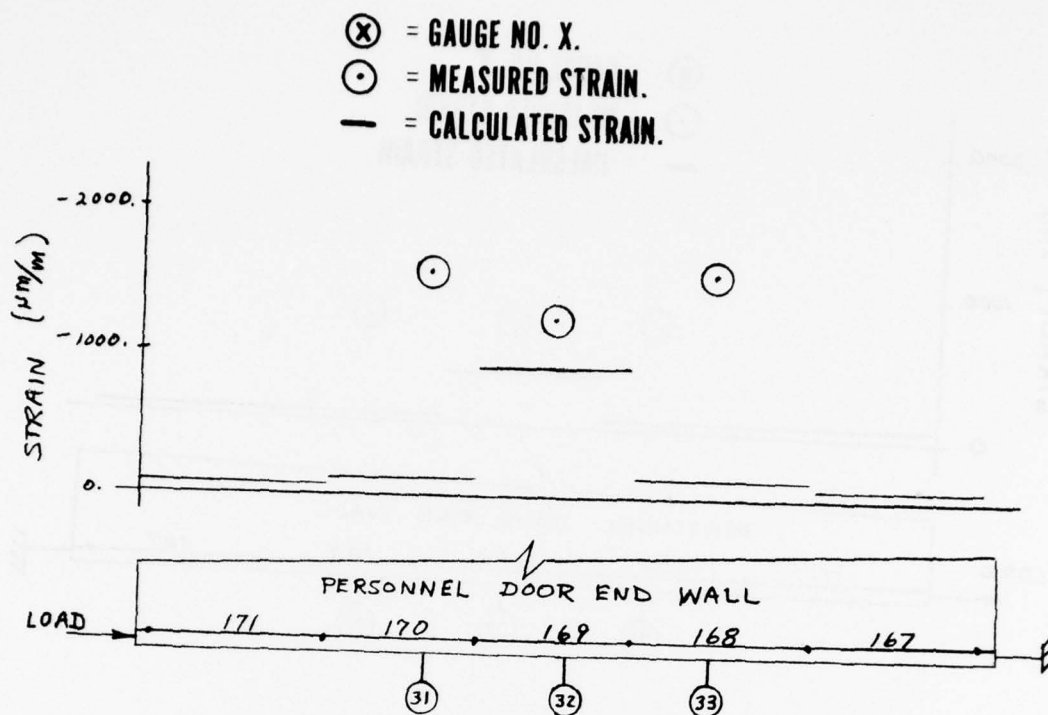


FIGURE 72. LASHING. COMPUTED AND MEASURED STRAINS FOR
 LOWER TRANSVERSE COMPRESSION TEST.

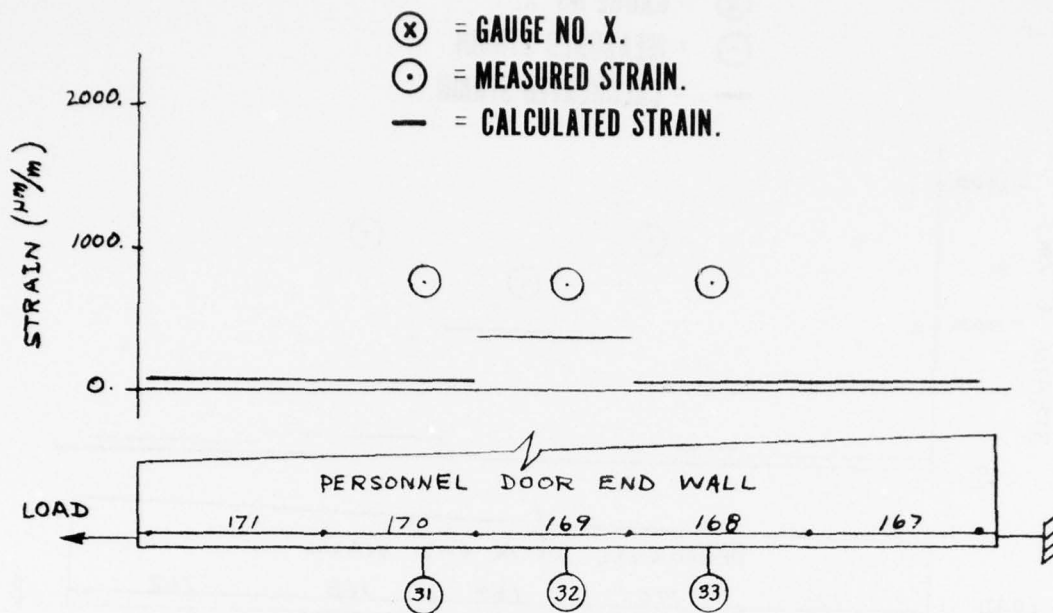


FIGURE 73. LASHING. COMPUTED AND MEASURED STRAINS FOR LOWER TRANSVERSE TENSION TEST.

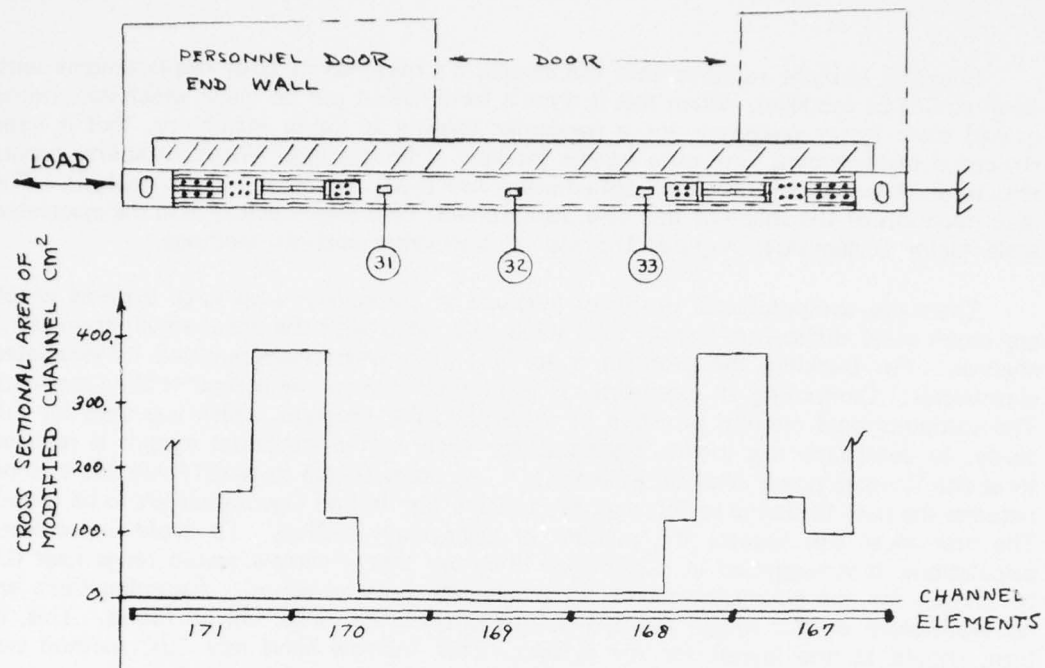


FIGURE 74. LASHING. DETAILED VIEW OF TRANSVERSE CHANNEL
AND CHANNEL CROSS SECTIONAL AREA.

Buckling analysis requires that the structure's response to large displacements with small strains be modeled. When this is done a formulation can be made which determines a load scale factor necessary for a particular loading to cause instability, that is large structural displacement without a further increase in the loading. When instability occurs structural elements deform to a configuration not predicted by the static analysis. The determination of the shape of this new displacement field (eigenvector), and the associated scale factor (eigenvalue) requires the use of eigenvalue analysis methods.

There are computational problems involved in eigenanalysis on large systems which are much more difficult to handle than those associated with the linear small strain static analysis. For buckling the problem is to find the lowest eigenvalue and its associated eigenvector. Computing all eigenstates is prohibited due to the computer time required. The computational method provided in the NASTRAN program, which was used for this study, to determine the lowest eigenstate for each of the structural models is referred to as the "inverse power method with shifts." As programmed in NASTRAN this method requires the user to define search regions in which the desired eigenvalues are to be found. The user must also request the number of eigenvalues desired. To avoid unnecessary calculations, it is suggested in NASTRAN literature that a narrow search range near 0.0 be chosen for the eigenvalue search by the inverse power method. Assuming there are no eigenvalues in this range, the lowest one outside the range will be found. This, in turn, should be the lowest for the system. This "narrow band near 0.0" method was found to be very useful.

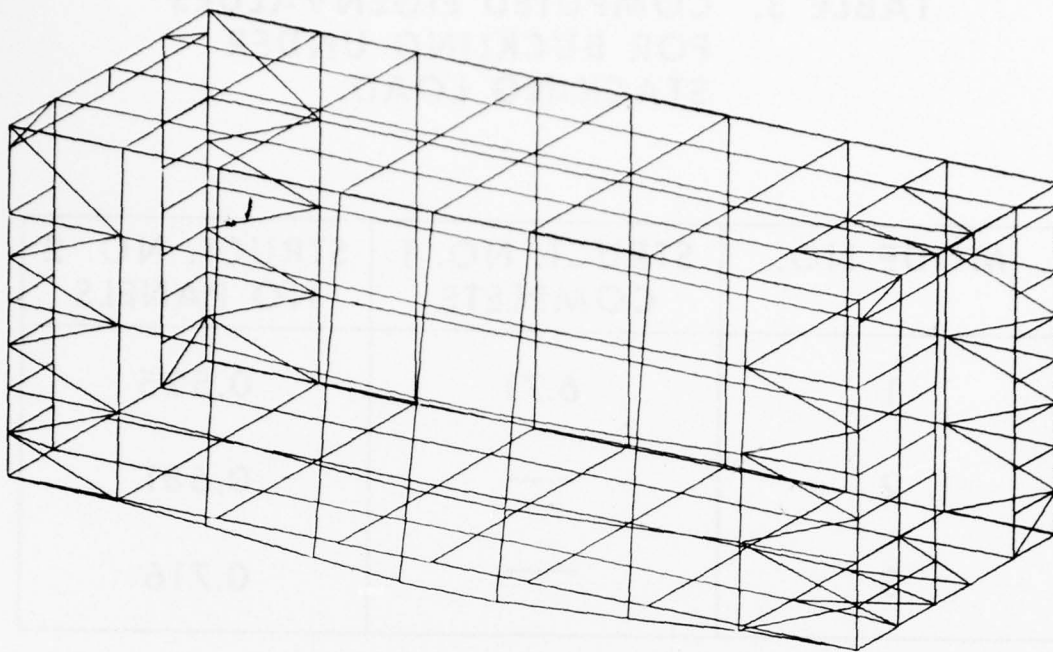
Table 3 gives the three lowest eigenvalues for the structural model which does not have wall and roof panels. The table also includes the lowest eigenvalue associated with the complete structure. To assure that these values were correct another set of computations were made in which the search range was expanded so that the upper bound of the search range was slightly less than the lowest eigenvalue previously predicted. The same eigenvalues were computed again, and thus there are none below these.

The table indicates that if all the beams and panels are acting together to resist the loading, then buckling is not a problem since the structure is stable until loaded by 6.7 times the design load. However, if the panels are not properly attached to the beams (structure without wall and roof panels) then the critical loading is only 0.52 times the design load that is, buckling will occur at half of the specified load. Thus, this buckling analysis has shown that it is imperative to use the panels as load-carrying members if the structure is to be subjected to the stacking load. In general, one could change the beam properties (especially the radius of gyration) of the frame members and determine other similar structures which resist buckling under the stacking load and for which the total frame weight is less.

It is interesting to study the eigenvectors (mode shapes) associated with the eigenvalues in Table 3. To this end Figure 75 is a plot of the first buckling mode of the structure which utilizes the wall and roof panels when responding to the loading. The plot indicates that when all four corners are "offset" loaded as indicated in Figure 24, the side wall farthest from the personnel door frame will bow out of plane when the buckling load is reached. It should be noted that this behavior of the complex structure was not obvious a priori and thus could not have been estimated by simpler numerical procedures.

**TABLE 3. COMPUTED EIGENVALUES
FOR BUCKLING UNDER
STACKING LOAD.**

MODE NO.	STRUCT. NO. 1 COMPLETE	STRUCT. NO. 2 NO PANELS
1	6.71	0.525
2	—	0.681
3	—	0.716



EIGENVALUE = 6.71

FIGURE 75. BUCKLING MODE NO. 1 FOR COMPLETE STRUCTURE SUBJECTED TO STACKING LOAD.

The first buckling mode for the structure without wall and roof panels subjected to the stacking load is indicated in Figure 76. The major frame members buckled into shapes similar to those one would expect by analogy to shapes predicted by the simpler Euler buckling analysis methods used on single frame members. Figure 77 indicates the second mode for this structure. It is interesting to note that in the second mode the frame members on the side farthest from the personnel door contain the maximum amplitude in the eigenvector. This is similar to the case for the first mode of the structure with wall and roof panels. However, the first mode of the structure without wall panels has its maximum component unexpectedly occurring on the side wall nearest to the personnel door.

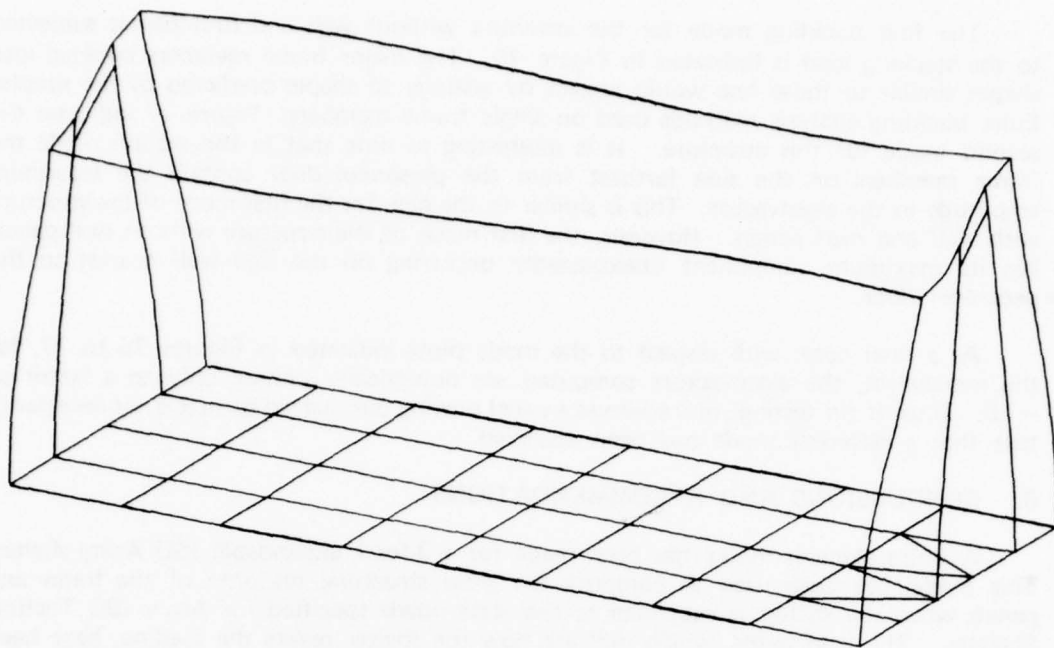
As a final note, with respect to the mode plots indicated in Figures 75 to 77, for the nonanalyst, the eigenvectors computed are numerically unique only to a factor of -1.0 . Thus, if (in testing) one observes a panel bowing out instead of in it is not necessarily true that a different mode has been observed.

6. CONCLUSIONS AND RECOMMENDATIONS

A finite element model has been made for a 3-for-1 expandable ISO Army shelter. This model has been used to compute the gross structural response of the frame and panels when the shelter is subjected to the static loads specified for Army ISO Tactical Shelters. The load paths, which indicate how the shelter resists the loading, have been displayed and described in detail for each load configuration. These load paths contain the type of technical information needed by shelter engineers interested in refining the design of the 3-for-1 shelter. The model has also been evaluated against measured data to determine what data can be used directly from this type of finite element analysis and what data must be determined by more refined analyses.

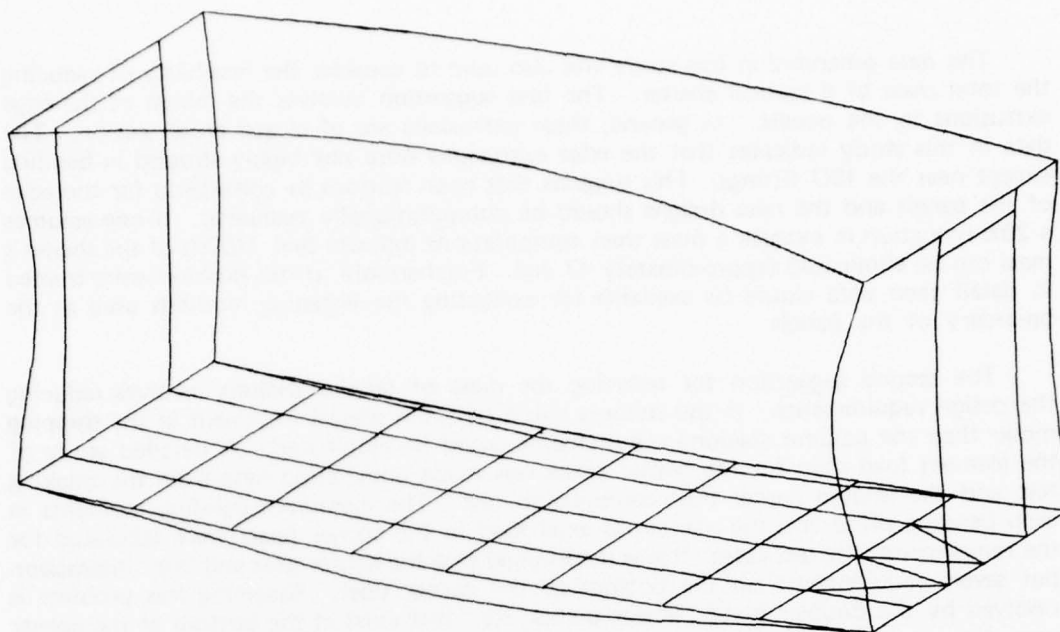
The data presented in this study indicated that the wall panels are essential structural members. They were shown to share a major portion of the "axial" loading with frame members. The wall panels were also shown to be useful for keeping low bending moments in the framework except near the ISO fittings. The section on buckling under the stacking load indicated that the shelter is much more stable when the frame and panels are designed to act together.

Finite element modeling and analyses of tactical shelters can be used to improve the design of these shelters. As an example of how it can be used, consider the main floor of the shelter. The data on the lift tests indicated that the floor was not designed well for these loads. Although there were high stresses involved, this analysis indicates the basic design itself is at fault. The floor was attached to fold-out floors along each longitudinal edge of the floor by a nonstructural hinge. The flexibility of the floor in the "Z-axis" direction was shown to be high in this analysis. The "Z-axis" flexibility of the fold-out floors in the shipping configuration is, of course, low since the panels are loaded in plane. This incompatibility of flexibilities is the design fault. The result is a highly stressed hinge which may either fail or eventually operate improperly. A suggested fix for this problem would be to connect the floor to the side wall in the shipping configuration or to design the fold-out floor hinges so that the fold-out floor can provide support for the main floor.



EIGENVALUE = 0.525

**FIGURE 76. BUCKLING MODE NO. 1 FOR STRUCTURE WITH NO WALL AND
ROOF PANELS SUBJECTED TO STACKING LOAD.**



EIGENVALUE = 0.681

**FIGURE 77. BUCKLING MODE NO. 2 FOR STRUCTURE WITH NO WALL AND ROOF PANELS
SUBJECTED TO STACKING LOAD.**

The data generated in this study was also used to consider the feasibility of reducing the total mass of a tactical shelter. The first suggestion involves the design of the edge extrusions in the panels. In general, these extrusions are of closed cross section. The data in this study indicates that the edge extrusions were not highly stressed in bending except near the ISO fittings. This suggests that open sections be considered for the edge of the panels and the new designs should be computationally evaluated. If one assumes a 20% reduction in extrusion mass then computations indicate that 1/50th of the shelter's mass can be eliminated (approximately 47 kg). Furthermore, if this problem were treated in detail then data would be available for evaluating the fastening methods used at the boundary of the panels.

The second suggestion for reducing the mass of tactical shelters involves reducing the design requirements. If the shelters could be given special treatment in the shipping mode then the column stacking requirements could be eliminated. A detailed study of the element load data for the corner posts was made eliminating data from the stacking test and the lashing corner post compression test. The maximum bending moments in each bending plane and the maximum axial load in the corner posts were tabulated for the remainder of the test cases. It was determined that the corner post and floor interaction put severe requirements on the bottom of the corner post. Assuming this problem is resolved by the doubler plates, gusset plates, etc., that exist at the bottom of the corner post, the maximum load data on the remainder of the corner posts was considered. The lifting tests and the transverse racking test were found to induce the highest loads in the corner posts. A conservative redesign of the corner post indicated the corner post mass could be cut by 45%. The total mass reduction for the four corner posts was then estimated as 24 kg (one percent of total shelter mass). Also, if the requirements were changed this drastically, then a new design of the entire structure would be required. However the other reductions would not be as extreme.

A summary of conclusions and recommendations is as follows:

- a. Finite element modeling of tactical shelters is useful for providing technical data on load paths in the shelter.
- b. A coarse finite element model of the entire structure provides load data valid everywhere except near supports, fasteners, and other mechanisms which cause high stress gradients.
- c. Moderate mass savings may be obtainable if the edge extrusions in the panels are redesigned for shelters which have corner posts separate from the panels.
- d. The method of hinging a fold-out panel to the main cargo floor is expected to place severe requirements on the hinge design. If hinge failures occur it is suggested that the cargo floor be connected to the outboard panel in the shipping mode by a method which reduces the hinge loading.
- e. Parameter studies should be conducted with the finite element model. In these studies the design requirements and/or various frame and panel structural combinations could be considered and varied. Such a study would yield technical data directing feasible alternative designs.

f. The wall panels have the ability to share significant portions of the static loadings with the basic framework.

This document reports research undertaken at the US Army Natick Research and Development Command and has been assigned No. Natick/TR-79/023 in the series of reports approved for publication.

REFERENCES

1. ANSI MH 5.1-1971, "Basic Requirements for Cargo Containers," November 18, 1971
2. Richard H. MacNeal. "The NASTRAN Theoretical Manual (Level 15)," COSMIC, University of Georgia, Georgia, April 1972
3. C. A. Felippa. "Refined Finite Element Analysis of Linear and Nonlinear Two-Dimensional Structures," Department of Civil Engineering, University of California, Berkeley, Report 66-22, October 1966
4. V. Dunder and S. Ridlon. "Practical Applications of Finite Element Method," Vol 104, No. ST1, ASCE Structural Division, January 1978, pp 9-21
5. J. E. Walz, R. E. Fulton and N. J. Cyrus. "Accuracy and Convergence of Finite Element Approximations," Proceedings of the Second Conference on Matrix Methods in Structural Mechanics, NTIS, December 1968
6. F. Barca. "Experimental Measurement of Strain and Acceleration Levels in a Rigid Wall Shelter Subjected to Environmental Loadings," Technical Report TR-79/024-AMEL, US Army Natick Research and Development Command, Natick, MA, 1978

APPENDIX

DATA DECKS FOR FINITE ELEMENT MODELS

Although the analysis methods used to obtain the data for the main body of this report were standard, these methods are still abstract to many engineers. Also, a complete study of this type should document the finite element models in detail. Thus, the inclusion of both finite element models, in the form of their data decks, is provided here to help clarify what data is required when preparing a model and to complete the documentation for this study.

It should be mentioned that not all the data is provided. Several runs were made to obtain eigenvalue information for buckling and special runs with different boundary conditions, beam properties, and applied loads were made with temporary data decks. The US Customary (inch-pound) System was used for the data decks since the structural drawings were in the US Customary System. Thus, length is expressed in inches, force in pounds, moments in inch-pounds, etc.

**DATA DECK FOR COMPLETE SHELTER WITH
WALL AND ROOF PANELS**

CARD COUNT	1	2	3	4	5	6	7	8	9	10
1-	1	1	1	1	1	1	1	1	1	1
2-	2	2	2	2	2	2	2	2	2	2
3-	3	3	3	3	3	3	3	3	3	3
4-	4	4	4	4	4	4	4	4	4	4
5-	5	5	5	5	5	5	5	5	5	5
6-	6	6	6	6	6	6	6	6	6	6
7-	7	7	7	7	7	7	7	7	7	7
8-	8	8	8	8	8	8	8	8	8	8
9-	9	9	9	9	9	9	9	9	9	9
10-	10	10	10	10	10	10	10	10	10	10
11-	11	11	11	11	11	11	11	11	11	11
12-	12	12	12	12	12	12	12	12	12	12
13-	13	13	13	13	13	13	13	13	13	13
14-	14	14	14	14	14	14	14	14	14	14
15-	15	15	15	15	15	15	15	15	15	15
16-	16	16	16	16	16	16	16	16	16	16
17-	17	17	17	17	17	17	17	17	17	17
18-	18	18	18	18	18	18	18	18	18	18
19-	19	19	19	19	19	19	19	19	19	19
20-	20	20	20	20	20	20	20	20	20	20
21-	21	21	21	21	21	21	21	21	21	21
22-	22	22	22	22	22	22	22	22	22	22
23-	23	23	23	23	23	23	23	23	23	23
24-	24	24	24	24	24	24	24	24	24	24
25-	25	25	25	25	25	25	25	25	25	25
26-	26	26	26	26	26	26	26	26	26	26
27-	27	27	27	27	27	27	27	27	27	27
28-	28	28	28	28	28	28	28	28	28	28
29-	29	29	29	29	29	29	29	29	29	29
30-	30	30	30	30	30	30	30	30	30	30
31-	31	31	31	31	31	31	31	31	31	31
32-	32	32	32	32	32	32	32	32	32	32
33-	33	33	33	33	33	33	33	33	33	33
34-	34	34	34	34	34	34	34	34	34	34
35-	35	35	35	35	35	35	35	35	35	35
36-	36	36	36	36	36	36	36	36	36	36
37-	37	37	37	37	37	37	37	37	37	37
38-	38	38	38	38	38	38	38	38	38	38
39-	39	39	39	39	39	39	39	39	39	39
40-	40	40	40	40	40	40	40	40	40	40
41-	41	41	41	41	41	41	41	41	41	41
42-	42	42	42	42	42	42	42	42	42	42
43-	43	43	43	43	43	43	43	43	43	43
44-	44	44	44	44	44	44	44	44	44	44
45-	45	45	45	45	45	45	45	45	45	45

CARD	1	2	3	4	5	6	7	8	9	10
COUNT
46-	CBAR	46	6	57	77	1.	0.0	1.	1.	1.
47-	CBAR	47	6	77	97	1.	0.0	1.	1.	1.
48-	CBAR	48	6	97	117	1.	0.0	1.	1.	1.
49-	CBAR	49	6	117	137	1.	0.0	1.	1.	1.
50-	CBAR	50	6	137	157	1.	0.0	1.	1.	1.
51-	CBAR	51	6	157	177	1.	0.0	1.	1.	1.
52-	CBAR	52	6	177	197	1.	0.0	1.	1.	1.
53-	CBAR	53	4	67	1	-1.	0.0	1.	1.	1.
54-	CBAR	54	4	87	67	-1.	0.0	1.	1.	1.
55-	CBAR	55	4	107	87	-1.	0.0	1.	1.	1.
56-	CBAR	56	4	127	107	-1.	0.0	1.	1.	1.
57-	CBAR	57	4	147	127	-1.	0.0	1.	1.	1.
58-	CBAR	58	4	167	147	-1.	0.0	1.	1.	1.
59-	CBAR	59	4	187	167	-1.	0.0	1.	1.	1.
60-	CBAR	60	4	207	187	-1.	0.0	1.	1.	1.
61-	CBAR	61	6	196	176	-1.	0.0	1.	1.	1.
62-	CBAR	62	6	176	156	-1.	0.0	1.	1.	1.
63-	CBAR	63	6	156	136	-1.	0.0	1.	1.	1.
64-	CBAR	64	6	136	116	-1.	0.0	1.	1.	1.
65-	CBAR	65	6	116	96	-1.	0.0	1.	1.	1.
66-	CBAR	66	6	96	76	-1.	0.0	1.	1.	1.
67-	CBAR	67	6	76	56	-1.	0.0	1.	1.	1.
68-	CBAR	68	6	56	36	-1.	0.0	1.	1.	1.
69-	CBAR	69	4	186	232	1.	0.0	1.	1.	1.
70-	CBAR	70	4	166	186	1.	0.0	1.	1.	1.
71-	CBAR	71	4	146	166	1.	0.0	1.	1.	1.
72-	CBAR	72	4	126	146	1.	0.0	1.	1.	1.
73-	CBAR	73	4	106	126	1.	0.0	1.	1.	1.
74-	CBAR	74	4	86	106	1.	0.0	1.	1.	1.
75-	CBAR	75	4	66	86	1.	0.0	1.	1.	1.
76-	CBAR	76	4	46	66	1.	0.0	1.	1.	1.
77-	CBAR	77	7	1	67	1.	0.0	1.	1.	1.
78-	+BAR77	77	7	0.	67	3.	-3.9	0.	3.	-3.9
79-	CBAR	78	7	67	87	1.	0.0	1.	1.	1.
80-	+BAR78	78	7	0.	87	3.	-3.9	0.	3.	-3.9
81-	CBAR	79	7	87	107	1.	0.0	1.	1.	1.
82-	+BAR79	79	7	0.	107	3.	-3.9	0.	3.	-3.9
83-	CBAR	80	7	107	127	1.	0.0	1.	1.	1.
84-	+BAR80	80	7	0.	127	3.	-3.9	0.	3.	-3.9
85-	CBAR	81	7	127	147	1.	0.0	1.	1.	1.
86-	+BAR81	81	7	0.	147	3.	-3.9	0.	3.	-3.9
87-	CBAR	82	7	147	167	1.	0.0	1.	1.	1.
88-	+BAR82	82	7	0.	167	3.	-3.9	0.	3.	-3.9
89-	CBAR	83	7	167	187	1.	0.0	1.	1.	1.
90-	+BAR83	83	7	0.	187	3.	-3.9	0.	3.	-3.9

CARD COUNT	1	2	3	4	5	6	7	8	9	10
91-	CBAR	84	187	233	1.	3.	0.0	1.	1	CBAR84
92-	+BAR84			0.	3.	-3.9	0.	0.	-3.9	CBAR85
93-	CBAR	85	65	40	-1.	0.0	0.0	1.	1	CBAR86
94-	+BAR85			0.	-3.	-3.9	0.	0.	-3.9	CBAR87
95-	CBAR	86	86	66	-1.	0.0	0.0	1.	1	CBAR88
96-	+BAR86			0.	-3.	-3.9	0.	0.	-3.9	CBAR89
97-	CBAR	87	105	86	-1.	0.0	0.0	1.	1	CBAR90
98-	+BAR87			0.	-3.	-3.9	0.	0.	-3.9	CBAR91
99-	CBAR	88	126	106	-1.	0.0	0.0	1.	1	CBAR92
100-	+BAR88			0.	-3.	-3.9	0.	0.	-3.9	CBAR93
101-	CBAR	89	146	126	-1.	0.0	0.0	1.	1	CBAR94
102-	+BAR89			0.	-3.	-3.9	0.	0.	-3.9	CBAR95
103-	CBAR	90	165	146	-1.	0.0	0.0	1.	1	CBAR96
104-	+BAR90			0.	-3.	-3.9	0.	0.	-3.9	CBAR97
105-	CBAR	91	186	166	-1.	0.0	0.0	1.	1	CBAR98
106-	+BAR91			0.	-3.	-3.9	0.	0.	-3.9	CBAR99
107-	CBAR	92	232	186	-1.	0.0	0.0	1.	1	CBAR100
108-	+BAR92			0.	-3.	-3.9	0.	0.	-3.9	CBAR101
109-	CBAR	93	10	71	1.	0.0	0.0	1.	1	CBAR102
110-	+BAR93			0.	-91	-4.05	0.	-2.45	-4.05	CBAR103
111-	CBAR	94	70	31	-1.	0.0	0.0	1.	1	CBAR104
112-	+BAR94			0.	-1.33	-4.05	0.	-3.71	-4.05	CBAR105
113-	CBAR	95	67	71	0.0	1.	1.	0.	0.	CBAR106
114-	+BAR95			0.	0.	-4.05	0.	0.	-4.05	CBAR107
115-	CBAR	96	71	72	0.0	0.0	1.	1.	0.	CBAR108
116-	+BAR96			0.	0.	-4.05	0.	0.	-4.05	CBAR109
117-	CBAR	97	72	70	0.0	0.0	1.	1.	0.	CBAR110
118-	+BAR97			0.	0.	-4.05	0.	0.	-4.05	CBAR111
119-	CBAR	98	70	66	0.0	1.	1.	0.	0.	CBAR112
120-	+BAR98			0.	0.	-4.05	0.	0.	-4.05	CBAR113
121-	CBAR	99	87	91	0.0	0.0	1.	1.	0.	CBAR114
122-	+BAR99			0.	0.	-4.05	0.	0.	-4.05	CBAR115
123-	CBAR	100	91	92	0.0	0.0	1.	1.	0.	CBAR116
124-	+BAR100			0.	0.	-4.05	0.	0.	-4.05	CBAR117
125-	CBAR	101	92	90	0.0	0.0	1.	1.	0.	CBAR118
126-	+BAR101			0.	0.	-4.05	0.	0.	-4.05	CBAR119
127-	CBAR	102	90	86	0.0	0.0	1.	1.	0.	CBAR120
128-	+BAR102			0.	0.	-4.05	0.	0.	-4.05	CBAR121
129-	CBAR	103	107	111	0.0	0.0	1.	1.	0.	CBAR122
130-	+BAR103			0.	0.	-3.5	0.	0.	-3.5	CBAR123
131-	CBAR	104	111	112	0.0	0.0	1.	1.	0.	CBAR124
132-	+BAR104			0.	0.	-3.5	0.	0.	-3.5	CBAR125
133-	CBAR	105	112	110	0.0	0.0	1.	1.	0.	CBAR126
134-	+BAR105			0.	0.	-3.5	0.	0.	-3.5	CBAR127
135-	CBAR	106	110	106	0.0	0.0	1.	1.	0.	CBAR128

CARD COUNT	1	2	3	4	5	6	7	8	9	10
136-	+BAR106	8	127	0.	0.	-3.5	0.	0.	-3.5	
137-	CBAR 107			131	0.0	0.0	1.	0.	0.	CBAR107
138-	+BAR107	8	131	0.	0.	-4.05	0.	1.	0.	-4.05
139-	CBAR 108			132	0.0	0.0	1.	0.	0.	CBAR108
140-	+BAR108	8	132	0.	0.	-4.05	0.	1.	0.	-4.05
141-	CBAR 109			130	0.0	0.0	1.	0.	0.	CBAR109
142-	+BAR109	8	130	0.	0.	-4.05	0.	1.	0.	-4.05
143-	CBAR 110			126	0.0	0.0	1.	0.	0.	CBAR110
144-	+BAR110	8	126	0.	0.	-4.05	0.	1.	0.	-4.05
145-	CBAR 111			151	0.0	0.0	1.	0.	0.	CBAR111
146-	+BAR111	9	147	0.	0.	-3.5	0.	1.	0.	-3.5
147-	CBAR 112			151	0.	0.0	1.	0.	0.	CBAR112
148-	+BAR112	9	151	0.	0.	-3.5	0.	1.	0.	-3.5
149-	CBAR 113			152	0.	0.0	1.	0.	0.	CBAR113
150-	+BAR113	9	152	0.	0.	-3.5	0.	1.	0.	-3.5
151-	CBAR 114			150	0.	0.0	1.	0.	0.	CBAR114
152-	+BAR114	9	150	0.	0.	-3.5	0.	1.	0.	-3.5
153-	CBAR 115			171	0.	0.0	-1.	0.	0.	CBAR115
154-	+BAR115	8	171	0.	0.	-4.05	0.	1.	0.	-4.05
155-	CBAR 116			172	0.	0.0	-1.	0.	0.	CBAR116
156-	+BAR116	8	172	0.	0.	-4.05	0.	1.	0.	-4.05
157-	CBAR 117			170	0.	0.0	-1.	0.	0.	CBAR117
158-	+BAR117	8	170	0.	0.	-4.05	0.	1.	0.	-4.05
159-	CBAR 118			166	0.	0.0	-1.	0.	0.	CBAR118
160-	+BAR118	8	166	0.	0.	-4.05	0.	1.	0.	-4.05
161-	CBAR 119			191	0.	0.0	-1.	0.	0.	CBAR119
162-	+BAR119	8	191	0.	0.	-4.05	0.	1.	0.	-4.05
163-	CBAR 120			192	0.	0.0	-1.	0.	0.	CBAR120
164-	+BAR120	8	192	0.	0.	-4.05	0.	1.	0.	-4.05
165-	CBAR 121			190	0.	0.0	-1.	0.	0.	CBAR121
166-	+BAR121	8	190	0.	0.	-4.05	0.	1.	0.	-4.05
167-	CBAR 122			186	0.	0.0	-1.	0.	0.	CBAR122
168-	+BAR122	8	186	0.	0.	-4.05	0.	1.	0.	-4.05
169-	CBAR 123			191	0.	1.	0.0	0.	0.	CBAR123
170-	+BAR123	8	191	0.	-2.45	-4.05	0.	1.	-2.45	-4.05
171-	CBAR 124			190	0.	-1.	0.0	0.	0.	CBAR124
172-	+BAR124	8	190	0.	-1.33	-4.05	0.	1.	-1.33	-4.05
173-	CBAR 125			231	0.0	0.0	1.	0.	0.	CBAR125
174-	CBAR 126	3	231	229	0.0	0.0	1.	1.	1.	
175-	CBAR 127	3	229	230	0.0	0.0	1.	1.	1.	
176-	CBAR 128	3	230	232	0.0	0.0	1.	1.	1.	
177-	CBAR 129	1	233	228	1.	0.0	0.0	1.	1.	
178-	CBAR 130	1	228	224	1.	0.0	0.0	1.	1.	
179-	CBAR 131	1	224	220	1.	0.0	0.0	1.	1.	
180-	CBAR 132	1	220	216	1.	0.0	0.0	1.	1.	

CARD COUNT	1	2	3	4	5	6	7	8	9	10
181-	CBAR	133	1	216	212	1	0.0	1	1	
182-	CBAR	134	1	212	208	1	0.0	1	1	
183-	CBAR	135	1	208	204	1	0.0	1	1	
184-	CBAR	136	1	204	197	1	0.0	1	1	
185-	CBAR	137	5	231	226	-1	0.0	1	1	
186-	CBAR	138	5	226	222	-1	0.0	1	1	
187-	CBAR	139	5	222	218	-1	0.0	1	1	
188-	CBAR	140	5	218	214	-1	0.0	1	1	
189-	CBAR	141	5	214	210	-1	0.0	1	1	
190-	CBAR	142	5	210	206	-1	0.0	1	1	
191-	CBAR	143	5	206	202	-1	0.0	1	1	
192-	CBAR	144	5	202	195	-1	0.0	1	1	
193-	CBAR	145	5	202	200	-1	1	0.0	1	
194-	CBAR	146	5	200	201	-1	1	0.0	1	
195-	CBAR	147	5	225	230	-1	0.0	-1	1	
196-	CBAR	148	5	221	225	-1	0.0	-1	1	
197-	CBAR	149	5	217	221	-1	0.0	-1	1	
198-	CBAR	150	5	213	217	-1	0.0	-1	1	
199-	CBAR	151	5	209	213	-1	0.0	-1	1	
200-	CBAR	152	5	205	209	-1	0.0	-1	1	
201-	CBAR	153	5	201	205	-1	0.0	-1	1	
202-	CBAR	154	5	194	201	-1	0.0	-1	1	
203-	CBAR	155	1	227	232	1	0.0	-1	1	
204-	CBAR	156	1	223	227	1	0.0	-1	1	
205-	CBAR	157	1	219	223	1	0.0	-1	1	
206-	CBAR	158	1	215	219	1	0.0	-1	1	
207-	CBAR	159	1	211	215	1	0.0	-1	1	
208-	CBAR	160	1	207	211	1	0.0	-1	1	
209-	CBAR	161	1	203	207	1	0.0	-1	1	
210-	CBAR	162	1	196	203	1	0.0	-1	1	
211-	CBAR	163	2	195	197	0.0	-1	1	1	
212-	CBAR	164	2	193	195	0.0	-1	1	1	
213-	CBAR	165	2	194	193	0.0	-1	1	1	
214-	CBAR	166	2	196	194	0.0	-1	1	1	
215-	CBAR	167	8	10	1	0.0	-1	1	1	CBAR167
216-	+BAR167			1.97		0.0	-4.05	1.97	0.0	-4.05
217-	CBAR	168	8	19	10	0.0	-1	1	1	CBAR168
218-	+BAR168			1.97		0.0	-4.05	1.97	0.0	-4.05
219-	CBAR	169	8	28	19	0.0	-1	1	1	CBAR169
220-	+BAR169			1.97		0.0	-4.05	1.97	0.0	-4.05
221-	CBAR	170	8	31	28	0.0	-1	1	1	CBAR170
222-	+BAR170			1.97		0.0	-4.05	1.97	0.0	-4.05
223-	CBAR	171	8	40	31	0.0	-1	1	1	CBAR171
224-	+BAR171			1.97		0.0	-4.05	1.97	0.0	-4.05
225-	CBAR	172	8	233	231	0.0	1	1	1	CBAR172

CARD	1	2	3	4	5	6	7	8	9	10
COUNT
226-	+BAR172	8	231	-1.97	0.	-4.05	-1.97	0.	-4.05	10
227-	CBAR	173	229	229	0.0	1.	1.	0.	CBAR173	
228-	+BAR173	8	229	-1.97	0.	-4.05	-1.97	0.	-4.05	
229-	CBAR	174	230	230	0.0	1.	1.	0.	CBAR174	
230-	+BAR174	8	230	-1.97	0.	-4.05	-1.97	0.	-4.05	
231-	CBAR	175	232	232	0.0	1.	1.	0.	CBAR175	
232-	+BAR175	8	232	-1.97	0.	-4.05	-1.97	0.	-4.05	
233-	CBAR	448	51	59	1.0	1.0	0.	1		
234-	CBAR	449	59	79	1.0	1.0	0.	1		
235-	CBAR	450	79	99	1.0	1.0	0.	1		
236-	CBAR	451	99	119	1.0	1.0	0.	1		
237-	CBAR	452	119	139	1.0	1.0	0.	1		
238-	CBAR	453	139	159	1.0	1.0	0.	1		
239-	CBAR	454	159	179	1.0	1.0	0.	1		
240-	CBAR	455	179	199	1.0	1.0	0.	1		
241-	CBAR	456	199	178	-1.0	-1.0	0.	1		
242-	CBAR	457	178	158	-1.0	-1.0	0.	1		
243-	CBAR	458	158	138	-1.0	-1.0	0.	1		
244-	CBAR	459	138	118	-1.0	-1.0	0.	1		
245-	CBAR	460	118	98	-1.0	-1.0	0.	1		
246-	CBAR	461	98	78	-1.0	-1.0	0.	1		
247-	CBAR	462	78	58	-1.0	-1.0	0.	1		
248-	CBAR	463	58	38	-1.0	-1.0	0.	1		
249-	CBAR	464	38	18	-1.0	-1.0	0.	1		
250-	CBAR	465	18	69	-1.0	1.0	0.	1		
251-	CBAR	466	69	89	-1.0	1.0	0.	1		
252-	CBAR	467	89	109	-1.0	1.0	0.	1		
253-	CBAR	468	109	129	-1.0	1.0	0.	1		
254-	CBAR	469	129	149	-1.0	1.0	0.	1		
255-	CBAR	470	149	169	-1.0	1.0	0.	1		
256-	CBAR	471	169	189	-1.0	1.0	0.	1		
257-	CBAR	472	189	209	-1.0	1.0	0.	1		
258-	CBAR	473	209	229	-1.0	1.0	0.	1		
259-	CBAR	474	229	249	-1.0	1.0	0.	1		
260-	CBAR	475	249	269	-1.0	1.0	0.	1		
261-	CBAR	476	269	289	-1.0	1.0	0.	1		
262-	CBAR	477	289	309	-1.0	1.0	0.	1		
263-	CBAR	478	309	329	-1.0	1.0	0.	1		
264-	CBAR	479	329	349	-1.0	1.0	0.	1		
265-	CELAS2	394	9	1	51	1	2	3		
266-	CELAS2	395	10	2	51	2	3	3		
267-	CELAS2	396	11	3	51	3	3	3		
268-	CELAS2	397	12	4	52	4	3	3		
269-	CELAS2	398	13	5	52	5	3	3		
270-	CELAS2	399	14	6	52	6	3	3		

CARD COUNT	1	2	3	4	5	6	7	8	9	10
271-	CELAS2	400	1.+10	57	1	59	1			
272-	CELAS2	401	1.+10	57	2	59	2			
273-	CELAS2	402	1.+10	57	3	59	3			
274-	CELAS2	403	1.+10	56	1	58	1			
275-	CELAS2	404	1.+10	56	2	58	2			
276-	CELAS2	405	1.+10	56	3	58	3			
277-	CELAS2	406	1.+10	77	1	79	1			
278-	CELAS2	407	1.+10	77	2	79	2			
279-	CELAS2	408	1.+10	77	3	79	3			
280-	CELAS2	409	1.+10	76	1	78	1			
281-	CELAS2	410	1.+10	76	2	78	2			
282-	CELAS2	411	1.+10	97	1	99	1			
283-	CELAS2	412	1.+10	97	2	99	2			
284-	CELAS2	413	1.+10	97	3	99	3			
285-	CELAS2	414	1.+10	96	1	98	1			
286-	CELAS2	415	1.+10	96	2	98	2			
287-	CELAS2	416	1.+10	96	3	98	3			
288-	CELAS2	417	1.+10	117	1	119	1			
289-	CELAS2	418	1.+10	117	2	119	2			
290-	CELAS2	419	1.+10	117	3	119	3			
291-	CELAS2	420	1.+10	116	1	118	1			
292-	CELAS2	421	1.+10	116	2	118	2			
293-	CELAS2	422	1.+10	116	3	118	3			
294-	CELAS2	423	1.+10	137	1	139	1			
295-	CELAS2	424	1.+10	137	2	139	2			
296-	CELAS2	425	1.+10	137	3	139	3			
297-	CELAS2	426	1.+10	136	1	138	1			
298-	CELAS2	427	1.+10	136	2	138	2			
299-	CELAS2	428	1.+10	136	3	138	3			
300-	CELAS2	429	1.+10	157	1	159	1			
301-	CELAS2	430	1.+10	157	2	159	2			
302-	CELAS2	431	1.+10	157	3	159	3			
303-	CELAS2	432	1.+10	156	1	158	1			
304-	CELAS2	433	1.+10	156	2	158	2			
305-	CELAS2	434	1.+10	156	3	158	3			
306-	CELAS2	435	1.+10	177	1	179	1			
307-	CELAS2	436	1.+10	177	2	179	2			
308-	CELAS2	437	1.+10	177	3	179	3			
309-	CELAS2	438	1.+10	176	1	178	1			
310-	CELAS2	439	1.+10	176	2	178	2			
311-	CELAS2	440	1.+10	176	3	178	3			
312-	CELAS2	441	1.+10	197	1	199	1			
313-	CELAS2	442	1.+10	197	2	199	2			
314-	CELAS2	443	1.+10	197	3	199	3			
315-	CELAS2	444	1.+10	197						

CARD COUNT	1	2	3	4	5	6	7	8	9	10	
316-	CELAS2	445	1.+10	196	1	198	1				
317-	CELAS2	446	1.+10	196	2	198	2				
318-	CELAS2	447	1.+10	196	3	198	3				
319-	CQUAD1	176	1	11	2	3	12				
320-	CQUAD1	177	1	12	3	4	13				
321-	CQUAD1	178	1	13	4	5	14				
322-	CQUAD1	179	1	14	5	6	15				
323-	CQUAD1	180	1	15	6	7	16				
324-	CQUAD1	181	1	16	7	8	17				
325-	CQUAD1	182	1	31	28	20	32				
326-	CQUAD1	183	1	32	20	21	33				
327-	CQUAD1	184	1	33	21	22	34				
328-	CQUAD1	185	1	34	22	23	35				
329-	CQUAD1	186	1	35	23	24	36				
330-	CQUAD1	187	1	36	24	25	37				
331-	CQUAD1	188	1	37	25	29	38				
332-	CQUAD1	189	1	26	17	18	27				
333-	CQUAD1	190	1	29	26	27	30				
334-	CQUAD1	191	1	38	29	30	39				
335-	CQUAD1	192	1	41	32	33	42				
336-	CQUAD1	193	1	42	33	34	43				
337-	CQUAD1	194	1	43	34	35	44				
338-	CQUAD1	195	1	44	35	36	45				
339-	CQUAD1	196	1	45	36	37	46				
340-	CQUAD1	197	1	46	37	38	47				
341-	CQUAD1	198	2	69	89	85	65				
342-	CQUAD1	199	2	65	85	83	63				
343-	CQUAD1	200	2	63	83	81	61				
344-	CQUAD1	201	2	61	81	79	59				
345-	CQUAD1	202	2	89	109	105	85				
346-	CQUAD1	203	2	85	105	103	83				
347-	CQUAD1	204	2	83	103	101	81				
348-	CQUAD1	205	2	81	101	99	79				
349-	CQUAD1	206	2	109	129	125	105				
350-	CQUAD1	207	2	105	125	123	103				
351-	CQUAD1	208	2	103	123	121	101				
352-	CQUAD1	209	2	101	121	119	99				
353-	CQUAD1	210	2	129	149	145	125				
354-	CQUAD1	211	2	125	145	143	123				
355-	CQUAD1	212	2	123	143	141	121				
356-	CQUAD1	213	2	121	141	139	119				
357-	CQUAD1	214	2	149	169	165	145				
358-	CQUAD1	215	2	145	165	163	143				
359-	CQUAD1	216	2	143	163	161	141				
360-	CQUAD1	217	2	141	161	159	139				

CARD COUNT	1	2	3	4	5	6	7	8	9	10

361-	CQUAD1	218	169	189	185	165	165	165	165	165
362-	CQUAD1	219	165	185	183	163	163	163	163	163
363-	CQUAD1	220	163	183	181	161	161	161	161	161
364-	CQUAD1	221	161	181	179	159	159	159	159	159
365-	CQUAD1	222	1	67	71	10	10	10	10	10
366-	CQUAD1	223	66	40	31	70	70	70	70	70
367-	CQUAD1	224	67	87	91	71	71	71	71	71
368-	CQUAD1	225	71	91	92	72	72	72	72	72
369-	CQUAD1	226	72	92	90	70	70	70	70	70
370-	CQUAD1	227	70	90	86	66	66	66	66	66
371-	CQUAD1	228	87	107	111	91	91	91	91	91
372-	CQUAD1	229	91	111	112	92	92	92	92	92
373-	CQUAD1	230	92	112	110	90	90	90	90	90
374-	CQUAD1	231	90	110	106	86	86	86	86	86
375-	CQUAD1	232	107	127	131	111	111	111	111	111
376-	CQUAD1	233	111	131	132	112	112	112	112	112
377-	CQUAD1	234	112	132	130	110	110	110	110	110
378-	CQUAD1	235	110	130	126	106	106	106	106	106
379-	CQUAD1	236	127	147	151	131	131	131	131	131
380-	CQUAD1	237	131	151	152	132	132	132	132	132
381-	CQUAD1	238	132	152	150	130	130	130	130	130
382-	CQUAD1	239	130	150	146	126	126	126	126	126
383-	CQUAD1	240	147	167	171	151	151	151	151	151
384-	CQUAD1	241	151	171	172	152	152	152	152	152
385-	CQUAD1	242	152	172	170	150	150	150	150	150
386-	CQUAD1	243	150	170	166	146	146	146	146	146
387-	CQUAD1	244	167	187	191	171	171	171	171	171
388-	CQUAD1	245	171	191	192	172	172	172	172	172
389-	CQUAD1	246	172	192	190	170	170	170	170	170
390-	CQUAD1	247	170	190	186	166	166	166	166	166
391-	CQUAD1	248	187	233	231	191	191	191	191	191
392-	CQUAD1	249	191	231	229	192	192	192	192	192
393-	CQUAD1	250	192	229	230	190	190	190	190	190
394-	CQUAD1	251	190	230	232	186	186	186	186	186
395-	CQUAD1	252	228	226	222	224	224	224	224	224
396-	CQUAD1	253	224	222	218	220	220	220	220	220
397-	CQUAD1	254	216	214	214	216	216	216	216	216
398-	CQUAD1	255	212	210	206	208	208	208	208	208
399-	CQUAD1	256	208	206	202	204	204	204	204	204
400-	CQUAD1	257	202	200	193	195	195	195	195	195
401-	CQUAD1	258	200	201	194	193	193	193	193	193
402-	CQUAD1	259	205	207	203	201	201	201	201	201
403-	CQUAD1	260	209	211	207	205	205	205	205	205
404-	CQUAD1	261	213	215	211	209	209	209	209	209
405-	CQUAD1	262	1	1	1	1	1	1	1	1

CARD	COUNT	1	2	3	4	5	6	7	8	9	10
406-	CQUAD1	263	1	1	217	219	215	213			
407-	CQUAD1	264	1	1	221	223	219	217			
408-	CQUAD1	265	1	1	225	227	223	221			
409-	CQUAD1	266	2	2	188	168	164	184			
410-	CQUAD1	267	2	2	184	164	162	182			
411-	CQUAD1	268	2	2	182	162	160	180			
412-	CQUAD1	269	2	2	180	160	158	178			
413-	CQUAD1	270	2	2	168	148	144	164			
414-	CQUAD1	271	2	2	164	144	142	162			
415-	CQUAD1	272	2	2	162	142	140	160			
416-	CQUAD1	273	2	2	160	140	138	158			
417-	CQUAD1	274	2	2	148	128	124	144			
418-	CQUAD1	275	2	2	144	124	122	142			
419-	CQUAD1	276	2	2	142	122	120	140			
420-	CQUAD1	277	2	2	140	120	118	138			
421-	CQUAD1	278	2	2	128	108	104	124			
422-	CQUAD1	279	2	2	124	104	102	122			
423-	CQUAD1	280	2	2	122	102	100	120			
424-	CQUAD1	281	2	2	120	100	98	118			
425-	CQUAD1	282	2	2	108	88	84	104			
426-	CQUAD1	283	2	2	104	84	82	102			
427-	CQUAD1	284	2	2	102	82	80	100			
428-	CQUAD1	285	2	2	100	80	78	98			
429-	CQUAD1	286	2	2	88	68	64	84			
430-	CQUAD1	287	2	2	84	64	62	82			
431-	CQUAD1	288	2	2	82	62	60	80			
432-	CQUAD1	289	2	2	80	60	58	78			
433-	CQUAD1	290	2	2	9	57	55	18			
434-	CQUAD1	291	2	2	56	48	39	54			
435-	CQUAD1	292	2	2	57	47	35	55			
436-	CQUAD1	293	2	2	55	45	33	53			
437-	CQUAD1	294	2	2	53	43	31	51			
438-	CQUAD1	295	2	2	54	44	32	52			
439-	CQUAD1	296	2	2	77	67	55	75			
440-	CQUAD1	297	2	2	75	65	53	73			
441-	CQUAD1	298	2	2	73	63	51	71			
442-	CQUAD1	299	2	2	74	64	52	72			
443-	CQUAD1	300	2	2	97	87	75	95			
444-	CQUAD1	301	2	2	95	85	73	93			
445-	CQUAD1	302	2	2	93	83	71	91			
446-	CQUAD1	303	2	2	94	84	72	92			
447-	CQUAD1	304	2	2	117	107	95	115			
448-	CQUAD1	305	2	2	115	105	93	113			
449-	CQUAD1	306	2	2	113	103	91	111			
450-	CQUAD1	307	2	2	114	104	92	112			

CARD	COUNT	1	2	3	4	5	6	7	8	9	10
451-	CQUAD1	308	2	3	137	157	155	135			
452-	CQUAD1	309	2	3	135	155	153	133			
453-	CQUAD1	310	2	3	133	153	154	134			
454-	CQUAD1	311	2	3	134	154	156	136			
455-	CQUAD1	312	2	3	157	177	175	155			
456-	CQUAD1	313	2	3	155	175	173	153			
457-	CQUAD1	314	2	3	153	173	174	154			
458-	CQUAD1	315	2	3	154	174	176	156			
459-	CQUAD1	316	2	3	177	197	195	175			
460-	CQUAD1	317	2	3	175	195	193	173			
461-	CQUAD1	318	2	3	173	193	194	174			
462-	CQUAD1	319	2	3	174	194	196	176			
463-	CTRIA1	320	1	3	10	1	2				
464-	CTRIA1	321	1	3	2	11	10				
465-	CTRIA1	322	1	3	17	3	18				
466-	CTRIA1	323	1	3	9	18	8				
467-	CTRIA1	324	1	3	40	31	41				
468-	CTRIA1	325	1	3	32	41	31				
469-	CTRIA1	326	1	3	47	38	39				
470-	CTRIA1	327	1	3	39	48	47				
471-	CTRIA1	328	2	3	1	69	2				
472-	CTRIA1	329	2	3	69	65	2				
473-	CTRIA1	330	2	3	65	3	2				
474-	CTRIA1	331	2	3	3	65	4				
475-	CTRIA1	332	2	3	65	63	4				
476-	CTRIA1	333	2	3	63	5	4				
477-	CTRIA1	334	2	3	5	63	6				
478-	CTRIA1	335	2	3	63	61	6				
479-	CTRIA1	336	2	3	61	7	6				
480-	CTRIA1	337	2	3	7	61	51				
481-	CTRIA1	338	2	3	59	51	61				
482-	CTRIA1	339	2	3	189	233	228				
483-	CTRIA1	340	2	3	185	189	228				
484-	CTRIA1	341	2	3	224	185	228				
485-	CTRIA1	342	2	3	185	224	220				
486-	CTRIA1	343	2	3	183	185	220				
487-	CTRIA1	344	2	3	216	183	220				
488-	CTRIA1	345	2	3	183	216	212				
489-	CTRIA1	346	2	3	181	183	212				
490-	CTRIA1	347	2	3	208	181	212				
491-	CTRIA1	348	2	3	181	208	199				
492-	CTRIA1	349	2	3	199	179	181				
493-	CTRIA1	350	3	3	10	71	19				
494-	CTRIA1	351	3	3	71	72	19				
495-	CTRIA1	352	3	3	28	19	72				

CARD COUNT	1	2	3	4	5	6	7	8	9	10
496-	CTRIA1 353	3	72	70	28					
497-	CTRIA1 354	3	31	28	70					
498-	CTRIA1 355	1	230	232	227					
499-	CTRIA1 356	1	227	225	230					
500-	CTRIA1 357	1	201	203	194					
501-	CTRIA1 358	1	196	194	203					
502-	CTRIA1 359	1	233	231	228					
503-	CTRIA1 360	1	226	228	231					
504-	CTRIA1 361	1	204	202	195					
505-	CTRIA1 362	1	195	197	204					
506-	CTRIA1 363	2	232	188	227					
507-	CTRIA1 364	2	184	184	227					
508-	CTRIA1 365	2	184	223	227					
509-	CTRIA1 366	2	223	184	219					
510-	CTRIA1 367	2	184	182	219					
511-	CTRIA1 368	2	182	215	219					
512-	CTRIA1 369	2	215	182	211					
513-	CTRIA1 370	2	182	180	211					
514-	CTRIA1 371	2	180	207	211					
515-	CTRIA1 372	2	207	180	198					
516-	CTRIA1 373	2	178	198	180					
517-	CTRIA1 374	2	68	40	41					
518-	CTRIA1 375	2	64	68	41					
519-	CTRIA1 376	2	42	64	41					
520-	CTRIA1 377	2	64	42	43					
521-	CTRIA1 378	2	62	64	43					
522-	CTRIA1 379	2	44	62	43					
523-	CTRIA1 380	2	62	44	45					
524-	CTRIA1 381	2	60	62	45					
525-	CTRIA1 382	2	46	60	45					
526-	CTRIA1 383	2	60	46	52					
527-	CTRIA1 384	2	52	58	60					
528-	CTRIA1 385	2	27	18	55					
529-	CTRIA1 386	2	55	53	27					
530-	CTRIA1 387	2	30	27	53					
531-	CTRIA1 388	2	53	54	30					
532-	CTRIA1 389	2	39	30	54					
533-	FORCE 100	9		1.01+5	.0					
534-	FORCE 100	48		1.01+5	.0					
535-	FORCE 100	196		1.01+5	.0					
536-	FORCE 100	197		1.01+5	.0					
537-	FORCE 110	48		6.75+4	.0					
538-	FORCE 400	1		1.35+3	-1.					
539-	FORCE 400	40		1.35+3	-1.					
540-	FORCE 410	1		1.35+3	1.					

CARD COUNT	1	2	3	4	5	6	7	8	9	10
541-	FORCE	40	..	1.35+3	1.
542-	FORCE	40	..	1.35+3	1.
543-	FORCE	40	..	1.35+3	1.
544-	FORCE	48	..	3.36+4
545-	FORCE	48	..	3.36+4
546-	FORCE	48	..	3.36+4
547-	FORCE	48	..	3.36+4
548-	FORCE	48	..	3.36+4
549-	FORCE	48	..	3.36+4
550-	FORCE	48	..	3.36+4
551-	FORCE	48	..	3.36+4
552-	FORCE	48	..	3.36+4
553-	FORCE	48	..	3.36+4
554-	FORCE	48	..	3.36+4
555-	FORCE	48	..	3.36+4
556-	FORCE	48	..	3.36+4
557-	FORCE	48	..	3.36+4
558-	FORCE	48	..	3.36+4
559-	FORCE	48	..	3.36+4
560-	FORCE	48	..	3.36+4
561-	FORCE	48	..	3.36+4
562-	FORCE	48	..	3.36+4
563-	FORCE	48	..	3.36+4
564-	FORCE	48	..	3.36+4
565-	FORCE	48	..	3.36+4
566-	FORCE	48	..	3.36+4
567-	FORCE	48	..	3.36+4
568-	FORCE	48	..	3.36+4
569-	FORCE	48	..	3.36+4
570-	FORCE	48	..	3.36+4
571-	FORCE	48	..	3.36+4
572-	FORCE	48	..	3.36+4
573-	FORCE	48	..	3.36+4
574-	FORCE	48	..	3.36+4
575-	FORCE	48	..	3.36+4
576-	FORCE	48	..	3.36+4
577-	FORCE	48	..	3.36+4
578-	FORCE	48	..	3.36+4
579-	GRAV	210	..	3.36+4
580-	GRID	1	..	3.36+4
581-	GRID	2	..	3.36+4
582-	GRID	3	..	3.36+4
583-	GRID	4	..	3.36+4
584-	GRID	5	..	3.36+4
585-	GRID	6	..	3.36+4

CARD	1	2	3	4	5	6	7	8	9	10
COUNT
586-	GRID	7	3.25	1.29	72.48					
587-	GRID	8	3.25	1.29	88.71					
588-	GRID	9	3.25	1.29	94.46					
589-	GRID	10	3.25	21.22	6.55					
590-	GRID	11	3.25	21.22	17.54					
591-	GRID	12	3.25	21.22	28.53					
592-	GRID	13	3.25	21.22	39.52					
593-	GRID	14	3.25	21.22	50.51					
594-	GRID	15	3.25	21.22	61.49					
595-	GRID	16	3.25	21.22	72.48					
596-	GRID	17	3.25	21.22	88.71					
597-	GRID	18	3.25	21.22	94.46					
598-	GRID	19	3.25	41.14	6.55					
599-	GRID	20	3.25	58.38	17.54					
600-	GRID	21	3.25	58.38	28.53					
601-	GRID	22	3.25	58.38	39.52					
602-	GRID	23	3.25	58.38	50.51					
603-	GRID	24	3.25	58.38	61.49					
604-	GRID	25	3.25	58.38	72.48					
605-	GRID	26	3.25	41.14	88.71					
606-	GRID	27	3.25	41.14	94.46					
607-	GRID	28	3.25	58.38	6.55					
608-	GRID	29	3.25	58.38	88.71					
609-	GRID	30	3.25	58.38	94.46					
610-	GRID	31	3.25	75.62	6.55					
611-	GRID	32	3.25	75.62	17.54					
612-	GRID	33	3.25	75.62	28.53					
613-	GRID	34	3.25	75.62	39.52					
614-	GRID	35	3.25	75.62	50.51					
615-	GRID	36	3.25	75.62	61.49					
616-	GRID	37	3.25	75.62	72.48					
617-	GRID	38	3.25	75.62	88.71					
618-	GRID	39	3.25	75.62	94.46					
619-	GRID	40	3.25	94.71	6.55					
620-	GRID	41	3.25	94.71	17.54					
621-	GRID	42	3.25	94.71	28.53					
622-	GRID	43	3.25	94.71	39.52					
623-	GRID	44	3.25	94.71	50.51					
624-	GRID	45	3.25	94.71	61.49					
625-	GRID	46	3.25	94.71	72.48					
626-	GRID	47	3.25	94.71	88.71					
627-	GRID	48	3.25	94.71	94.46					
628-	GRID	49	119.25	1.29	295.38					
629-	GRID	50	119.25	94.71	295.38					
630-	GRID	51	3.25	1.29	94.46					

4 4 4 4 4 4

456 456

CARD	1	2	3	4	5	6	7	8	9	10
COUNT	52	53	54	55	56	57	58	59	60	61
GRID	GRID	GRID	GRID	GRID	GRID	GRID	GRID	GRID	GRID	GRID
631-	3.25	94.71	94.46	94.46	94.46	94.46	94.46	94.46	94.46	94.46
632-	33.86	48.0	94.46	94.46	94.46	94.46	94.46	94.46	94.46	94.46
633-	33.86	73.24	94.46	94.46	94.46	94.46	94.46	94.46	94.46	94.46
634-	33.86	22.76	94.46	94.46	94.46	94.46	94.46	94.46	94.46	94.46
635-	33.86	94.71	94.46	94.46	94.46	94.46	94.46	94.46	94.46	94.46
636-	33.86	1.29	94.46	94.46	94.46	94.46	94.46	94.46	94.46	94.46
637-	33.86	94.71	94.46	94.46	94.46	94.46	94.46	94.46	94.46	94.46
638-	33.86	1.29	94.46	94.46	94.46	94.46	94.46	94.46	94.46	94.46
639-	33.86	94.71	94.46	94.46	94.46	94.46	94.46	94.46	94.46	94.46
640-	33.86	1.29	94.46	94.46	94.46	94.46	94.46	94.46	94.46	94.46
641-	33.86	94.71	94.46	94.46	94.46	94.46	94.46	94.46	94.46	94.46
642-	33.86	1.29	94.46	94.46	94.46	94.46	94.46	94.46	94.46	94.46
643-	33.86	94.71	94.46	94.46	94.46	94.46	94.46	94.46	94.46	94.46
644-	33.86	1.29	94.46	94.46	94.46	94.46	94.46	94.46	94.46	94.46
645-	33.86	94.71	94.46	94.46	94.46	94.46	94.46	94.46	94.46	94.46
646-	33.86	1.29	94.46	94.46	94.46	94.46	94.46	94.46	94.46	94.46
647-	33.86	94.71	94.46	94.46	94.46	94.46	94.46	94.46	94.46	94.46
648-	33.86	1.29	94.46	94.46	94.46	94.46	94.46	94.46	94.46	94.46
649-	33.86	94.71	94.46	94.46	94.46	94.46	94.46	94.46	94.46	94.46
650-	33.86	1.29	94.46	94.46	94.46	94.46	94.46	94.46	94.46	94.46
651-	33.86	94.71	94.46	94.46	94.46	94.46	94.46	94.46	94.46	94.46
652-	33.86	1.29	94.46	94.46	94.46	94.46	94.46	94.46	94.46	94.46
653-	33.86	94.71	94.46	94.46	94.46	94.46	94.46	94.46	94.46	94.46
654-	33.86	1.29	94.46	94.46	94.46	94.46	94.46	94.46	94.46	94.46
655-	33.86	94.71	94.46	94.46	94.46	94.46	94.46	94.46	94.46	94.46
656-	33.86	1.29	94.46	94.46	94.46	94.46	94.46	94.46	94.46	94.46
657-	33.86	94.71	94.46	94.46	94.46	94.46	94.46	94.46	94.46	94.46
658-	33.86	1.29	94.46	94.46	94.46	94.46	94.46	94.46	94.46	94.46
659-	33.86	94.71	94.46	94.46	94.46	94.46	94.46	94.46	94.46	94.46
660-	33.86	1.29	94.46	94.46	94.46	94.46	94.46	94.46	94.46	94.46
661-	33.86	94.71	94.46	94.46	94.46	94.46	94.46	94.46	94.46	94.46
662-	33.86	1.29	94.46	94.46	94.46	94.46	94.46	94.46	94.46	94.46
663-	33.86	94.71	94.46	94.46	94.46	94.46	94.46	94.46	94.46	94.46
664-	33.86	1.29	94.46	94.46	94.46	94.46	94.46	94.46	94.46	94.46
665-	33.86	94.71	94.46	94.46	94.46	94.46	94.46	94.46	94.46	94.46
666-	33.86	1.29	94.46	94.46	94.46	94.46	94.46	94.46	94.46	94.46
667-	33.86	94.71	94.46	94.46	94.46	94.46	94.46	94.46	94.46	94.46
668-	33.86	1.29	94.46	94.46	94.46	94.46	94.46	94.46	94.46	94.46
669-	33.86	94.71	94.46	94.46	94.46	94.46	94.46	94.46	94.46	94.46
670-	33.86	1.29	94.46	94.46	94.46	94.46	94.46	94.46	94.46	94.46
671-	33.86	94.71	94.46	94.46	94.46	94.46	94.46	94.46	94.46	94.46
672-	33.86	1.29	94.46	94.46	94.46	94.46	94.46	94.46	94.46	94.46
673-	33.86	94.71	94.46	94.46	94.46	94.46	94.46	94.46	94.46	94.46
674-	33.86	1.29	94.46	94.46	94.46	94.46	94.46	94.46	94.46	94.46
675-	33.86	94.71	94.46	94.46	94.46	94.46	94.46	94.46	94.46	94.46

ISO SHELTER FINITE ELEMENT ANALYSIS.

NOVEMB 14, 1978 NASTRAN 4/30/75 PAGE 18

CARD	COUNT	1	2	3	4	5	6	7	8	9	10
576-	GRID	97	1.29	93.11	1.29	94.46	94.46				
577-	GRID	98	93.11	94.71	94.46	94.46					
578-	GRID	99	93.11	1.29	94.46	94.46					
579-	GRID	100	93.11	94.71	72.48	72.48	5				
580-	GRID	101	93.11	1.29	72.48	72.48	5				
581-	GRID	102	93.11	94.71	50.51	50.51	5				
582-	GRID	103	93.11	1.29	50.51	50.51	5				
583-	GRID	104	93.11	94.71	28.53	28.53	5				
584-	GRID	105	93.11	1.29	28.53	28.53	5				
585-	GRID	106	93.11	94.71	6.55	6.55					
586-	GRID	107	93.11	1.29	6.55	6.55					
587-	GRID	108	93.11	94.71	6.55	6.55					
588-	GRID	109	93.11	1.29	6.55	6.55					
589-	GRID	110	93.11	73.24	6.55	6.55					
590-	GRID	111	93.11	22.76	6.55	6.55					
591-	GRID	112	93.11	48.0	6.55	6.55					
592-	GRID	113	119.7	48.0	94.46	94.46	6				
593-	GRID	114	119.7	73.24	94.46	94.46	6				
594-	GRID	115	119.7	22.76	94.46	94.46	6				
595-	GRID	116	119.7	94.71	94.46	94.46					
596-	GRID	117	119.7	1.29	94.46	94.46					
597-	GRID	118	119.7	94.71	94.46	94.46					
598-	GRID	119	119.7	1.29	94.46	94.46					
599-	GRID	120	119.7	94.71	72.48	72.48	5				
700-	GRID	121	119.7	1.29	72.48	72.48	5				
701-	GRID	122	119.7	94.71	50.51	50.51	5				
702-	GRID	123	119.7	1.29	50.51	50.51	5				
703-	GRID	124	119.7	94.71	28.53	28.53	5				
704-	GRID	125	119.7	1.29	28.53	28.53	5				
705-	GRID	126	119.7	94.71	6.55	6.55					
706-	GRID	127	119.7	1.29	6.55	6.55					
707-	GRID	128	119.7	94.71	6.55	6.55					
708-	GRID	129	119.7	1.29	6.55	6.55					
709-	GRID	130	119.7	73.24	6.55	6.55					
710-	GRID	131	119.7	22.76	6.55	6.55					
711-	GRID	132	119.7	48.0	6.55	6.55					
712-	GRID	133	145.21	48.0	94.46	94.46	6				
713-	GRID	134	145.21	73.24	94.46	94.46	6				
714-	GRID	135	145.21	22.76	94.46	94.46	6				
715-	GRID	136	145.21	94.71	94.46	94.46					
716-	GRID	137	145.21	1.29	94.46	94.46					
717-	GRID	138	145.21	94.71	94.46	94.46					
718-	GRID	139	145.21	1.29	94.46	94.46					
719-	GRID	140	145.21	94.71	72.48	72.48	5				
720-	GRID	141	145.21	1.29	72.48	72.48	5				

CARD	COUNT	1	2	3	4	5	6	7	8	9	10	ECHO
721-	GRID	142	145.21	94.71	50.51							
722-	GRID	143	145.21	1.29	50.51			5				
723-	GRID	144	145.21	94.71	28.53			5				
724-	GRID	145	145.21	1.29	28.53			5				
725-	GRID	146	145.21	94.71	6.55							
726-	GRID	147	145.21	1.29	6.55							
727-	GRID	148	145.21	94.71	6.55							
728-	GRID	149	145.21	1.29	6.55							
729-	GRID	150	145.21	73.24	6.55							
730-	GRID	151	145.21	22.76	6.55							
731-	GRID	152	145.21	48.0	6.55							
732-	GRID	153	178.14	48.0	94.46							6
733-	GRID	154	178.14	73.24	94.46							6
734-	GRID	155	178.14	22.76	94.46							6
735-	GRID	156	178.14	94.71	94.46							
736-	GRID	157	178.14	1.29	94.46							
737-	GRID	158	178.14	94.71	94.46							
738-	GRID	159	178.14	1.29	94.46							
739-	GRID	160	178.14	94.71	72.48							5
740-	GRID	161	178.14	1.29	72.48							5
741-	GRID	162	178.14	94.71	50.51							5
742-	GRID	163	178.14	1.29	50.51							5
743-	GRID	164	178.14	94.71	28.53							5
744-	GRID	165	178.14	1.29	28.53							5
745-	GRID	166	178.14	94.71	6.55							5
746-	GRID	167	178.14	1.29	6.55							
747-	GRID	168	178.14	94.71	6.55							
748-	GRID	169	178.14	1.29	6.55							
749-	GRID	170	178.14	73.24	6.55							
750-	GRID	171	178.14	22.76	6.55							
751-	GRID	172	178.14	48.0	6.55							6
752-	GRID	173	204.56	48.0	94.46							6
753-	GRID	174	204.56	73.24	94.46							6
754-	GRID	175	204.56	22.76	94.46							
755-	GRID	176	204.56	94.71	94.46							
756-	GRID	177	204.56	1.29	94.46							
757-	GRID	178	204.56	94.71	94.46							
758-	GRID	179	204.56	1.29	94.46							
759-	GRID	180	204.56	94.71	72.48							5
760-	GRID	181	204.56	1.29	72.48							5
761-	GRID	182	204.56	94.71	50.51							5
762-	GRID	183	204.56	1.29	50.51							5
763-	GRID	184	204.56	94.71	28.53							5
764-	GRID	185	204.56	1.29	28.53							5
765-	GRID	186	204.56	94.71	6.55							

ISO SHELTER FINITE ELEMENT ANALYSIS.

NOVEMBER 14, 1978 NASTRAN 4/30/75 PAGE 20

CARD COUNT	1	2	3	4	5	6	7	8	9	10
GRID	187	204.56	1.29	6.55						
GRID	188	204.56	94.71	6.55						
GRID	189	204.56	1.29	6.55						
GRID	190	204.56	73.24	6.55						
GRID	191	204.56	22.76	6.55						
GRID	192	204.56	48.0	6.55						
GRID	193	235.25	48.0	94.46						
GRID	194	235.25	73.24	94.46						
GRID	195	235.25	22.76	94.46						
GRID	196	235.25	94.71	94.46						
GRID	197	235.25	1.29	94.46						
GRID	198	235.25	94.71	94.46						
GRID	199	235.25	1.29	94.46						
GRID	200	235.25	48.0	88.71						
GRID	201	235.25	73.24	88.71						
GRID	202	235.25	22.76	88.71						
GRID	203	235.25	94.71	88.71						
GRID	204	235.25	1.29	88.71						
GRID	205	235.25	73.24	72.48						
GRID	206	235.25	22.76	72.48						
GRID	207	235.25	94.71	72.48						
GRID	208	235.25	1.29	72.48						
GRID	209	235.25	73.24	61.49						
GRID	210	235.25	22.76	61.49						
GRID	211	235.25	94.71	61.49						
GRID	212	235.25	1.29	61.49						
GRID	213	235.25	73.24	50.51						
GRID	214	235.25	22.76	50.51						
GRID	215	235.25	94.71	50.51						
GRID	216	235.25	1.29	50.51						
GRID	217	235.25	73.24	39.52						
GRID	218	235.25	22.76	39.52						
GRID	219	235.25	94.71	39.52						
GRID	220	235.25	1.29	39.52						
GRID	221	235.25	73.24	28.53						
GRID	222	235.25	22.76	28.53						
GRID	223	235.25	94.71	28.53						
GRID	224	235.25	1.29	28.53						
GRID	225	235.25	73.24	17.54						
GRID	226	235.25	22.76	17.54						
GRID	227	235.25	94.71	17.54						
GRID	228	235.25	1.29	17.54						
GRID	229	235.25	48.0	6.55						
GRID	230	235.25	73.24	6.55						
GRID	231	235.25	22.76	6.55						

CARD	1	2	3	4	5	6	7	8	9	10
COUNT	232	233	200	1.	1.	220	1.25-5			
811-	GRID	232	235.25	94.71	6.55					
812-	GRID	233	235.25	1.29	6.55					
813-	LOAD	200	1.	210	1.					
814-	MAT1	1	10.+6	.33	3.04-3					
815-	MAT1	2	1.5+4	.3						
816-	MOMENT	100	9	1.21+5	-1.0	.0				
817-	MOMENT	100	9	7.56+5	.0	-1.0	.0			
818-	MOMENT	100	48	1.21+5	-1.0	.0	.0			
819-	MOMENT	100	48	7.56+5	.0	-1.0	.0			
820-	MOMENT	100	196	1.21+5	-1.0	.0	.0			
821-	MOMENT	100	196	7.56+5	.0	-1.0	.0			
822-	MOMENT	100	197	1.21+5	-1.0	.0	.0			
823-	MOMENT	100	197	7.56+5	.0	-1.0	.0			
824-	MOMENT	110	48	5.05+5	.0	1.0	.0			
825-	MOMENT	110	48	8.09+4	1.0	.0	.0			
826-	PSAR	1	1	2.30	11.23	13.53	0.0			PAAR1
827-	+AAR1	1.2	3.9	.7	-1.9	-2.4	-5	3.9		PAAR2
828-	PBAR	2	1	2.22	1.68	3.36	0.0	1.8		PAAR3
829-	+AAR2	1.9	1.8	.9	-1.7	-1.2	-4	1.2		PAAR4
830-	PBAR	3	1	2.8	4.02	8.78	0.0	.86		PAAR5
831-	+AAR3	2.3	2.1	.5	-2.4	-2.5	-8	1.2		PAAR6
832-	PBAR	4	1	1.63	1.84	2.59	0.0	.86		PAAR7
833-	+AAR4	1.5	.86	1.5	-1.5	-1.5	-1.5	1.325		PAAR8
834-	PBAR	5	1	1.43	1.09	1.99	0.0	.86		PAAR9
835-	+AAR5	1.31	1.33	1.31	-1.18	-1.175	-1.194	1.325		PAAR10
836-	PBAR	6	1	2.43	4.58	6.50	0.0	1.16		
837-	+AAR6	2.24	1.16	2.239	-1.59	-2.01	-2.01	1.16		
838-	PBAR	7	1	2.687	12.079	14.579	0.0	1.884		
839-	+AAR7	2.345	1.884	2.348	-2.304	-2.652	-2.652	1.884		
840-	PBAR	8	1	1.613	5.878	6.46	0.0	.514		
841-	+AAR8	2.5	.514	2.5	-1.486	-2.5	-2.5	.514		
842-	PBAR	9	1	7.661	31.94	218.772	0.0	6.0		
843-	+AAR9	1.946	8.0	1.946	-8.0	-2.804	-2.804	6.0		
844-	PBAR	10	1	.8	.4	.8	.0	.89		
845-	+AAR10	1.04	.89	.85	-.96	-.96	-.96	.89		
846-	PLOAD2	100	-969	222	THRU	251				
847-	PLOAD2	100	-969	350	THRU	354				
848-	PLOAD2	220	-1.571	222	THRU	251				
849-	PLOAD2	220	-1.571	350	THRU	354				
850-	PLOAD2	400	-415	222	THRU	251				
851-	PLOAD2	400	-415	350	THRU	354				
852-	PLOAD2	410	-415	222	THRU	251				
853-	PLOAD2	410	-415	350	THRU	354				
854-	PLOAD2	420	-415	222	THRU	251				
855-	PLOAD2	420	-415	350	THRU	354				

CARD	COUNT	1	2	3	4	5	6	7	8	9	10
856-	PLOAD2	430	1.29	-.415	222	THRU	251				
857-	PLOAD2	430	1.04	-.415	350	THRU	354				
858-	PLOAD2	700	1.55	-.7343	176	THRU	197				
859-	PLOAD2	700	1.29	-.7343	320	THRU	327				
860-	PLOAD2	710	1.04	-.7343	176	THRU	197				
861-	PLOAD2	710	1.55	-.7343	320	THRU	327				
862-	PLOAD2	800	1.29	-.2957	198	THRU	221				
863-	PLOAD2	800	1.04	-.2957	328	THRU	349				
864-	PLOAD2	810	1.55	-.2957	198	THRU	221				
865-	PLOAD2	810	1.29	-.2957	328	THRU	349				
866-	PLOAD2	900	1.04	-.2509	301	THRU	305				
867-	PLOAD2	1	1.55	-.2509	301	THRU	305				
868-	+QUADA	1	1.29	-1.29	.0664	1	.129	2	2.50	.0	PQUADA
869-	+QUADI	2	1.04	-1.04	.0664	1	.0832	2	2.00	.0	PQUADB
870-	+QUADB	3	1.55	-1.55	.083	1	.2326	2	3.00	.0	PQUADC
871-	+QUADC	1	1.29	-1.29	.0664	1	.129	2	2.50	.0	PTRI1
872-	PROD	1	1.04	-1.04	.0664	1	.0832	2	2.00	.0	PTRI2
873-	PTRI1	1	1.55	-1.55	.083	1	.2326	2	3.00	.0	PTRI3
874-	+TRI1	1	1.29	-1.29	.0664	1	.129	2	2.50	.0	
875-	+TRI1	2	1.04	-1.04	.0664	1	.0832	2	2.00	.0	
876-	+TRI2	2	1.55	-1.55	.083	1	.2326	2	3.00	.0	
877-	+TRI2	3	1.29	-1.29	.0664	1	.129	2	2.50	.0	
878-	+TRI3	1	1.04	-1.04	.0664	1	.0832	2	2.00	.0	
879-	+TRI3	1	1.55	-1.55	.083	1	.2326	2	3.00	.0	
880-	SPC	100	1	1.29	123	.0	40	3	.0		
881-	SPC	100	49	123	123	.0	50	123	.0		
882-	SPC	100	232	3	123	.0	233	23	.0		
883-	SPC	110	40	123	123	.0	48	2	.0		
884-	SPC	110	49	123	123	.0	50	123	.0		
885-	SPC	110	196	2	123	.0	232	23	.0		
886-	SPC	200	9	123	123	0.0	48	13	0.0		
887-	SPC	200	49	123	123	.0	50	123	.0		
888-	SPC	200	196	3	123	0.0	197	23	0.0		
889-	SPC	400	1	23	23	.0	40	3	.0		
890-	SPC	400	49	123	123	.0	50	123	.0		
891-	SPC	400	232	13	123	.0	233	123	.0		
892-	SPC	500	1	123	123	.0	40	3	.0		
893-	SPC	500	49	123	123	.0	50	123	.0		
894-	SPC	500	232	3	123	.0	233	123	.0		
895-	SPC	600	1	23	23	.0	40	3	.0		
896-	SPC	600	49	123	123	.0	50	123	.0		
897-	SPC	600	232	3	123	.0	233	123	.0		
898-	SPC	601	9	23	23	.0	48	3	.0		
899-	SPC	601	49	123	123	.0	50	123	.0		
900-	SPC	601	196	3	123	.0	197	123	.0		

CARD COUNT	1	2	3	4	5	6	7	8	9	10
SPC	602	40	23	23	48	2	7	..	9	10
SPC	602	49	123	123	50	123
SPC	602	196	13	13	232	23
SPC	700	1	123	123	9	12
SPC	700	40	1	1	48	1
SPC	700	49	123	123	50	123
SPC	800	1	123	123	9	12
SPC	800	49	123	123	50	123
SPC	800	197	2	2	233	2
SPC	900	1	123	123	40	13
SPC	900	49	123	123	50	123
SPC	900	232	3	3	233	3

ENDDATA

```

* 36.9 CPU-S 90.8 COR-S 226 ELP-S. DO IFP
* 55.8 CPU-S 113.8 COR-S 345 ELP-S. END IFP
* 55.8 CPU-S 113.8 COR-S 345 ELP-S. XGPI
      *NO ERRORS FOUND - EXECUTE NASTRAN PROGRAM**
* 63.7 CPU-S 123.3 COR-S 383 ELP-S. SEM1 END
* 63.7 CPU-S 123.9 COR-S 384 ELP-S. ---- LINK NS02 ----

```

140

@TEST TNE/1/56
INTERVENING STATEMENTS SKIPPED

@TEST TNE/2/56

```

@XQT *NASTRAN.LINK2
* 64.0 CPU-S 126.8 COR-S 390 ELP-S. ---- LINK END ----
* 64.0 CPU-S 126.8 COR-S 390 ELP-S. XSFA
* 64.5 CPU-S 130.8 COR-S 391 ELP-S. XSFA
* 64.5 CPU-S 130.8 COR-S 391 ELP-S. 4 GPI BEGN
* 67.5 CPU-S 135.8 COR-S 418 ELP-S. 4 GPI END

```

**DATA DECK FOR SHELTER WITHOUT WALL
AND ROOF PANELS**

CARD COUNT	1	2	3	4	5	6	7	8	9	10
1-	1	1	1	1	1	1	1	1	1	1
2-	2	2	2	2	2	2	2	2	2	2
3-	3	3	3	3	3	3	3	3	3	3
4-	4	4	4	4	4	4	4	4	4	4
5-	5	5	5	5	5	5	5	5	5	5
6-	6	6	6	6	6	6	6	6	6	6
7-	7	7	7	7	7	7	7	7	7	7
8-	8	8	8	8	8	8	8	8	8	8
9-	9	9	9	9	9	9	9	9	9	9
10-	10	10	10	10	10	10	10	10	10	10
11-	11	11	11	11	11	11	11	11	11	11
12-	12	12	12	12	12	12	12	12	12	12
13-	13	13	13	13	13	13	13	13	13	13
14-	14	14	14	14	14	14	14	14	14	14
15-	15	15	15	15	15	15	15	15	15	15
16-	16	16	16	16	16	16	16	16	16	16
17-	17	17	17	17	17	17	17	17	17	17
18-	18	18	18	18	18	18	18	18	18	18
19-	19	19	19	19	19	19	19	19	19	19
20-	20	20	20	20	20	20	20	20	20	20
21-	21	21	21	21	21	21	21	21	21	21
22-	22	22	22	22	22	22	22	22	22	22
23-	23	23	23	23	23	23	23	23	23	23
24-	24	24	24	24	24	24	24	24	24	24
25-	25	25	25	25	25	25	25	25	25	25
26-	26	26	26	26	26	26	26	26	26	26
27-	27	27	27	27	27	27	27	27	27	27
28-	28	28	28	28	28	28	28	28	28	28
29-	29	29	29	29	29	29	29	29	29	29
30-	30	30	30	30	30	30	30	30	30	30
31-	31	31	31	31	31	31	31	31	31	31
32-	32	32	32	32	32	32	32	32	32	32
33-	33	33	33	33	33	33	33	33	33	33
34-	34	34	34	34	34	34	34	34	34	34
35-	35	35	35	35	35	35	35	35	35	35
36-	36	36	36	36	36	36	36	36	36	36
37-	37	37	37	37	37	37	37	37	37	37
38-	38	38	38	38	38	38	38	38	38	38
39-	39	39	39	39	39	39	39	39	39	39
40-	40	40	40	40	40	40	40	40	40	40
41-	41	41	41	41	41	41	41	41	41	41
42-	42	42	42	42	42	42	42	42	42	42
43-	43	43	43	43	43	43	43	43	43	43
44-	44	44	44	44	44	44	44	44	44	44
45-	45	45	45	45	45	45	45	45	45	45

CARD COUNT	1	2	3	4	5	6	7	8	9	10
46-	CBAR	46	6	57	77	1.	0.0	1.
47-	CBAR	47	6	77	97	1.	0.0	1.
48-	CBAR	48	6	97	117	1.	0.0	1.
49-	CBAR	49	6	117	137	1.	0.0	1.
50-	CBAR	50	6	137	157	1.	0.0	1.
51-	CBAR	51	6	157	177	1.	0.0	1.
52-	CBAR	52	6	177	197	1.	0.0	1.
53-	CBAR	53	4	67	1	-1.	0.0	1.
54-	CBAR	54	4	87	67	-1.	0.0	1.
55-	CBAR	55	4	107	87	-1.	0.0	1.
56-	CBAR	56	4	127	107	-1.	0.0	1.
57-	CBAR	57	4	147	127	-1.	0.0	1.
58-	CBAR	58	4	167	147	-1.	0.0	1.
59-	CBAR	59	4	187	167	-1.	0.0	1.
60-	CBAR	60	4	233	187	-1.	0.0	1.
61-	CBAR	61	6	196	176	-1.	0.0	1.
62-	CBAR	62	6	176	156	-1.	0.0	1.
63-	CBAR	63	6	156	136	-1.	0.0	1.
64-	CBAR	64	6	136	116	-1.	0.0	1.
65-	CBAR	65	6	116	96	-1.	0.0	1.
66-	CBAR	66	6	96	76	-1.	0.0	1.
67-	CBAR	67	6	76	56	-1.	0.0	1.
68-	CBAR	68	6	56	48	-1.	0.0	1.
69-	CBAR	69	4	186	232	1.	0.0	1.
70-	CBAR	70	4	166	186	1.	0.0	1.
71-	CBAR	71	4	146	166	1.	0.0	1.
72-	CBAR	72	4	126	146	1.	0.0	1.
73-	CBAR	73	4	106	126	1.	0.0	1.
74-	CBAR	74	4	86	106	1.	0.0	1.
75-	CBAR	75	4	66	86	1.	0.0	1.
76-	CBAR	76	4	40	66	1.	0.0	1.
77-	CBAR	77	7	1	67	1.	0.0	1.
78-	+BAR77	78	7	67	0.	3.	-3.9	0.	3.	CBAR77 -3.9
79-	CBAR	79	7	87	87	1.	0.0	1.	3.	CBAR78 -3.9
80-	+BAR78	80	7	87	0.	3.	-3.9	0.	3.	CBAR79 -3.9
81-	CBAR	81	7	107	107	1.	0.0	1.	3.	CBAR80 -3.9
82-	+BAR79	82	7	107	0.	3.	-3.9	0.	3.	CBAR81 -3.9
83-	CBAR	83	7	127	127	1.	0.0	1.	3.	CBAR82 -3.9
84-	+BAR80	84	7	127	0.	3.	-3.9	0.	3.	CBAR83 -3.9
85-	CBAR	85	7	147	147	1.	0.0	1.	3.	..
86-	+BAR81	86	7	147	0.	3.	-3.9	0.	3.	..
87-	CBAR	87	7	167	167	1.	0.0	1.	3.	..
88-	+BAR82	88	7	167	0.	3.	-3.9	0.	3.	..
89-	CBAR	89	7	187	187	1.	0.0	1.	3.	..
90-	+BAR83	90	7	187	0.	3.	-3.9	0.	3.	..

CARD COUNT	1	2	3	4	5	6	7	8	9	10
91-	CBAR	84	187	233	1.	0.0	0.0	1.	9	CBAR84
92-	+BAR84			0.	3.	-3.9	0.	3.	-3.9	CBAR85
93-	CBAR	85	66	40	-1.	0.0	1.	1.	-3.9	CBAR86
94-	+BAR85			0.	-3.	-3.9	0.	-3.	-3.9	CBAR87
95-	CBAR	86	86	66	-1.	0.0	1.	1.	-3.9	CBAR88
96-	+BAR86			0.	-3.	-3.9	0.	-3.	-3.9	CBAR89
97-	CBAR	87	106	86	-1.	0.0	1.	1.	-3.9	CBAR90
98-	+BAR87			0.	-3.	-3.9	0.	-3.	-3.9	CBAR91
99-	CBAR	88	126	106	-1.	0.0	1.	1.	-3.9	CBAR92
100-	+BAR88			0.	-3.	-3.9	0.	-3.	-3.9	CBAR93
101-	CBAR	89	146	126	-1.	0.0	1.	1.	-3.9	CBAR94
102-	+BAR89			0.	-3.	-3.9	0.	-3.	-3.9	CBAR95
103-	CBAR	90	166	146	-1.	0.0	1.	1.	-3.9	CBAR96
104-	+BAR90			0.	-3.	-3.9	0.	-3.	-3.9	CBAR97
105-	CBAR	91	186	166	-1.	0.0	1.	1.	-3.9	CBAR98
106-	+BAR91			0.	-3.	-3.9	0.	-3.	-3.9	CBAR99
107-	CBAR	92	232	186	-1.	0.0	1.	1.	-3.9	CBAR100
108-	+BAR92			0.	-3.	-3.9	0.	-3.	-3.9	CBAR101
109-	CBAR	93	10	71	1.	0.0	1.	-2.45	-4.05	CBAR102
110-	+BAR93			0.	-91	-4.05	0.	-3.71	-4.05	CBAR103
111-	CBAR	94	70	31	-1.	0.0	1.	0.	-4.05	CBAR104
112-	+BAR94			0.	-1.33	-4.05	0.	0.	-4.05	CBAR105
113-	CBAR	95	67	71	0.	0.0	1.	1.	-4.05	CBAR106
114-	+BAR95			0.	0.	-4.05	0.	0.	-4.05	CBAR107
115-	CBAR	96	71	72	0.	0.0	1.	1.	-4.05	CBAR108
116-	+BAR96			0.	0.	-4.05	0.	0.	-4.05	CBAR109
117-	CBAR	97	72	70	0.	0.0	1.	1.	-4.05	CBAR110
118-	+BAR97			0.	0.	-4.05	0.	0.	-4.05	CBAR111
119-	CBAR	98	70	66	0.	0.0	1.	1.	-4.05	CBAR112
120-	+BAR98			0.	0.	-4.05	0.	0.	-4.05	CBAR113
121-	CBAR	99	87	91	0.	0.0	1.	1.	-4.05	CBAR114
122-	+BAR99			0.	0.	-4.05	0.	0.	-4.05	CBAR115
123-	CBAR	100	91	92	0.	0.0	1.	1.	-4.05	CBAR116
124-	+BAR100			0.	0.	-4.05	0.	0.	-4.05	CBAR117
125-	CBAR	101	92	90	0.	0.0	1.	1.	-4.05	CBAR118
126-	+BAR101			0.	0.	-4.05	0.	0.	-4.05	CBAR119
127-	CBAR	102	90	86	0.	0.0	1.	1.	-4.05	CBAR120
128-	+BAR102			0.	0.	-4.05	0.	0.	-4.05	CBAR121
129-	CBAR	103	107	111	0.	0.0	1.	1.	-3.5	CBAR122
130-	+BAR103			0.	0.	-3.5	0.	0.	-3.5	CBAR123
131-	CBAR	104	111	112	0.	0.0	1.	1.	-3.5	CBAR124
132-	+BAR104			0.	0.	-3.5	0.	0.	-3.5	CBAR125
133-	CBAR	105	112	110	0.	0.0	1.	1.	-3.5	CBAR126
134-	+BAR105			0.	0.	-3.5	0.	0.	-3.5	CBAR127
135-	CBAR	106	112	106	0.	0.0	1.	1.	-3.5	CBAR128

CARD COUNT	1	2	3	4	5	6	7	8	9	10
136-	+BAR106	8	127	0.	0.	-3.5	0.	0.	-3.5	CBAR107
137-	CBAR	107	131	0.	0.0	-4.05	1.	1.	-4.05	CBAR108
138-	+BAR107	8	131	0.	0.	-4.05	1.	1.	-4.05	CBAR109
139-	CBAR	108	132	0.	0.	-4.05	1.	1.	-4.05	CBAR110
140-	+BAR108	8	132	0.	0.	-4.05	1.	1.	-4.05	CBAR111
141-	CBAR	109	130	0.	0.	-4.05	1.	1.	-4.05	CBAR112
142-	+BAR109	8	130	0.	0.	-4.05	1.	1.	-4.05	CBAR113
143-	CBAR	110	147	0.	0.	-4.05	1.	1.	-4.05	CBAR114
144-	+BAR110	8	147	0.	0.	-4.05	1.	1.	-4.05	CBAR115
145-	CBAR	111	151	0.	0.	-3.5	1.	1.	-3.5	CBAR116
146-	+BAR111	9	151	0.	0.	-3.5	1.	1.	-3.5	CBAR117
147-	CBAR	112	152	0.	0.	-3.5	1.	1.	-3.5	CBAR118
148-	+BAR112	9	152	0.	0.	-3.5	1.	1.	-3.5	CBAR119
149-	CBAR	113	150	0.	0.	-3.5	1.	1.	-3.5	CBAR120
150-	+BAR113	9	150	0.	0.	-3.5	1.	1.	-3.5	CBAR121
151-	CBAR	114	171	0.	0.	-4.05	1.	1.	-4.05	CBAR122
152-	+BAR114	8	171	0.	0.	-4.05	1.	1.	-4.05	CBAR123
153-	CBAR	115	172	0.	0.	-4.05	1.	1.	-4.05	CBAR124
154-	+BAR115	8	172	0.	0.	-4.05	1.	1.	-4.05	CBAR125
155-	CBAR	116	170	0.	0.	-4.05	1.	1.	-4.05	CBAR126
156-	+BAR116	8	170	0.	0.	-4.05	1.	1.	-4.05	CBAR127
157-	CBAR	117	166	0.	0.	-4.05	1.	1.	-4.05	CBAR128
158-	+BAR117	8	166	0.	0.	-4.05	1.	1.	-4.05	CBAR129
159-	CBAR	118	191	0.	0.	-4.05	1.	1.	-4.05	CBAR130
160-	+BAR118	8	191	0.	0.	-4.05	1.	1.	-4.05	CBAR131
161-	CBAR	119	192	0.	0.	-4.05	1.	1.	-4.05	CBAR132
162-	+BAR119	8	192	0.	0.	-4.05	1.	1.	-4.05	CBAR133
163-	CBAR	120	190	0.	0.	-4.05	1.	1.	-4.05	CBAR134
164-	+BAR120	8	190	0.	0.	-4.05	1.	1.	-4.05	CBAR135
165-	CBAR	121	186	0.	0.	-4.05	1.	1.	-4.05	CBAR136
166-	+BAR121	8	186	0.	0.	-4.05	1.	1.	-4.05	CBAR137
167-	CBAR	122	191	0.	0.	-4.05	1.	1.	-4.05	CBAR138
168-	+BAR122	8	191	0.	0.	-4.05	1.	1.	-4.05	CBAR139
169-	CBAR	123	230	0.	0.	-4.05	1.	1.	-4.05	CBAR140
170-	+BAR123	8	230	0.	0.	-4.05	1.	1.	-4.05	CBAR141
171-	CBAR	124	233	0.	0.	-4.05	1.	1.	-4.05	CBAR142
172-	+BAR124	8	233	0.	0.	-4.05	1.	1.	-4.05	CBAR143
173-	CBAR	125	229	0.	0.	-4.05	1.	1.	-4.05	CBAR144
174-	+BAR125	8	229	0.	0.	-4.05	1.	1.	-4.05	CBAR145
175-	CBAR	126	230	0.	0.	-4.05	1.	1.	-4.05	CBAR146
176-	+BAR126	8	230	0.	0.	-4.05	1.	1.	-4.05	CBAR147
177-	CBAR	127	233	0.	0.	-4.05	1.	1.	-4.05	CBAR148
178-	+BAR127	8	233	0.	0.	-4.05	1.	1.	-4.05	CBAR149
179-	CBAR	128	228	0.	0.	-4.05	1.	1.	-4.05	CBAR150
180-	+BAR128	8	228	0.	0.	-4.05	1.	1.	-4.05	CBAR151

CARD COUNT	1	2	3	4	5	6	7	8	9	10
181-	CBAR	133	1	216	212	1	0.0	1		
182-	CBAR	134	1	212	208	1	0.0	1		
183-	CBAR	135	1	208	204	1	0.0	1		
184-	CBAR	136	1	204	197	1	0.0	1		
185-	CBAR	137	5	231	225	-1	0.0	1		
186-	CBAR	138	5	226	222	-1	0.0	1		
187-	CBAR	139	5	222	216	-1	0.0	1		
188-	CBAR	140	5	218	214	-1	0.0	1		
189-	CBAR	141	5	214	210	-1	0.0	1		
190-	CBAR	142	5	210	206	-1	0.0	1		
191-	CBAR	143	5	206	202	-1	0.0	1		
192-	CBAR	144	5	202	195	-1	0.0	1		
193-	CBAR	145	5	202	200	-1	1	0.0		
194-	CBAR	146	5	200	201	-1	1	0.0		
195-	CBAR	147	5	225	230	-1	0.0	1		
196-	CBAR	148	5	221	225	-1	0.0	1		
197-	CBAR	149	5	217	221	-1	0.0	1		
198-	CBAR	150	5	213	217	-1	0.0	1		
199-	CBAR	151	5	209	213	-1	0.0	1		
200-	CBAR	152	5	205	209	-1	0.0	1		
201-	CBAR	153	5	201	205	-1	0.0	1		
202-	CBAR	154	5	194	201	-1	0.0	1		
203-	CBAR	155	1	227	232	1	0.0	1		
204-	CBAR	156	1	223	227	1	0.0	1		
205-	CBAR	157	1	219	223	1	0.0	1		
206-	CBAR	158	1	215	219	1	0.0	1		
207-	CBAR	159	1	211	215	1	0.0	1		
208-	CBAR	160	1	207	211	1	0.0	1		
209-	CBAR	161	1	203	207	1	0.0	1		
210-	CBAR	162	1	196	203	1	0.0	1		
211-	CBAR	163	2	195	197	0.0	-1	1		
212-	CBAR	164	2	193	195	0.0	-1	1		
213-	CBAR	165	2	194	193	0.0	-1	1		
214-	CBAR	166	2	196	194	0.0	-1	1		
215-	CBAR	167	8	10	1	0.0	-1	1		
216-	+BAR167	167		1.97	1	0.0	-4.05	1.97		CBAR167
217-	CBAR	168	8	19	10	0.0	-1	1		-4.05 CBAR168
218-	+BAR168	168		1.97	1	0.0	-4.05	1.97		-4.05
219-	CBAR	169	8	28	19	0.0	-1	1		CBAR169
220-	+BAR169	169		1.97	1	0.0	-4.05	1.97		-4.05
221-	CBAR	170	8	31	28	0.0	-1	1		CBAR170
222-	+BAR170	170		1.97	1	0.0	-4.05	1.97		-4.05
223-	CBAR	171	8	40	31	0.0	-1	1		CBAR171
224-	+BAR171	171		1.97	1	0.0	-4.05	1.97		-4.05
225-	CBAR	172	8	233	231	0.0	1	1		CBAR172

CARD	1	2	3	4	5	6	7	8	9	10
COUNT
226-	+BAR172	173	8	231	229	0.	-1.97	0.	-4.05	1.0
227-	CBAR	173	8	231	229	0.	-1.97	0.	-4.05	1.0
228-	+BAR173	174	8	229	230	0.	-1.97	0.	-4.05	1.0
229-	CBAR	174	8	229	230	0.	-1.97	0.	-4.05	1.0
230-	+BAR174	175	8	230	232	0.	-1.97	0.	-4.05	1.0
231-	CBAR	175	8	230	232	0.	-1.97	0.	-4.05	1.0
232-	+BAR175	448	10	51	59	1.0	1.0	1.0	-1.97	0.
233-	CBAR	448	10	51	59	1.0	1.0	1.0	-1.97	0.
234-	CBAR	449	10	59	79	1.0	1.0	1.0	-1.97	0.
235-	CBAR	450	10	79	99	1.0	1.0	1.0	-1.97	0.
236-	CBAR	451	10	99	119	1.0	1.0	1.0	-1.97	0.
237-	CBAR	452	10	119	139	1.0	1.0	1.0	-1.97	0.
238-	CBAR	453	10	139	159	1.0	1.0	1.0	-1.97	0.
239-	CBAR	454	10	159	179	1.0	1.0	1.0	-1.97	0.
240-	CBAR	455	10	179	199	1.0	1.0	1.0	-1.97	0.
241-	CBAR	456	10	199	178	1.0	1.0	1.0	-1.97	0.
242-	CBAR	457	10	178	158	1.0	1.0	1.0	-1.97	0.
243-	CBAR	458	10	158	138	1.0	1.0	1.0	-1.97	0.
244-	CBAR	459	10	138	118	1.0	1.0	1.0	-1.97	0.
245-	CBAR	460	10	118	98	1.0	1.0	1.0	-1.97	0.
246-	CBAR	461	10	98	78	1.0	1.0	1.0	-1.97	0.
247-	CBAR	462	10	78	58	1.0	1.0	1.0	-1.97	0.
248-	CBAR	463	10	58	38	1.0	1.0	1.0	-1.97	0.
249-	CBAR	464	10	38	18	1.0	1.0	1.0	-1.97	0.
250-	CBAR	465	10	18	1	1.0	1.0	1.0	-1.97	0.
251-	CBAR	466	10	1	69	1.0	1.0	1.0	-1.97	0.
252-	CBAR	467	10	69	89	1.0	1.0	1.0	-1.97	0.
253-	CBAR	468	10	89	109	1.0	1.0	1.0	-1.97	0.
254-	CBAR	469	10	109	129	1.0	1.0	1.0	-1.97	0.
255-	CBAR	470	10	129	149	1.0	1.0	1.0	-1.97	0.
256-	CBAR	471	10	149	169	1.0	1.0	1.0	-1.97	0.
257-	CBAR	472	10	169	189	1.0	1.0	1.0	-1.97	0.
258-	CBAR	473	10	189	209	1.0	1.0	1.0	-1.97	0.
259-	CBAR	474	10	209	229	1.0	1.0	1.0	-1.97	0.
260-	CBAR	475	10	229	249	1.0	1.0	1.0	-1.97	0.
261-	CBAR	476	10	249	269	1.0	1.0	1.0	-1.97	0.
262-	CBAR	477	10	269	289	1.0	1.0	1.0	-1.97	0.
263-	CBAR	478	10	289	309	1.0	1.0	1.0	-1.97	0.
264-	CBAR	479	10	309	329	1.0	1.0	1.0	-1.97	0.
265-	CELAS2	394	1.0	9	1	1.0	1.0	1.0	-1.97	0.
266-	CELAS2	395	1.0	9	2	1.0	1.0	1.0	-1.97	0.
267-	CELAS2	396	1.0	9	3	1.0	1.0	1.0	-1.97	0.
268-	CELAS2	397	1.0	48	1	1.0	1.0	1.0	-1.97	0.
269-	CELAS2	398	1.0	48	2	1.0	1.0	1.0	-1.97	0.
270-	CELAS2	399	1.0	48	3	1.0	1.0	1.0	-1.97	0.

CARD COUNT	1	2	3	4	5	6	7	8	9	10
271-	CELAS2	400	1.+10	57	1	59	1			
272-	CELAS2	401	1.+10	57	2	59	2			
273-	CELAS2	402	1.+10	57	3	59	3			
274-	CELAS2	403	1.+10	58	1	58	1			
275-	CELAS2	404	1.+10	56	2	58	2			
276-	CELAS2	405	1.+10	55	3	58	3			
277-	CELAS2	406	1.+10	77	1	79	1			
278-	CELAS2	407	1.+10	77	2	79	2			
279-	CELAS2	408	1.+10	77	3	79	3			
280-	CELAS2	409	1.+10	76	1	78	1			
281-	CELAS2	410	1.+10	76	2	78	2			
282-	CELAS2	411	1.+10	76	3	78	3			
283-	CELAS2	412	1.+10	97	1	99	1			
284-	CELAS2	413	1.+10	97	2	99	2			
285-	CELAS2	414	1.+10	97	3	99	3			
286-	CELAS2	415	1.+10	96	1	98	1			
287-	CELAS2	416	1.+10	96	2	98	2			
288-	CELAS2	417	1.+10	96	3	98	3			
289-	CELAS2	418	1.+10	117	1	119	1			
290-	CELAS2	419	1.+10	117	2	119	2			
291-	CELAS2	420	1.+10	117	3	119	3			
292-	CELAS2	421	1.+10	116	1	118	1			
293-	CELAS2	422	1.+10	116	2	118	2			
294-	CELAS2	423	1.+10	116	3	118	3			
295-	CELAS2	424	1.+10	137	1	139	1			
296-	CELAS2	425	1.+10	137	2	139	2			
297-	CELAS2	426	1.+10	137	3	139	3			
298-	CELAS2	427	1.+10	136	1	138	1			
299-	CELAS2	428	1.+10	136	2	138	2			
300-	CELAS2	429	1.+10	136	3	138	3			
301-	CELAS2	430	1.+10	157	1	159	1			
302-	CELAS2	431	1.+10	157	2	159	2			
303-	CELAS2	432	1.+10	157	3	159	3			
304-	CELAS2	433	1.+10	156	1	158	1			
305-	CELAS2	434	1.+10	156	2	158	2			
306-	CELAS2	435	1.+10	156	3	158	3			
307-	CELAS2	436	1.+10	177	1	179	1			
308-	CELAS2	437	1.+10	177	2	179	2			
309-	CELAS2	438	1.+10	177	3	179	3			
310-	CELAS2	439	1.+10	176	1	178	1			
311-	CELAS2	440	1.+10	176	2	178	2			
312-	CELAS2	441	1.+10	176	3	178	3			
313-	CELAS2	442	1.+10	197	1	199	1			
314-	CELAS2	443	1.+10	197	2	199	2			
315-	CELAS2	444	1.+10	197	3	199	3			

CARD COUNT	1	2	3	4	5	6	7	8	9	10
316-	CELAS2	445	1.+10	196	1	198	1			
317-	CELAS2	446	1.+10	196	2	198	2			
318-	CELAS2	447	1.+10	196	3	198	3			
319-	QUAD1	222	3	66	67	71	10			
320-	QUAD1	223	3	66	40	31	70			
321-	QUAD1	224	3	67	87	91	71			
322-	QUAD1	225	3	71	51	92	72			
323-	QUAD1	226	3	72	92	90	70			
324-	QUAD1	227	3	70	90	86	66			
325-	QUAD1	228	3	87	107	111	91			
326-	QUAD1	229	3	51	111	112	92			
327-	QUAD1	230	3	92	112	110	90			
328-	QUAD1	231	3	90	110	106	86			
329-	QUAD1	232	3	107	127	131	111			
330-	QUAD1	233	3	111	131	132	112			
331-	QUAD1	234	3	112	132	130	110			
332-	QUAD1	235	3	110	130	126	106			
333-	QUAD1	236	3	127	147	151	131			
334-	QUAD1	237	3	131	151	152	132			
335-	QUAD1	238	3	132	152	150	130			
336-	QUAD1	239	3	130	150	146	126			
337-	QUAD1	240	3	147	167	171	151			
338-	QUAD1	241	3	151	171	172	152			
339-	QUAD1	242	3	152	172	170	150			
340-	QUAD1	243	3	150	170	166	146			
341-	QUAD1	244	3	167	187	191	171			
342-	QUAD1	245	3	171	191	192	172			
343-	QUAD1	246	3	172	192	190	170			
344-	QUAD1	247	3	170	190	186	166			
345-	QUAD1	248	3	187	233	231	191			
346-	QUAD1	249	3	191	231	229	192			
347-	QUAD1	250	3	192	229	230	190			
348-	QUAD1	251	3	190	230	232	186			
349-	TRIA1	350	3	10	71	19				
350-	TRIA1	351	3	71	72	19				
351-	TRIA1	352	3	28	19	72				
352-	TRIA1	353	3	72	70	28				
353-	TRIA1	354	3	31	28	70				
354-	FORCE	100	9	1.01+5	0	0	-1.0			
355-	FORCE	100	48	1.01+5	0	0	-1.0			
356-	FORCE	100	196	1.01+5	0	0	-1.0			
357-	FORCE	100	197	1.01+5	0	0	-1.0			
358-	FORCE	110	48	6.75+4	0	0	-1.0			
359-	FORCE	400	1	1.35+3	-1.	0	0			
360-	FORCE	400	40	1.35+3	-1.	0	0			

CARD COUNT	1	2	3	4	5	6	7	8	9	10
361-	FORCE	410	1	1.35+3	1.	0	0	0		
362-	FORCE	410	40	1.35+3	1.	0	0	0		
363-	FORCE	420	40	1.35+3	1.	0	0	0		
364-	FORCE	430	40	1.35+3	1.	0	0	0		
365-	FORCE	500	48	3.36+4	0	-1.	0	0		
366-	FORCE	510	48	3.36+4	0	1.	0	0		
367-	FORCE	520	48	3.36+4	1.	0	0	0		
368-	FORCE	530	48	3.36+4	1.	0	0	0		
369-	FORCE	600	9	2.24+4	0	1.	0	0		
370-	FORCE	600	48	2.24+4	0	-1.	0	0		
371-	FORCE	501	48	2.24+4	0	-1.	0	0		
372-	FORCE	610	9	3.36+4	0	-1.	0	0		
373-	FORCE	610	48	3.36+4	0	1.	0	0		
374-	FORCE	611	48	3.36+4	0	-1.	0	0		
375-	FORCE	620	40	3.36+4	0	-1.	0	0		
376-	FORCE	630	40	3.36+4	0	-1.	0	0		
377-	FORCE	640	48	6.72+4	0	0	0	-1.		
378-	FORCE	641	48	6.72+4	0	0	0	-1.		
379-	FORCE	650	48	2.24+4	0	0	0	1.		
380-	FORCE	651	48	2.24+4	0	0	0	1.		
381-	FORCE	660	48	2.24+4	-1.	0	0	0		
382-	FORCE	660	196	2.24+4	1.	0	0	0		
383-	FORCE	661	48	2.24+4	-1.	0	0	0		
384-	FORCE	670	40	3.36+4	1.	0	0	0		
385-	FORCE	670	232	3.36+4	-1.	0	0	0		
386-	FORCE	680	40	3.36+4	-1.	0	0	0		
387-	FORCE	680	232	3.36+4	1.	0	0	0		
388-	FORCE	700	11	374.	-1.	0	0	0		
389-	FORCE	700	14	374.	-1.	0	0	0		
390-	FORCE	700	16	374.	-1.	0	0	0		
391-	FORCE	700	20	374.	-1.	0	0	0		
392-	FORCE	700	23	374.	-1.	0	0	0		
393-	FORCE	700	25	374.	-1.	0	0	0		
394-	FORCE	710	11	374.	1.	0	0	0		
395-	FORCE	710	14	374.	1.	0	0	0		
396-	FORCE	710	16	374.	1.	0	0	0		
397-	FORCE	710	20	374.	1.	0	0	0		
398-	FORCE	710	23	374.	1.	0	0	0		
399-	FORCE	710	25	374.	1.	0	0	0		
400-	GRAV	210		0	0	-1.				
401-	GRID	1		3.25	6.55					
402-	GRID	2		1.29	17.54					
403-	GRID	3		3.25	28.53					
404-	GRID	4		3.25	39.52					
405-	GRID	5		3.25	50.51					

CARD	1	2	3	4	5	6	7	8	9	10
COUNT
406-	GRID	6	3.25	1.29	61.49					
407-	GRID	7	3.25	1.29	72.48					
408-	GRID	8	3.25	1.29	88.71					
409-	GRID	9	3.25	1.29	94.46					
410-	GRID	10	3.25	21.22	6.55					
411-	GRID	11	3.25	21.22	17.54					
412-	GRID	12	3.25	21.22	28.53					
413-	GRID	13	3.25	21.22	39.52					
414-	GRID	14	3.25	21.22	50.51					
415-	GRID	15	3.25	21.22	61.49					
416-	GRID	16	3.25	21.22	72.48					
417-	GRID	17	3.25	21.22	88.71					
418-	GRID	18	3.25	21.22	94.46					
419-	GRID	19	3.25	41.14	6.55					
420-	GRID	20	3.25	58.38	17.54					
421-	GRID	21	3.25	58.38	28.53					
422-	GRID	22	3.25	58.38	39.52					
423-	GRID	23	3.25	58.38	50.51					
424-	GRID	24	3.25	58.38	61.49					
425-	GRID	25	3.25	58.38	72.48					
426-	GRID	26	3.25	41.14	88.71					
427-	GRID	27	3.25	41.14	94.46					
428-	GRID	28	3.25	58.38	6.55					
429-	GRID	29	3.25	58.38	17.54					
430-	GRID	30	3.25	58.38	28.53					
431-	GRID	31	3.25	58.38	39.52					
432-	GRID	32	3.25	75.62	6.55					
433-	GRID	33	3.25	75.62	17.54					
434-	GRID	34	3.25	94.71	28.53					
435-	GRID	35	3.25	94.71	39.52					
436-	GRID	36	3.25	94.71	50.51					
437-	GRID	37	3.25	94.71	61.49					
438-	GRID	38	3.25	94.71	72.48					
439-	GRID	39	3.25	94.71	88.71					
440-	GRID	40	3.25	94.71	94.46					
441-	GRID	41	119.25	1.29	295.38					
442-	GRID	42	119.25	1.29	295.38					
443-	GRID	43	3.25	1.29	94.46					
444-	GRID	44	3.25	94.71	94.46					
445-	GRID	45	33.86	1.29	94.46					
446-	GRID	46	33.86	1.29	94.46					
447-	GRID	47	33.86	94.71	94.46					
448-	GRID	48	33.86	94.71	94.46					
449-	GRID	49	33.86	1.29	94.46					
450-	GRID	50	33.86	94.71	94.46					
		51								
		52								
		53								
		54								
		55								
		56								
		57								
		58								
		59								
		60								
		61								
		62								
		63								
		64								
		65								
		66								
		67								
		68								
		69								
		70								
		71								
		72								
		73								
		74								
		75								
		76								
		77								
		78								
		79								
		80								
		81								
		82								
		83								
		84								
		85								
		86								
		87								
		88								
		89								
		90								
		91								
		92								
		93								
		94								
		95								
		96								
		97								
		98								
		99								
		100								

456
456

CARD COUNT	1	2	3	4	5	6	7	8	9	10
451-	GRID	67	33.85	1.29	6.55					
452-	GRID	69	33.86	94.71	6.55					
453-	GRID	69	33.86	1.29	6.55					
454-	GRID	70	33.86	73.24	6.55					
455-	GRID	71	33.86	22.76	6.55					
456-	GRID	72	33.86	48.0	6.55					
457-	GRID	76	60.55	94.71	94.46					
458-	GRID	77	60.55	1.29	94.46					
459-	GRID	78	60.55	94.71	94.46					
460-	GRID	79	60.55	1.29	94.46					
461-	GRID	86	60.55	94.71	6.55					
462-	GRID	87	60.55	1.29	6.55					
463-	GRID	88	60.55	94.71	6.55					
464-	GRID	89	60.55	1.29	6.55					
465-	GRID	90	60.55	73.24	6.55					
466-	GRID	91	60.55	22.76	6.55					
467-	GRID	92	60.55	48.0	6.55					
468-	GRID	96	93.11	94.71	94.46					
469-	GRID	97	93.11	1.29	94.46					
470-	GRID	98	93.11	94.71	94.46					
471-	GRID	99	93.11	1.29	94.46					
472-	GRID	106	93.11	94.71	6.55					
473-	GRID	107	93.11	1.29	6.55					
474-	GRID	108	93.11	94.71	6.55					
475-	GRID	109	93.11	1.29	6.55					
476-	GRID	110	93.11	73.24	6.55					
477-	GRID	111	93.11	22.76	6.55					
478-	GRID	112	93.11	48.0	6.55					
479-	GRID	116	119.7	94.71	94.46					
480-	GRID	117	119.7	1.29	94.46					
481-	GRID	118	119.7	94.71	94.46					
482-	GRID	119	119.7	1.29	94.46					
483-	GRID	126	119.7	94.71	6.55					
484-	GRID	127	119.7	1.29	6.55					
485-	GRID	128	119.7	94.71	6.55					
486-	GRID	129	119.7	1.29	6.55					
487-	GRID	130	119.7	73.24	6.55					
488-	GRID	131	119.7	22.76	6.55					
489-	GRID	132	119.7	48.0	6.55					
490-	GRID	136	145.21	94.71	94.46					
491-	GRID	137	145.21	1.29	94.46					
492-	GRID	138	145.21	94.71	94.46					
493-	GRID	139	145.21	1.29	94.46					
494-	GRID	146	145.21	94.71	6.55					
495-	GRID	147	145.21	1.29	6.55					

CARD COUNT	1	2	3	4	5	6	7	8	9	10
496-	GRID 148	145.21	94.71	6.55						
497-	GRID 149	145.21	1.29	6.55						
498-	GRID 150	145.21	73.24	6.55						
499-	GRID 151	145.21	22.76	6.55						
500-	GRID 152	145.21	48.0	6.55						
501-	GRID 156	178.14	94.71	94.46						
502-	GRID 157	178.14	1.29	94.46						
503-	GRID 158	178.14	94.71	94.46						
504-	GRID 159	178.14	1.29	94.46						
505-	GRID 166	178.14	94.71	6.55						
506-	GRID 167	178.14	1.29	6.55						
507-	GRID 168	178.14	94.71	6.55						
508-	GRID 169	178.14	1.29	6.55						
509-	GRID 170	178.14	73.24	6.55						
510-	GRID 171	178.14	22.76	6.55						
511-	GRID 172	178.14	48.0	6.55						
512-	GRID 176	204.56	94.71	94.46						
513-	GRID 177	204.56	1.29	94.46						
514-	GRID 178	204.56	94.71	94.46						
515-	GRID 179	204.56	1.29	94.46						
516-	GRID 186	204.56	94.71	6.55						
517-	GRID 187	204.56	1.29	6.55						
518-	GRID 188	204.56	94.71	6.55						
519-	GRID 189	204.56	1.29	6.55						
520-	GRID 190	204.56	73.24	6.55						
521-	GRID 191	204.56	22.76	6.55						
522-	GRID 192	204.56	48.0	6.55						
523-	GRID 193	235.25	48.0	94.46						
524-	GRID 194	235.25	73.24	94.46						
525-	GRID 195	235.25	22.76	94.46						
526-	GRID 196	235.25	94.71	94.46						
527-	GRID 197	235.25	1.29	94.46						
528-	GRID 198	235.25	94.71	94.46						
529-	GRID 199	235.25	1.29	94.46						
530-	GRID 200	235.25	48.0	88.71						
531-	GRID 201	235.25	73.24	88.71						
532-	GRID 202	235.25	22.76	88.71						
533-	GRID 203	235.25	94.71	88.71						
534-	GRID 204	235.25	1.29	88.71						
535-	GRID 205	235.25	73.24	72.48						
536-	GRID 206	235.25	22.76	72.48						
537-	GRID 207	235.25	94.71	72.48						
538-	GRID 208	235.25	1.29	72.48						
539-	GRID 209	235.25	73.24	61.49						
540-	GRID 210	235.25	22.76	61.49						

CARD	CCOUNT	1	2	3	4	5	6	7	8	9	10
541-	GRID	211	235.25	94.71	61.49						
542-	GRID	212	235.25	1.29	61.49						
543-	GRID	213	235.25	73.24	50.51						
544-	GRID	214	235.25	22.76	50.51						
545-	GRID	215	235.25	94.71	50.51						
546-	GRID	216	235.25	1.29	50.51						
547-	GRID	217	235.25	73.24	39.52						
548-	GRID	218	235.25	22.76	39.52						
549-	GRID	219	235.25	94.71	39.52						
550-	GRID	220	235.25	1.29	39.52						
551-	GRID	221	235.25	73.24	28.53						
552-	GRID	222	235.25	22.76	28.53						
553-	GRID	223	235.25	94.71	28.53						
554-	GRID	224	235.25	1.29	28.53						
555-	GRID	225	235.25	73.24	17.54						
556-	GRID	226	235.25	22.76	17.54						
557-	GRID	227	235.25	94.71	17.54						
558-	GRID	228	235.25	1.29	17.54						
559-	GRID	229	235.25	48.0	6.55						
560-	GRID	230	235.25	73.24	6.55						
561-	GRID	231	235.25	22.76	6.55						
562-	GRID	232	235.25	94.71	6.55						
563-	GRID	233	235.25	1.29	6.55						
564-	LOAD	200	1.	210	1.	220	1.	220	1.25-5		
565-	MAT1	1	10.+6	.33	3.04-3						
566-	MAT1	2	1.5+4	.3							
567-	MOMENT	100	9	1.21+5	-1.0	.0	.0	.0	.0		
568-	MOMENT	100	9	7.56+5	.0	-1.0	.0	.0	.0		
569-	MOMENT	100	48	1.21+5	-1.0	.0	.0	.0	.0		
570-	MOMENT	100	48	7.56+5	.0	-1.0	.0	.0	.0		
571-	MOMENT	100	196	1.21+5	-1.0	.0	.0	.0	.0		
572-	MOMENT	100	196	7.56+5	.0	-1.0	.0	.0	.0		
573-	MOMENT	100	197	1.21+5	-1.0	.0	.0	.0	.0		
574-	MOMENT	100	197	7.56+5	.0	-1.0	.0	.0	.0		
575-	MOMENT	110	48	5.05+5	.0	1.0	.0	.0	.0		
576-	MOMENT	110	48	8.09+4	1.0	.0	.0	.0	.0		
577-	PBAR	1	2.99	2.30	11.23	13.53	0.0	0.0	0.0	PAAR1	
578-	+AAR1	1.2	.7	-1.9	-1.8	-2.4	-5	3.9	0.0	PAAR2	
579-	PBAR	2	2.22	1.68	1.68	3.36	0.0	0.0	0.0	PAAR2	
580-	+AAR2	1.9	.9	-3	-1.7	-1.2	-4	1.3	0.0	PAAR3	
581-	PBAR	3	2.8	4.02	4.76	8.78	0.0	0.0	0.0	PAAR3	
582-	+AAR3	2.3	.5	-2.4	-2.1	-2.5	-8	1.2	0.0	PAAR4	
583-	PBAR	4	1.63	1.84	.75	2.59	0.0	.86	0.0	PAAR4	
584-	+AAR4	1.5	1.5	-3.6	-1.5	-1.5	-1.5	.86	0.0	PAAR5	
585-	PBAR	5	1.43	1.09	.90	1.99	0.0	0.0	0.0	PAAR5	

CARD	1	2	3	4	5	6	7	8	9	10
COUNT	1	2	3	4	5	6	7	8	9	10
586-	1.31	1.33	1.31	1.31	1.18	1.75	1.175	1.194	1.325	
587-	6	1	2.43	4.56	4.56	1.92	6.50	0.0		PAAR6
588-	2.24	1.16	2.239	1.59	1.59	2.01	1.839	2.01	1.16	
589-	7	1	2.587	12.079	12.079	2.50	14.579	0.0		PAAR7
590-	2.345	1.884	2.348	2.304	2.304	2.652	2.652	2.652	1.884	
591-	8	1	1.613	5.878	5.878	5.82	6.46	0.0		PAAR8
592-	2.5	.514	2.5	1.486	1.486	2.5	1.486	2.5	.514	
593-	9	1	7.561	31.94	31.94	186.832	218.772	0.0		PAAR9
594-	1.945	8.0	1.945	8.0	8.0	2.804	2.804	6.0		PAAR10
595-	10	1	.8	.4	.4	.4	.4	.4		
596-	1.04	.89	.85	.85	.85	.96	.96	.96	.89	
597-	100	100	100	100	100	100	100	100	100	
598-	100	100	100	100	100	100	100	100	100	
599-	220	220	220	220	220	220	220	220	220	
600-	220	220	220	220	220	220	220	220	220	
601-	400	400	400	400	400	400	400	400	400	
602-	400	400	400	400	400	400	400	400	400	
603-	410	410	410	410	410	410	410	410	410	
604-	410	410	410	410	410	410	410	410	410	
605-	420	420	420	420	420	420	420	420	420	
606-	420	420	420	420	420	420	420	420	420	
607-	430	430	430	430	430	430	430	430	430	
608-	430	430	430	430	430	430	430	430	430	
609-	1	1	.0664	.0664	1	.129	2	2.50	.0	PQUADA
610-	1.29	1.29	1.29	1.29	1	.0832	2	2.00	.0	PQUADB
611-	2	1	1.04	1.04	1	.2326	2	3.00	.0	PQUADC
612-	3	1	1.55	1.55	1	1.	.01			
613-	1	1	2.67	2.67	1.	.129	2	2.50	.0	PTRI1
614-	1	1	.0664	.0664	1	.0832	2	2.00	.0	PTRI2
615-	1	1	1.29	1.29	1	.2326	2	3.00	.0	PTRI3
616-	2	1	1.04	1.04	1	.0832	2	2.00	.0	
617-	1	1	1.55	1.55	1	.0832	2	2.00	.0	
618-	1	1	1.29	1.29	1	.2326	2	3.00	.0	
619-	2	1	1.04	1.04	1	.0832	2	2.00	.0	
620-	1	1	1.55	1.55	1	.0832	2	2.00	.0	
621-	3	1	1.29	1.29	1	.2326	2	3.00	.0	
622-	100	100	100	100	100	100	100	100	100	
623-	100	100	100	100	100	100	100	100	100	
624-	100	100	100	100	100	100	100	100	100	
625-	110	110	110	110	110	110	110	110	110	
626-	110	110	110	110	110	110	110	110	110	
627-	110	110	110	110	110	110	110	110	110	
628-	200	200	200	200	200	200	200	200	200	
629-	400	400	400	400	400	400	400	400	400	
630-	400	400	400	400	400	400	400	400	400	

CARD COUNT	1	2	3	4	5	6	7	8	9	10
SPC	400	232	13			233	123			
SPC	500	1	123			40	3			
SPC	500	49	123			50	123			
SPC	500	232	3			233	123			
SPC	600	1	23			40	3			
SPC	600	49	123			50	123			
SPC	600	232	3			233	123			
SPC	601	9	23			46	3			
SPC	601	49	123			50	123			
SPC	601	196	3			197	123			
SPC	602	40	23			48	2			
SPC	602	49	123			50	123			
SPC	602	196	13			232	23			
SPC	700	1	123			9	12			
SPC	700	40	1			48	1			
SPC	700	49	123			50	123			
SPC	800	1	123			9	12			
SPC	800	49	123			50	123			
SPC	800	197	2			233	2			
SPC	900	1	123			40	13			
SPC	900	49	123			50	123			
SPC	900	232	3			233	3			

ENDDATA

```

* 24.5 CPU-S 78.2 COR-S 303 ELP-S. DO IFP
* 38.1 CPU-S 95.4 COR-S 439 ELP-S. END IFP
* 38.1 CPU-S 95.4 COR-S 439 ELP-S. XGPI

**NO ERRORS FOUND - EXECUTE NASTRAN PROGRAM**

* 45.4 CPU-S 104.4 COR-S 480 ELP-S. SEM1 END
* 45.4 CPU-S 104.4 COR-S 480 ELP-S. ---- LINK NS02 ----

```

@TEST TNE/1/56
INTERVENING STATEMENTS SKIPPED

@TEST TNE/2/56

@XQT *NASTRAN.LINK2